SERIAL NO. SSC-56

Fourth

PROGRESS REPORT

(Project SR-119)

on

WELDED REINFORCEMENT OF OPENINGS IN STRUCTURAL STEEL MEMBERS:

Cleavage Fracture and Plastic Flow in Structural Steel Plates with Openings

by

D. VASARHELYI, R. A. HECHTMAN AND Y. T. YOSHIMI
University of Washington

Under Bureau of Ships Contract NObs-50238
(BuShips Project NS-731-034)

for

SHIP STRUCTURE COMMITTEE

Convened by
The Secretary of the Treasury

Member Agencies—Ship Structure Committee

Bureau of Ships, Dept. of Navy
Military Sea Transportation Service, Dept. of Navy
United States Coast Guard, Treasury Dept.
Maritime Administration, Dept. of Commerce
American Bureau of Shipping

Address Correspondence To:

Secretary
Ship Structure Committee
U. S. Coast Guard Headquarters
Washington 25, D. C.

SERIAL NO. SSC-56
BuShips Project NS-731-034

March 1, 1954

SHIP STRUCTURE COMMITTEE

MEMBER AGENCIES:

BUREAU OF SHIPS, DEPT. OF NAVY
MILITARY SEA TRANSPORTATION SERVICE, DEPT. OF NAVY
UNITED STATES COAST GUARD, TREASURY DEPT.
MARITIME ADMINISTRATION, DEPT. OF COMMERCE
AMERICAN BUREAU OF SHIPPING

ADDRESS CORRESPONDENCE TO:

SECRETARY
SHIP STRUCTURE COMMITTEE
U. S. COAST GUARD HEADQUARTERS
WASHINGTON 25, D. C.

March 1, 1954

Dear Sir:

As part of its research program related to the improvement of hull structures of ships, the Ship Structure Committee is sponsoring an investigation on the welded reinforcement of openings in structural steel members at the University of Washington. Herewith is a copy of the Fourth Progress Report, SSC-56, of the investigation, entitled "Welded Reinforcement of Openings in Structural Steel Members: Cleavage Fracture and Plastic Flow in Structural Steel Plates with Openings" by D. Vasarhelyi, R. A. Hechtman and Y. T. Yoshimi.

Any questions, comments criticism or other matters pertaining to the Report should be addressed to the Secretary, Ship Structure Committee.

This Report is being distributed to those individuals and agencies associated with and interested in the work of the Ship Structure Committee.

Yours sincerely,

K. K. COWART
Rear Admiral, U. S. Coast Guard
Chairman, Ship Structure
Committee.

Fourth

Progress Report
(Project SR-119)

on

WELDED REINFORCEMENT OF OPENINGS IN STRUCTURAL STEEL MEMBERS:

Cleavage Fracture and Plastic Flow in Structural Steel Plates with Openings

by

D. Vasarhelyi, R. A. Hechtman, and Y. T. Yoshimi

UNIVERSITY OF WASHINGTON

under

Department of the Navy
Bureau of Ships Contract NObs-50238
BuShips Project No. NS-731-034

for

SHIP STRUCTURE COMMITTEE

CLEAVAGE FRACTURE AND PLASTIC FLOW IN STRUCTURAL STEEL PLATES WITH OPENINGS

TABLE OF CONTENTS

		Page
I.	Synopsis	1
II.	Introduction	2
III.	Tests of Plates with Openings	4
	1. Details of Specimens	4
	2. Methods of Plastic Analysis and Calibration Tests	9
	3. General Behavior During Test and Fracture of Plates with Openings	9
IV.	Elastic Stress Distribution in Plates with Openings	10
V.	Plastic Stress Distribution in Plates with Openings	14
VI.	Plastic Energy Distribution in Plates with Openings	20
VII.	Conditions for the Initiation of Fracture	25
VIII.	Conclusions	28
IX.	Acknowledgments	30
X.	Bibliography	31
	Appendix A: Calibration Tensile Tests	58
	Appendix B: Test of Specimen No. 85	62
	List of Figures	ii
	List of Tables	ix

LIST OF FIGURES

Fig. No.	Title	Page
1.	Plate with Circular Opening. Spec. No. 69.	32
2.	Plate with Reinforced Square Opening with Rounded Corners. Specs. No. 70 and 71	32
3.	Details of Specs. No. 4, 5, 17, 37, 38, and 38A	33
4.	Details of Specs. No. 95 and 96	33
5.	Location of SR-4 Gages and Slide-Wire Gages	34
6.	Arrangement of Grid-Wire Gages for Spec. No. 69	34
7.	Arrangement of Grid-Wire Gages for Specs. No. 95 and 96	35
8.	Arrangement of Grid-Wire Gages for Specs. No. 70 and 71	35
9.	Load-Average Elongation Curves. Specs. No. 37, 38, 69, 95 and 96.	36
10.	Load-Average Elongation Curves. Specs. No. 70 and 71	36
11.	Photographs of Plates after Failure. Specs. No. 69, 70 and 71.	37
12.	Photographs of Plates after Failure. Specs. No. 95 and 96	37
13.	Particular Cases of Plates with Unreinforced Openings Analyzed by Elastic Theory. Plates (a), (b) and (c).	38
14.	Particular Cases of Plates with Reinforced Openings Analyzed by Elastic Theory. Plates (d) and (e).	38
15.	Stress Concentration Contours in y-Direction for Plate of Infinite Width with Circular Hole by Elastic Theory. Plate (a)	39

Fig. No.	Title	Page
16.	Stress Concentration Contours in y-Direction for Plate of Finite Width with Circular Hole by Elastic Theory. Plate (b)	39
17.	Elastic Unit Strain Concentration Contours for Plate of Finite Width with Circular Opening Plotted from SR-4 Strain Gage Readings. Spec. No. 69	39
18.	Stress Concentration Contours in y-Direction for Plate of Infinite Width with Square Opening with Rounded Corners by Elastic Theory. Plate (c).	39
19.	Elastic Unit Strain Concentration Contours for Plate of Finite Width with Square Opening with Rounded Corners Plotted from SR-4 Strain Gage Readings. Spec. No. 38A	40
20.	Elastic Unit Strain Concentration Contours for Plate of Finite Width with Square Opening. Plotted from SR-4 Strain Gage Readings. Spec. No. 95. 76°F.	40
21.	Elastic Unit Strain Concentration Contours for Plate of Finite Width with Square Opening. Plotted from SR-4 Strain Gage Readings. Spec. No. 96. -46°F	40
22.	Stress Concentration Contours in y-Direction for Plate of Infinite Width with Circular Opening with Face Bar Reinforcement by Elastic Theory. Plate (d).	41
23.	Elastic Unit Strain Concentration Curve for Plate of Finite Width with Circular Opening with Face Bar Reinforcement. Spec. No. 5	41
24.	Stress Concentration Contours in y-Direction for Plate of Infinite Width with Circular Opening with Insert Plate Reinforcement by Elastic Theory. Plate (e)	42
25.	Elastic Unit Strain Concentration Curve for Plate of Finite Width. Insert Plate Reinforcement. Spec. No. 17	42

Fig. No.	Title	Page
26.	Stress Concentration Contours for σ_y for Plate with Circular Opening for Load of 650 kips, 77 Per Cent of Maximum Load. Spec. No. 69. 76°F . .	43
27.	Stress Concentration Contours for σ_y for Plate with Circular Opening for Load of 845 kips, Maximum Load. Spec. No. 69. 76°F	43
28.	Comparison of Elastic and Plastic Stress Concentration Curves for σ_y for a Plate with Circular Opening. Spec. No. 69	43
29.	Stress Concentration Contours for σ_y for Plate with Square Opening, Rounded Corners, Load of 800 kips, Maximum Load. Spec. No. 37. 76°F . . .	44
30.	Comparison of Elastic and Plastic Stress Concentration Curves for σ_y for Plate with Square Opening with Rounded Corners. Spec. No. 37. 76°F	44
31.	Stress Concentration Contours for σ_y for Plate with Square Opening with Rounded Corners, Load of 915 kips. Maximum Load. Spec. No. 38. -20°F.	44
32.	Comparison of Elastic and Plastic Stress Concentration Curves for σ_y for Plate with Square Opening with Rounded Corners. Spec. No. 38. -20°F.	44
33.	Stress Concentration Contours for σ_y for Plate with Square Opening, Load of 575 kips, 81 Per Cent of Maximum Load. Spec. No. 95. 76°F.	45
34.	Stress Concentration Contours for σ_y for Plate with Square Opening. Load of 710 kips. Maximum Load. Spec. No. 95. 76°F	45
35.	Comparison of Elastic and Plastic Stress Concentration Curves for σ_y for Plate with Square Opening. Spec. No. 95. 76°F.	45
36.	Stress Concentration Contours for σ_y for Plate with Square Opening. Load of 648 kips. Maximum Load. Spec. No. 96. -46°F.	46

Fig. No.	Title	Page
37.	Comparison of Elastic and Plastic Stress Concentration Curves for σ_Y for Plate with Square Opening. Spec. No. 96. -46°F	46
38.	Stress Concentration Contours for σ_Y for Plate with Reinforced Square Opening with Rounded Corners for Load of 1150 kips, 90 Per Cent of Maximum Load. Spec. No. 70. 76°F	47
39.	Stress Concentration Contours for σ_Y for Plate with Reinforced Square Opening with Rounded Corners for Load of 1276 kips, Maximum Load. Spec. No. 70, 76°F	47
40.	Comparison of Elastic and Plastic Stress Concentration Curves for σ_Y for Plate with Reinforced Square Opening with Rounded Corners. Spec. No. 70. 76°F.	47
41.	Stress Concentration Contours for σ_Y for Plate with Reinforced Square Opening with Rounded Corners for Load of 1150 kips, 98 Per Cent of Maximum Load. Spec. No. 71. -46°F.	48
42.	Stress Concentration Contours for σ_Y for Plate with Reinforced Square Opening with Rounded Corners for Load of 1176 kips, Maximum Load. Spec. No. 71. -46°F	48
43.	Comparison of Elastic and Plastic Stress Concentration Curves for σ_Y for Plate with Reinforced Square Opening with Rounded Corners. Spec. No. 71. -46°F	48
44.	Stress Concentration Factor in Plastic Range as Failure is Approached.	49
45.	Effect of Testing Temperature Upon Plastic Stress Distribution at Maximum Load	49
46.	Unit Strain Energy Contours for Plate of Finite Width with Circular Opening for Load of 650 kips, 77 Per Cent of Maximum Load. Spec. No. 69. 76°F.	50

Fig. No.	Title	Page
47.	Unit Strain Energy Contours for Plate of Finite Width with Circular Opening for Load of 845 kips, Maximum Load. Spec. No. 69. 76°F . . .	50
48.	Unit Strain Energy Contours for Plate of Finite Width with Square Opening, for Load of 575 kips, 81 Per Cent of the Load. Spec. No. 95. 76°F	50
49.	Unit Strain Energy Contours for Plate of Finite Width with Square Opening, for Load of 710 kips, Maximum Load. Spec. No. 95. 76°F . . .	50
50.	Unit Strain Energy Contours for Plate of Finite Width with Square Opening, for Load of 648 kips. Maximum Load. Spec. No. 96. -46°F . .	51
51.	Unit Strain Energy Contours for Plate of Finite Width with Reinforced Opening with Rounded Corners for Load of 1150 kips, 90 Per Cent of Maximum Load. Spec. No. 70. 76°F	51
52.	Unit Strain Energy Contours for Plate of Finite Width with Reinforced Square Opening with Rounded Corners for Load of 1276 kips, Maximum Load. Spec. No. 70. 76°F	51
53.	Unit Strain Energy Contours for Plate of Finite Width with Reinforced Square Opening with Rounded Corners for Load of 1150 kips, 98 Per Cent of Maximum Load. Spec. No. 71. -46°F. .	52
54.	Unit Strain Energy Contours for Plate of Finite Width with Reinforced Square Opening with Rounded Corners for Load of 1176 kips. Maximum Load. Spec. No. 71. -46°F.	52
55.	Contours of Equal Rate of Energy Absorption. Spec. No. 69. 76°F.	52
56.	Contours of Equal Rate of Energy Absorption. Spec. No. 37. 76°F.	53
57.	Contours of Equal Rate of Energy Absorption. Spec. No. 38. -20°F	53

Fig. No.	Title	Page
58.	Contours of Equal Rate of Energy Absorption. Spec. No. 95. 76°F.	53
59.	Contours of Equal Rate of Energy Absorption. Spec. No. 96. -46°F	53
60.	Contours of Equal Rate of Energy Absorption. Spec. No. 70. 76°F.	54
61.	Contours of Equal Rate of Energy Absorption. Spec. No. 71. -46°F	54
62.	Effect of Testing Temperature upon Plastic Energy Distribution at Maximum Load. Spec. No. 37 and 38	55
63.	Effect of Testing Temperature upon Plastic Energy Distribution at Maximum Load. Spec. No. 70 and 71	55
64.	Effect of Testing Temperature upon Plastic Energy Distribution at Maximum Load. Spec. No. 95 and 96	56
65.	Stress Concentration Factor, Maximum Strain and Maximum Unit Energy as Fracture is Approached. Specs. No. 69, 37, 38, 70, and 71.	57
66.	Stress Concentration Factor, Maximum Strain and Maximum Unit Energy as Fracture is Approached. Specs. No. 95 and 96	57

Appendix A

1a	Calibration Test. True Stress-(Natural) Strain Curve for Plate No. 1 and 3.	60
2a	Calibration Test. Octahedral Stress-Strain Curve for Plate No. 1 and 3.	60
3a	Relation of Unit Strain Energy Absorption and Octahedral Shear Strain for Calibration Test Specimen from Plate No. 1 and 3.	61
4a	Plot of E_t as a Function of Natural Strain, Plate No. 1 and 3.	61

Appendix B	Title	Page
1b	Details of Spec. No. 85.	65
2b	Distribution across Plate of Elongation on 36-in. Gage Length. Spec. No. 85. Square Opening with Rounded Corners, Face Bar and Insert Plate Reinforcement.	65
3b	Load and Average Elongation on 36-in. Gage Length for Spec. No. 85.	66
4b	Unit Strain Concentration in Region of Opening. Spec. No. 85.	66
5b	Photograph of Spec. No. 85 after Failure.	67

LIST OF TABLES

Table No.	Title	Page
I	Description of Specimens with 9 in. x 9 in. Openings with 1-1/8 in. Corner Radius.	5
II	List of Plates Used for Fabrication of Each Specimen	6
III	Mechanical Properties of Plates of Different Thicknesses Semi-Killed Steel U as Rolled. . .	7
IV	Strength and Energy Absorption of 36 in. x 1/2 in. and 48 in. x 1/2 in. Plates With Openings at Room and at Low Temperature .	8
V	Comparison of Load Computed From True Stress Distribution and Testing Machine Load.	19
VI	Comparison of the Total Energy Obtained by the Octahedral Theory and from the Load-Elongation Curve.	24
Appendix A.		
Ia	Results of Calibration Tensile Tests	59
Appendix B.		
Ib	Description and Test Results of Spec. No. 85 .	63
IIb	General Yielding and Fracture of Spec. No. 85.	64

CLEAVAGE FRACTURE AND PLASTIC FLOW IN STRUCTURAL STEEL PLATES WITH OPENINGS

I. SYNOPSIS

The study of welded reinforcement of openings in structural steel plates has as an objective the development of better design specifications. A thorough investigation of the plastic behavior of the plates was deemed necessary as a phase of this project. This avenue of approach led to energy and stress studies which utilized experimental techniques and theoretical concepts whose applicability had to be verified. The Second Progress Report[2] presented the first results thus obtained, which were sufficiently encouraging to justify the continuation of this type of analysis. It dealt only with notched plates without reinforcement.

The present Fourth Progress Report broadens the subject, including more theoretical and basic data on one hand and the application of the methods of plastic analysis to reinforced plates on the other. It covers the tests of an unreinforced plate with a circular opening, two unreinforced plates with a square opening, and two plates with a reinforced square opening with rounded corners. The methods of plastic analysis previously applied to unreinforced plates[2] gave satisfactory results for reinforced plates. The test results of two plates with a square opening with rounded

corners from the Second Report[2] are included where direct comparison is necessary.

II. INTRODUCTION

1. Previous Work

The tests of twenty-three 1/4-in. plates in the First Progress Report[1] with and without welded reinforcement drew attention to the importance of the behavior of these plates in the plastic range. A more detailed study of the unit strain energy and of the stress distribution in the plastic range was decided upon. The plastic analysis employed Nadai's octahedral theory[4] and a method of stress determination developed by this investigation[2].

The results of tests at both room and low temperature of three 36-in. x 1/2-in. plates with an unreinforced square opening with rounded corners were reported in the Second Progress Report[2], and the following main conclusions were drawn with respect to their behavior in the plastic range.

1. The octahedral theory proved to be a practicable means to study the distribution of the distortional energy in the plastic range of steel.
2. The true stresses in the plastic range were satisfactorily found by a method of analysis developed

by R. A. Hechtman for the purpose.

3. Both the distortional energy and the true stress analysis gave values in good agreement with the values obtained by entirely different methods.

4. The maximum values of the true tensile stress occurred in the regions where the greatest unit energy absorption was found.

5. A drop in the testing temperature from 76°F to -20°F, which changed the type of fracture from shear to cleavage, caused no significant increase or decrease in the energy absorption but made the unit energy gradients steeper in the region of the opening.

These conclusions suggested the nature of the subsequent program. The present investigation has had these additional objectives:

1. To analyze both the unit distortional energy and the true stresses in a plate with a circular unreinforced opening and to correlate these data with the elastic stresses computed by the mathematical solutions available for this problem.

2. To determine both the unit strain energy and the true stresses in plates with a sharp notch, the square opening, and to correlate the data with the results obtained with much less severe notches, the circular opening and the square opening with rounded corners.

3. To prove the applicability of the methods of plastic analysis to the case of a specimen with welded reinforcement both at room and at low temperature.

The theoretical and experimental data of this report will be presented in the following general order:

1. Elastic stress distribution in plates with openings.

2. Plastic stress distribution in plates with openings.

3. Plastic energy distribution in plates with openings.

The data for Specs. No. 37, 38A, and 38 from the Second Progress Report[2] have been used in this report wherever correlation with the present test results was desirable.

III. TESTS OF PLATES WITH OPENINGS

1. Details of Specimens.

The specimens covered by this report and described in Table I and Figs. 1--4 were fabricated from the same Steel U as-rolled as was used for the previous tests. The plates from which the details of each specimen were cut are given in Table II, and their mechanical properties in Table III.

The methods of fabrication and testing have been previously described[1,2]. The welds between the body plate and the reinforcement, designed for 100 per cent efficiency, were in accordance with Navy Specification Navship 451. The welding electrode met AWS Specification E-6010.

TABLE I

DESCRIPTION OF SPECIMENS WITH 9 in. x 9 in. OPENINGS
WITH 1-1/8 in. CORNER RADIUS

Spec. No.	Size of Reinforcement In.	Percentage Of Reinforcement	Cross - Section Area - Sq. Inch Gross	Net	Testing Temp. deg F
37	None	0	18.00	13.50	76
38A	None	0	18.00	13.50	0
38	None	0	18.00	13.50	-20
69	None None	0	18.00	13.50	76
70	12-3/4 x 12-3/4 x 1*	39	24.00	21.38	76
71	12-3/4 x 12-3/4 x 1*	39	24.00	21.38	-46
95	None	0	18.00	13.50	76
96	None	0	18.00	13.50	-46

* Insert Plates

TABLE II

LIST OF PLATES USED FOR FABRICATION OF EACH SPECIMEN

Spec. No.	Plate No. Used For:	
	Body Plate	Reinforcement
37	26	--
38A	4	--
38	4	--
69	3	--
70	3	10
71	3	10
95	1	--
96	1	--

TABLE III

MECHANICAL PROPERTIES OF PLATES OF DIFFERENT THICKNESSES
SEMI-KILLED STEEL U AS ROLLED

Plate No.	Plate Thickness	Testing Temp.	Tensile Properties*				Tear-Test Transition** Temperature
			Upper Yield Point	Ultimate Strength	Elong. in 8 in.	Red. of Area	
	in.	deg F	psi	psi	per cent	per cent	deg F
1	1/2	76	36,600	62,400	27.8	55.8	
1	1/2	-46	42,300	69,900	23.4	51.2	
3	1/2	76	34,900	61,200	32.9	61.9	
3	1/2	-46	44,100	71,400	29.1	55.8	
4	1/2	76	34,900	60,200	32.2	60.7	40
4	1/2	-20	40,700	66,300	32.1	56.8	
10	1	76	32,800	61,100	32.6	55.6	120
26	1/2	76	36,900	62,300	29.7	79.7	

* Standard ASTM flat tensile coupons of full plate thickness used for tensile tests.
** Determined by Navy tear-test specimens of full plate thickness.

Chemical analysis of Steel U as Rolled:

C	Mn	P	S	Si
0.23	0.50	0.053	0.051	0.07

TABLE IV

STRENGTH AND ENERGY ABSORPTION OF 36" x 1/2" AND 48" x 1/2" PLATES WITH OPENINGS AT ROOM AND AT LOW TEMPERATURE

Spec. No.	Per Cent of Reinf.	Test Temp. deg.F	Fracture* Per Cent C	S	Unbroken	General Yielding- Load kips	Ave. Stress Gross ksi	Net ksi	Ultimate Strength Load kips	Ave. Stress Gross ksi	Net ksi	Energy Absorp.** To Ultimate 1000's	To Failure In.Lbs	Nature of Final Fracture
36" x 1/2" Body Plate. No Reinforcement.														
37	0	76	0	54	46	450	25.0	33.3	800	44.5	59.3	1700	2179	Thru Opening
38A	0	0	87	13	0	500	27.8	37.0	898	49.9	66.5	2890	3470	Thru Opening
38	0	-20	91	9	0	500	27.8	37.0	915	50.8	67.7	2778	2778	Thru Opening
69	0	76	0	67	33	500	27.8	37.0	845	47.0	62.5	1739	2533	Thru Opening
95	0	76	0	89	11	547	26.5	35.4	710	39.4	52.6	1100	1597	Thru Opening
96	0	-46	100	0	0	550	30.6	40.7	648	36.0	48.0	486	486	Thru Opening
48" x 1/2" Body Plate. Insert Plate Reinforcement.														
70	39	76	1	50	49	800	33.3	37.6	1276	53.1	59.7	3362	3699	Weld to Rein.
71	39	-46	100	0	0	800	33.3	37.6	1176	48.8	55.0	2084	2084	Thru Opening

* Proportion in per cent of total net cross-section area at fracture surface including fracture and unbroken section, if any. C = Cleavage. S = Shear.

** 36-in. gage length for 36" x 1/2" plates. 48-in. gage length for 48" x 1/2" plates.

2. Methods of Plastic Analysis and Calibration Tests.

A description of the application of Nadai's octahedral theory to the determination of the unit energy distribution in notched plates, as well as the tangent method of plastic stress analysis and its derivation, was given in the Second Progress Report[2]. Both methods utilize the measured strains in the plastic range of the material. The data of the calibration tests are given in Appendix A.

3. General Behavior during Test and Fracture of Plates with Openings.

A comparison of the applied load and the average elongation on a gage length equal to the half-width of the plate for these plates is shown in Figs. 9 and 10. This gage length extended vertically upwards from the transverse centerline of the specimen and enclosed the area in which the grid of slide-wire resistance gages was mounted. Thus the area under these load-average elongation curves up to a particular load represents the same quantity of energy as was obtained by the application of the octahedral theory to the elongations measured by the grid system at that load.

It is interesting that a change in the mode of fracture from shear to cleavage was accompanied by little change in the load-average elongation curves for the plates with the less severe stress-raisers, such as the circular opening and square opening with rounded corners. In contrast a drastic change occurred in the shape of the load-average

elongation curves and thereby a large reduction of energy absorption in the case of the sharp stress-raiser, the square opening. This observation suggests the manner in which the plastic energy absorption and the subsequent type of fracture were related to the degree of triaxiality of the stress condition at the notch.

Photographs of Specs. No. 69, 70, 71, 95 and 96 after failure are shown in Figs. 11 and 12. The deformation and fracture of Specs. No. 69, 70 and 71 were described in the Third Progress Report[3], and the reader is referred thereto for a more complete discussion of these points.

The data of these tests are summarized in Table IV.

IV. ELASTIC STRESS DISTRIBUTION IN PLATES WITH OPENINGS

The elastic stress distribution was computed by theoretical formulas wherever a solution was available for a case similar to or like that of the test specimens. The theoretical stresses and the experimentally measured unit strains could then be compared. The stresses were computed for the following five cases:

a. A plate of infinite width with a circular opening.

b. A plate of finite width with a circular opening, the width being four times the diameter of the opening. The proportions of this plate were the same as those of Spec. No. 69, for which an experimental stress

analysis was made in both the elastic and the plastic ranges.

c. A plate of infinite width with a square opening with rounded corners, similar to Specs. No. 4 and 38A of the First and Second Progress Reports[1,2], whose width was four times the diameter of the hole.

d. A plate of infinite width with a circular opening reinforced with a face-bar reinforcement, similar to Spec. No. 5 of the First Progress Report[1], whose width was four times the diameter of the hole.

e. A plate of infinite width with a circular hole reinforced with an insert plate, similar to Spec. No. 17 of the First Progress Report[1], whose width was four times the diameter of the hole.

Sketches of these plates are shown in Figs. 1, 3, 13, and 14.

The results are presented as elastic unit stress or unit strain contours in Figs. 15 to 25, in which only the stress or strain component parallel to the direction of loading is shown. The theoretical background of and formulas for the stress computation are not given in this paper. The reader is referred to References 5 to 9, inclusive, in the Bibliography.

If the theoretically computed elastic stress concentration contours for unreinforced plates in Fig. 15, 16, and 18 are compared, a number of points of similarity may be noted.

The stresses some distance from the opening in these particular cases are not substantially affected either by the shape of the opening or the width of the plate. The contour for unit stress concentration lies at almost the same angle and in almost the same location for all of these cases. At the edge of the opening the maximum stress concentration of 3.00 for the plate of infinite width with a circular opening in Fig. 15 increases to only 3.23 when the plate width is decreased to four times the diameter of the opening (Fig. 16). The maximum stress concentration for the plate of infinite width with a square opening with rounded corners in Fig. 18 is 3.09, and for a plate width of four times the width of the opening would be somewhat greater. Thus for plate widths greater than about four times the diameter of the opening and for a corner radius of the opening greater than about one-eighth the diameter of the opening, the theoretical elastic stress distributions are very similar, and the maximum stress concentration varies only between the limits of 3.00 and a maximum slightly greater than 3.23. This similarity with respect to both stress distribution and stress concentration factor explains why both the energy absorption and the ultimate strength of the plates in the First Progress Report[1] with a circular opening and a square opening with rounded corners having a radius of D/8 were essentially of the same order of magnitude.

The experimentally determined unit strain concentration contours in Figs. 17 and 19 were in good agreement with the theoretically computed stress contours in Figs. 16 and 18. Some allowance must be made in comparing Figs. 18 and 19, since the experimental results were obtained for a plate of finite width and the theoretical values for a plate of infinite width.

When the experimentally determined unit strain contours in Figs. 20 and 21 for the square opening with the 1/32-in. corner radius are compared with the similar plot in Fig. 19 for the square opening with the rounded corner, it may be seen that the high values of strain were concentrated more closely around the opening in the two plates with the sharp corner radius. The maximum value indicated was computed from the reading on a SR-4 gage of 1/4-in. gage length located as close as possible to the point where the maximum was expected. Consequently the value shown here may be somewhat smaller than the true maximum.

The effect of reinforcement upon the stress or strain distribution is shown in Figs. 22--25. It would appear that the Beskin solution[6] for these two cases gives a fairly good picture of the elastic stress distribution and the maximum elastic stress concentration.

When Figures 22 and 24 are compared with Fig. 15, it may be seen that the stress concentration contours in the

plates with reinforcement around the opening because of its greater stiffness restrains the boundary of the opening and develops transverse tensile stress in the region of the weld between the reinforcement and the body plate above and below the opening, where compressive stress would be present in an unreinforced plate. In the case of certain types of reinforcement which have relatively high rigidity, a different approach to the analysis of the stresses in the body plate may be advisable. The reinforcing ring in such cases should perhaps be considered as a rigid inclusion restraining the circumferential deformation of the opening in a manner which according to Reference 8 in the Bibliography brings about very high shear stresses in the body plate. These high shear stresses are located at the corners in the case of a square opening with rounded corners. The fact that in previous tests[1] the plates with face bars having the larger percentage of reinforcement broke in the weld in a fashion indicating high shear stresses in this location points to the need for additional theoretical work along these lines.

V. PLASTIC STRESS DISTRIBUTION IN PLATES WITH OPENINGS

The stresses in the plastic range of the steel were computed from the measured strains by the tangent modulus method of stress analysis first described in the Second Progress Report[2]. The stress concentration contours and

distributions in Figs. 26--43 show the ratio of the true stress at any point in the y-direction, the direction of loading, to the uniform true stress on the gross area of the specimen in a region remote from the opening. Contour maps at a number of loads in the plastic range were plotted for Specs. No. 69, 37, 38, 70, 71, 95, and 96; but only one or two of these are shown for each plate, one of which is for maximum load, the instant at which fracture was initiated.

When the elastic stress concentration contour maps in Figs. 15--25 are compared with those in the plastic range, a number of similarities may be seen. The pattern of the contours, the distribution of the high and low values, and the location of the stress concentration contour of unit value are very much alike for the same type of specimen. Moreover, the shape of the opening affected the contours only in the vicinity of the opening. The general similarities between the elastic and the plastic stress distributions substantiate to some degree the common assumptions of the theory of plasticity that the principal stress directions and the general stress pattern are not changed by the transition from the elastic to the plastic state.

The effect of increasing the plastic stress level upon the values of the stress concentrations was a tendency of the stresses to approach uniformity. The maximum stress concentration, commonly called the stress concentration factor,

is compared with the percentage of the ultimate load in Fig. 44. In these plots the experimental value of the elastic stress concentration factor has been plotted at the relative load at which general yielding began. It was found that the plastic stress concentration factors for the plates with the circular or the square opening with rounded corners, Specs. No. 37, 38, 69, 70, and 71, plotted as one family of curves, one curve for unreinforced plates and one for reinforced plates, regardless of the type of fracture. In Section IV of this report in Figs. 15--19, it was found that the elastic stress concentration factor and the elastic stress distribution were quite similar for the circular opening and the square opening with the rounded corner. It is not surprising therefore that the stress concentration factors in the plastic range were closely similar.

However, a different curve resulted for Specs. No. 95 and 96 with the square opening. In the case of this sharper corner, the plastic stress concentration factor fell off much more rapidly than for the less severe corner radii, and this reduction took place closer to the maximum load.

The stress concentration factor was always maximum in the elastic range, decreased as the plastic stress or load level increased, and approached a constant and also a minimum value as the ultimate strength of the plate was reached. That is, fracture began when the stress concentration factor approached a constant value, which was also a minimum value. This observation

suggests that perhaps the low-energy cleavage fracture of some welded elements, which is often accompanied by low ultimate strength, may result in part because the amount of plastic flow which has occurred is not large enough to bring about a sufficient reduction in the plastic stress concentration factor.

The plastic stress distribution shown in Figs. 26--43 was examined with the view of determining whether it may be correlated with the type of fracture in any way. A statistical analysis in the gaged area of the frequency of the various values of stress concentration is shown in Fig. 45, which compares the results for a shear fracture with those for a predominately cleavage fracture, both for reinforced and unreinforced plates.

The manner in which this analysis was developed will be explained. The gaged area referred to is the area of the specimen covered by the grid-wire system as shown in Figs. 6--8. For example, in the plot for Spec. No. 37 at the top of Fig. 45, approximately 3 per cent of this gaged area developed a stress concentration of 0.4, 19 per cent of the area 0.8, and so on. Thus Fig. 45 is a distribution curve with respect to stress concentration and indicates what proportionate parts of the specimens were under either high or low values of plastic stress.

In each comparison in Fig. 45 are shown the analyses for a room temperature specimen and an identical low-temperature specimen, where the predominate mode of fracture was shear in the former and cleavage in the latter. In this figure when

the analyses for the two identical specimens tested at the two temperatures are compared, it may be seen that a larger portion of the area in the low-temperature specimen developed the lower values of stress concentration, while a correspondingly smaller area developed the higher values. The specimens sustaining a predominately cleavage fracture did not produce the same plastic stress distribution as those with a shear fracture. For the plates with a cleavage mode of fracture, the higher plastic stresses were concentrated in a smaller region around the opening; that is, the stress gradients were steeper. Cleavage fracture was accompanied by a less efficient stress distribution in the plastic range than shear fracture.

When the true stresses on any transverse cross-section of the specimen were summed up with due respect to the plate thickness, the resultant was the total force on the cross section. A comparison of the values obtained in this manner with the testing machine load is given in Table V. Agreement within fifteen per cent was attained for most of the computed values.

It would be well to analyze the principal sources of error in the plastic stress analyses. These are as follows:

1. The minimum of the two biaxial stresses frequently fell in the incipient yield range where the values of the tangent modulus and Poisson's ratio were uncertain.

TABLE V

COMPARISON OF LOAD COMPUTED FROM
TRUE STRESS DISTRIBUTION AND TESTING MACHINE LOAD

Spec. No.	Machine Load kips	Computed Load at Cross Section, kips* A	B	C	D
	Distance of	3 3/4"	5 3/4"	7 3/4"	9 3/4"
37	800	897	750	784	720
38	915	1060	1126	1100	1016
	Distance of	1 1/2"	4 3/4"	7 1/4"	9 3/4"
69	650	642	770	750	700
	845	1053	1010	990	944
95	575	507	597	458	450
	710	836	985	902	858
96	568	542	551	557	553
	648	662	620	564	535
	Distance of	2 3/4"	7 1/4"	12 3/4"	18 1/4"
70	1150	1140	1200	1120	1130
	1276	1380	1500	1450	1520
71	1150	1096	1290	1250	1199
	1176	1052	1202	1126	1069

* Distance of cross section measured from transverse centerline of specimen, which is also the horizontal axis of the opening.

2. The assumption that the x- and y-directions were principal directions was more in error, the closer the gage point was to the opening. The poorest correlation between the testing machine load and the computed load was usually found on cross sections near or through the opening where the deviation of the principal directions from the coordinate axes was greatest.

3. The selected cross sections of the specimen, which were initially straight lines, became considerably distorted as the maximum load was approached. Integration of the values along this somewhat curved cross section produced an error, since no correction for the shear stresses thus introduced was made.

4. The slid-wire grid system, which was designed for large strains, was not sensitive to an elongation in any gage length smaller than 0.001 inches. The sensitivity of the system was therefore in the yield range of the material.

After a review of the errors in the computed values, it appeared that the preceding reasons were responsible for the errors and not some inadequacy of the stress equations themselves.

VI. PLASTIC ENERGY DISTRIBUTION IN PLATES WITH OPENINGS

The unit energy distribution in the vicinity of the opening

was computed by the octahedral theory of A. Nadai[4]. The experimental and analytical procedure was described in the Second Progress Report[2].

Contour maps showing the unit energy distribution in the plastic range appear in Figs. 46--54. Although this analysis was made for each plate at a number of load levels in the plastic range, only a few typical energy contours are shown in this report.

It is interesting to point out that the contour line for the average unit energy absorption in the plastic range, the total energy absorption in the gaged area divided by the volume corresponding to this area, fell in almost the same location in each plate as contour line for unit stress concentration for both the elastic and plastic stress states. Moreover, the higher values of the unit energy absorption appeared in the regions where the higher values of the plastic and elastic stresses occurred, and vice versa.

The maximum unit energy absorption, which always occurred adjacent to the opening, was much greater in the unreinforced plates than in the reinforced plates, as Figs. 46--54 show. It should be pointed out that the grid system of one-inch squares was not fine enough to determine either the exact location or the true value of the absolute maximum. The maximum values in these figures are probably less than the unit energy which existed at the point where fracture was

initiated. Fracture started in these specimens at maximum load.

The Second Progress Report showed that the unit energy absorption u at any point increased in the plastic range in accordance with the empirical equation,

$$u = e^{A + BP},$$

where A and B were numerical quantities and P the applied load. It was observed that A remained almost constant. The significant variable was B, the slope of the semi-logarithmic curve relating u and P. From semi-logarithmic plots of u against P for each point of the grid system, the values of B were obtained. A similar semi-logarithmic plot with respect to the average unit energy absorption u_{Av} for the entire gaged area gave the average value of B or B_{Av}. The ratio B/B_{Av} has been called the relative rate of increase of the unit energy absorption. Maps showing the contours of equal values of B/B_{Av} appear in Figs. 55--61.

The major differences which were found in these figures with respect to the strain energy distribution in the plastic range were:

1. The maximum value of the unit energy absorption at ultimate load was about twice as great in the unreinforced plates as in the reinforced plates.
2. The distribution of the energy was more nearly uniform in the reinforced plates with less of a spread between the maximum and the minimum values.
3. The distribution of the energy over the gaged area was

more nearly uniform in the unreinforced plates with circular openings or square openings with rounded corners than in the unreinforced plates with square openings. A concentration of the high values in the vicinity of the sharp corners of the square opening was noticeable.

When the unit strain energy values for a given load in Figs. 46--54 were integrated, they could be compared, as shown in Table VI, with those values obtained from the load-average elongation curves. Reasonably good correlation was obtained so long as the plastic strains were fairly large. However, poorer agreement occurred in all the plates at low loads where much of the gaged area had not begun to yield and in those plates with the square opening where the yielding was concentrated almost entirely at the corners of the opening. The resistance-wire grid system used to measure the plastic strains was designed to measure large values of strain and was therefore not sufficiently sensitive when yielding was just beginning.

In the plastic stress concentration contour plots in Figs. 29, 31, 34, 36, 39, and 42, and in Fig. 45, it was shown that the plastic stress gradients were steeper in the specimens with a predominately cleavage fracture than in identical specimens with a shear fracture. A similar type of analysis of the unit energy frequency distribution was made for the same specimens and is shown in Figs. 62--64. A similar trend is revealed in that a larger proportion of the area of specimens with a predominately

TABLE VI

COMPARISON OF THE TOTAL ENERGY
OBTAINED BY THE OCTAHEDRAL THEORY AND FROM THE LOAD-ELONGATION CURVE

Spec. No.	Load	Energy by Octahedral Theory			Total Energy by Load-Elong. Curve
		Body Plate	Insert Plate	Total	
	kips	in-kips	in-kips	in-kips	in-kips
37	500	19.4		79.4	60.6
	650	243.0		243.0	270.0
	720	426.0		426.0	452.0
	800	1056.0		1056.0	884.0
38	650	282.9		282.9	225.0
	720	444.5		444.5	370.0
	800	683.8		683.8	638.0
	870	1103.8		1103.8	1021.0
	915	1450.2		1450.2	1389.0
69	650	329.0		329.0	324.0
	720	483.0		483.0	462.0
	800	813.0		813.0	768.0
	845	1237.0		1237.0	1284.0
70	1000	562.0	41.0	603.0	540.0
	1150	947.0	82.0	1029.0	1025.0
	1276	2031.0	197.0	2228.0	1988.0
71	1000	283.0	27.0	310.0	255.6
	1150	850.0	48.0	898.0	742.5
	1176	748.0	715	819.5	787.5
95	575	179.0		179.0	176.0
	700	443.2		443.2	459.0
	710	770.0		770.0	736.0
96	648	227.2		227.2	226.9

cleavage fracture developed the lower values of unit energy than of those with a shear fracture. The gradual development of this divergent behavior as the loads increased may be seen in Fig. 62 for Specs. No. 37 and 38 if the unit energy distribution is examined at the different loads

VII. CONDITIONS FOR THE INITIATION OF FRACTURE

It would be well at this point to examine the experimental data for information pertaining to the initiation of fracture. The simplest of the common theories of fracture assume that fracture begins at a point at the moment a certain limiting value of the principal stress, principal strain, or unit energy characteristic of the material at the given temperature has been exceeded. Such theories, it should be pointed out, do not differentiate between types of fracture, cleavage or shear, or take into account strain-aging and other metallurgical changes in the material.

Data are available herein to examine the applicability of these three simple hypotheses of failure, since the information from which the stress concentration and unit energy contour maps were computed give the observed maximum values of stress, unit strain, and unit energy at ultimate, or maximum load where fracture was initiated.

The maximum true stresses computed from the observed strains were as follows:

Spec. No.	Testing Temp., °F	Percentage of Fracture		Max. True Stress ksi
		Cleavage	Shear	
37	76	0	54	90.0
38	-20	91	9	105.0
69	76	0	67	81.0
70	76	1	50	87.0
71	-46	100	--	81.0
95	76	0	89	90.7
96	-46	100	--	68.5

These are principal stresses at the boundary of the opening. While these values are of the same general order of magnitude, it would not seem that a maximum stress theory could predict failure in these specimens with sufficient accuracy.

The maximum unit nominal strains developed in the unreinforced and reinforced specimens are shown in Fig. 65. The unit strains in the unreinforced plates were approximately double those in the reinforced plates. The plot in Fig. 66 for the unreinforced plates with a square opening indicates that the maximum unit strain for this more severe notch was related to the type of fracture. The maximum unit strain hypothesis of failure would not apply to these specimens.

The maximum unit distortional energy in the specimens is also shown in Figs. 65 and 66. It is obvious that a limiting value of the maximum unit distortional energy would not properly indicate the imminence of failure.

Since the maximum stress occurred at the boundary of

the opening where the stress in the normal direction was zero and the stress in the direction of the thickness of the plate extremely small, the maximum principal shearing stress would be a function of only the maximum stress in the y-direction. Since the maximum stress theory did not hold for these specimens, the maximum shearing stress theory would not apply in this case either.

It would appear that any theory of failure must consider other factors, such as testing temperature, the mechanical and/or heat treatment of the metal, and the anisotropy of the metal, as well as the geometry of the specimen. The maximum stress, maximum unit strain, and maximum unit distortional energy are related to all these factors and not just to the geometry.

The data in this report appear to establish the following facts concerning the conditions for the initiation of fracture:

1. Fracture was initiated when the stress concentration factor for a given specimen was approaching or reached a minimum and constant value.
2. The plastic stress and unit energy gradients were steeper in the specimens with a predominately cleavage fracture than in those with a shear fracture.
3. When the stress-raiser became sufficiently severe, the energy and the strain absorbing capacity of the plates was substantially less in the case of a predominately cleavage fracture than for a shear fracture.

The second and third observations would rule out the possibility that a specimen developing a shear fracture could accurately describe the plastic stress and strain energy conditions of an identical specimen at a temperature which would cause cleavage fracture.

The theories which were used to develop the unit energy and stress distributions in the plastic range are based on the assumption that all stresses and strains are the result of the applied loading. Reasonably good checks were found between the values computed by these theories and the applied load and energy input. Therefore, it would appear that the initial residual stresses from welding have no appreciable effect upon the stress and energy distribution in the plastic range of the material.

VIII. CONCLUSIONS

The following tentative conclusions have resulted from the investigation of plastic energy and stress distribution:

1. The maximum values of elastic and plastic stress, elastic and plastic strain and of unit distortional energy were located at the same point, the point where failure started.
2. Apparently, no theory of failure based upon a limiting value of stress, strain or energy would yield a numerical value accurately indicating the imminence of failure. Such factors as the metallurgical characteristics

and testing conditions should be considered.

3. The effect of increasing the plastic stress level upon the values of the stress concentrations was a tendency of the stresses to approach uniformity. The stress concentration factor was always maximum in the elastic range, decreased as the plastic stress or load level increased, and approached a constant and also a minimum value as the ultimate strength of the plate was reached.

4. The low energy cleavage fracture of some welded elements, which is often accompanied by low ultimate strength, may result in part because the amount of plastic flow which has occurred is not large enough to bring about a sufficient reduction in the plastic stress concentration factor.

5. The effect of low temperature was a steeper gradient of stress and unit energy in the neighborhood of peak values and the occurrence of low values over a larger area of the specimen. Cleavage fracture was accompanied by a less efficient stress distribution in the plastic range than shear fracture.

6. Tests of structural elements resulting in shear fractures would not predict the stress and strain energy distribution of identical elements undergoing cleavage fracture.

7. The addition of reinforcement brought about a more uniform plastic stress and energy distribution, with smaller

differences between the extreme values.

8. The analysis of the stress distribution both in the elastic and the plastic ranges substantiated the theoretical assumption of no change of principal stress directions in the transition from the elastic to the plastic range.
9. The applicability of both unit energy and plastic stress methods of analysis was established in the use of plates with welded reinforcement.

IX. ACKNOWLEDGMENTS

This investigation, at the University of Washington, sponsored by the Ship Structure Committee, is in progress in the Structural Research Laboratory of the Department of Civil Engineering, of which Professor R. B. Van Horn is head. This research program is directed by Dr. R. A. Hechtman, Associate Professor of Structural Research. Dr. D. Vasarhelyi, Assistant Professor of Civil Engineering, the project engineer, was assisted by Mr. Y. T. Yoshimi, Mr. Robert McHugh, and Mr. P. Roy Choudhury.

The authors express their appreciation to Mr. John Vasta of the Bureau of Ships, Navy Department, Dr. Finn Jonassen of the National Research Council, and Dean H. E. Wessman and Professor F. B. Farquharson of the University of Washington for their suggestions and encouragement.

X. BIBLIOGRAPHY

1. D. Vasarhelyi and R. A. Hechtman, "Welded Reinforcement of Openings in Structural Steel Members", First Progress Report, Ship Structure Committee, Serial Number SSC-39, 15 December 1951.

2. D. Vasarhelyi and R. A. Hechtman, "Welded Reinforcement of Openings in Structural Steel Members: A Determination of Strain Energy Distribution and True Stresses in the Plastic Range in Plates with Openings", Second Progress Report, Ship Structure Committee, Serial Number SSC-50, 10 March 1952.

3. D. Vasarhelyi and R. A. Hechtman, "Welded Reinforcement of Openings in Structural Steel Members: Room and Low Temperature Tests of Plates with Reinforced Openings", Third Progress Report, Ship Structure Committee, Serial Number SSC-55, 30 June 1953.

4. A. Nadai, "Energy of Distortion Absorbed by Plastic Deformation of Thin Steel Plates," Research Report SR-182, Westinghouse Research Laboratories, April, 1943.

5. R. C. Y. Howland, "Stresses in the Neighborhood of a Circular Hole in a strip under Tension," Royal Society of London, Phil. Trans., 1930, Vol. 229, p. 49.

6. L. Beskin, "Strengthening of Circular Holes in Plates under Edge Loads," Journ. Appl. Mech., 1944, p. A-140.

7. M. Greenspan, "Effect of a Small Hole on the Stresses in a Uniformly Loaded Plate," Quart. of Appl. Math., April 1944

8. Yi-Yuan Yu, "Solution for the Exterior of a General Ovaloid under Arbitrary Loading," Dissert. PhD, Eng. Mech., Northwestern University, 1951.

9. C. Guerney, "An Analysis of the Stresses in a Flat Plate with Reinforced Circular Hole under Edge Forces," Brit. Res. Memo., No. 1834, 1938.

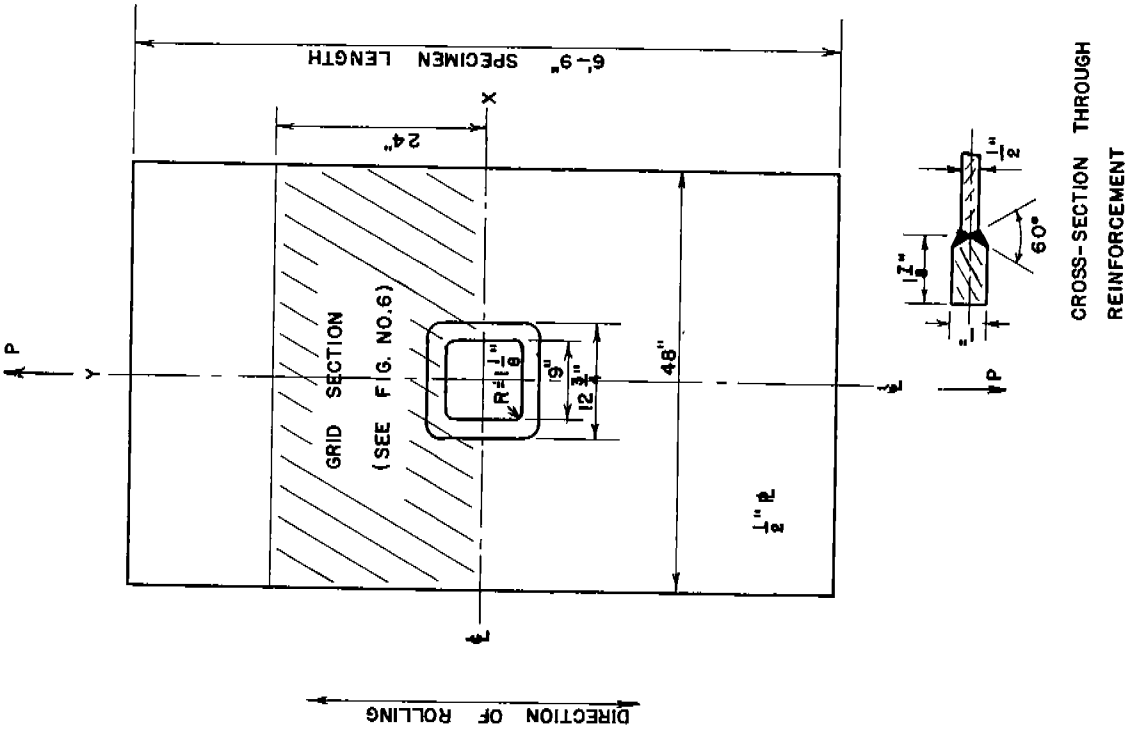

Fig. 2. Plate with Reinforced Square Opening with Rounded Corners. Spec. No. 70 and 71.

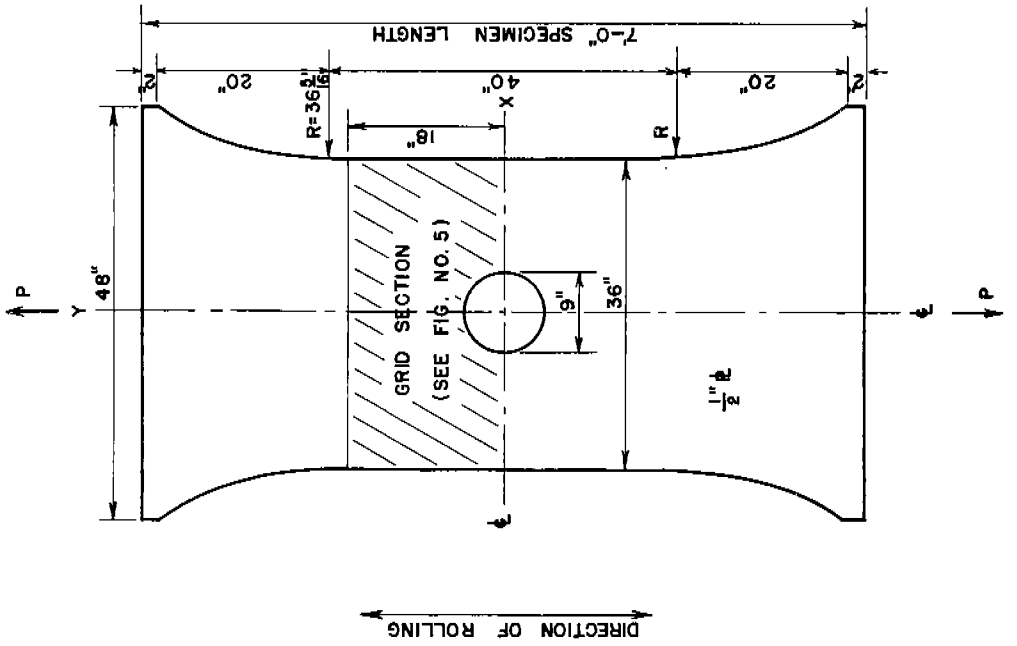

Fig. 1. Plate with Circular Opening. Spec. No. 69.

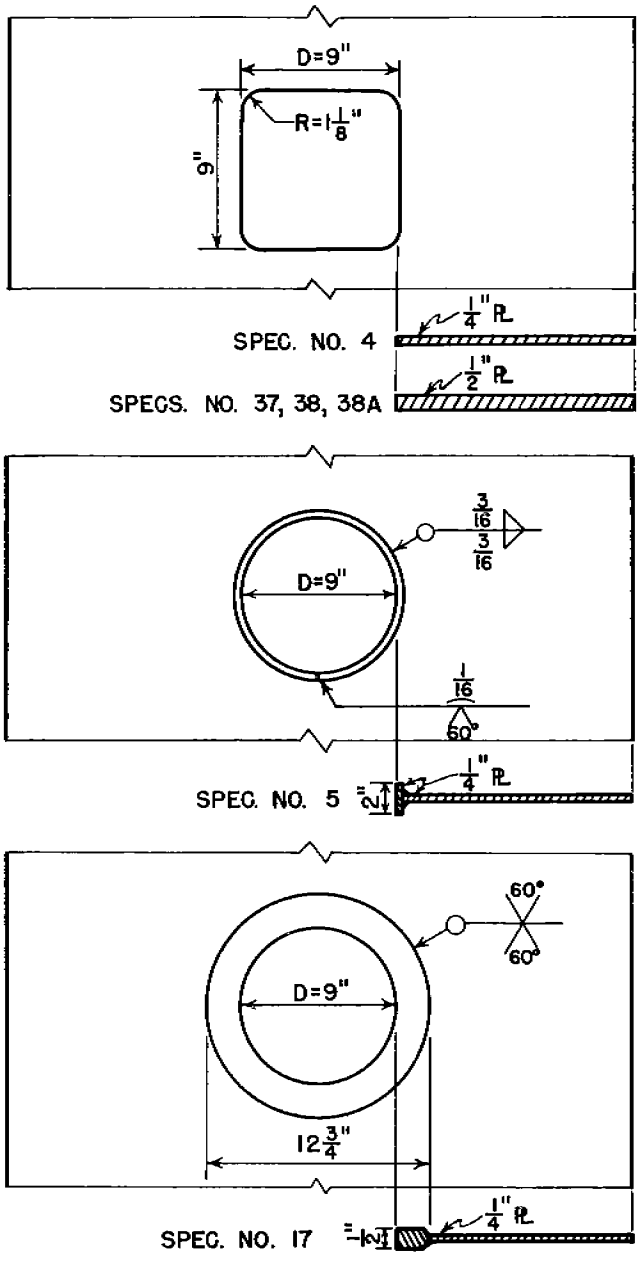

Fig. 3 . Details of Specs. No. 4, 5, 17, 37, 38, and 38A.

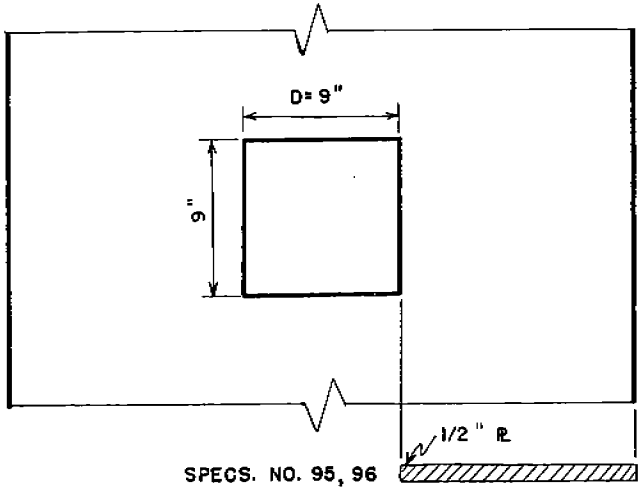

Fig. No. 4 . Details of Specs. No. 95 and 96.

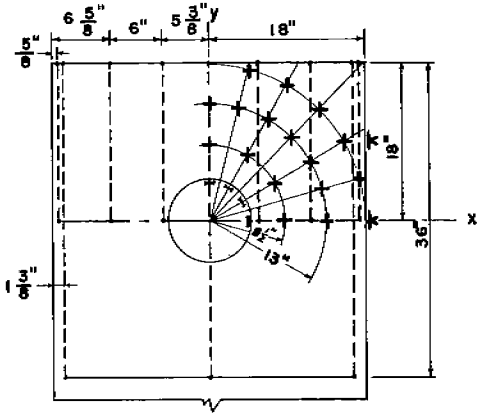

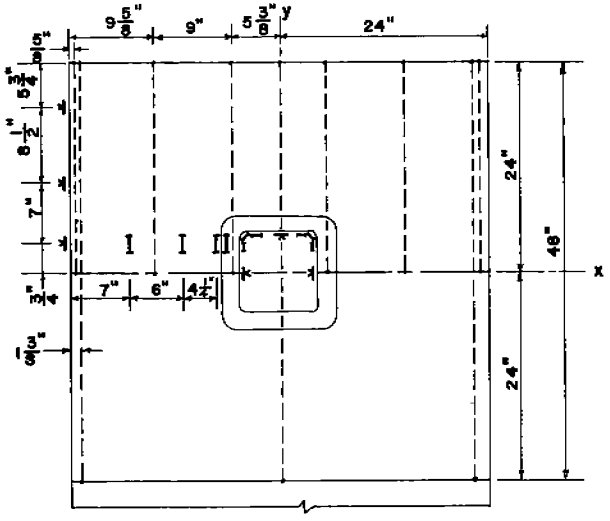

LEGENDS

I	SR-4 STRAIN GAGE TYPE A-7
⊢	SR-4 STRAIN GAGE TYPE A-12
+	SR-4 STRAIN GAGE TYPE AX-5
----	SLIDE-WIRE STRAIN GAGES

Fig. 5 . Location of SR-4 Gages and Slide-Wire Gages.

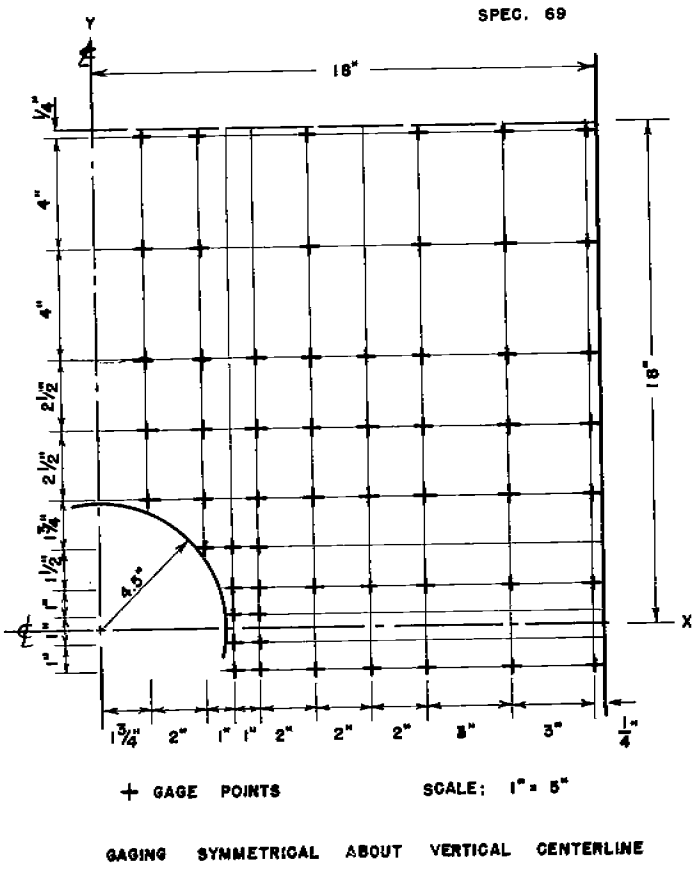

Fig. 6. Arrangement of Grid-Wire Gages for Spec. No. 69.

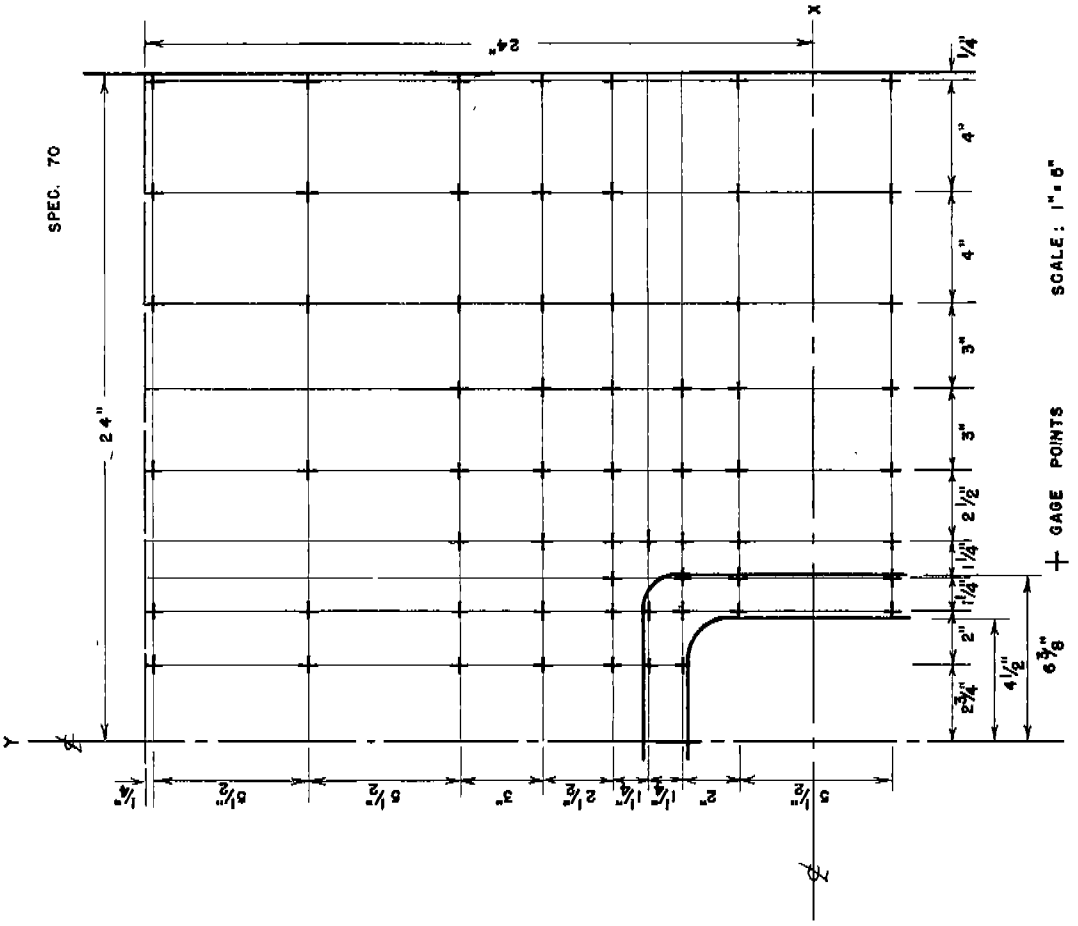

Fig. 8. Arrangement of Grid-Wire Gages for Spec. No. 70. and 71.

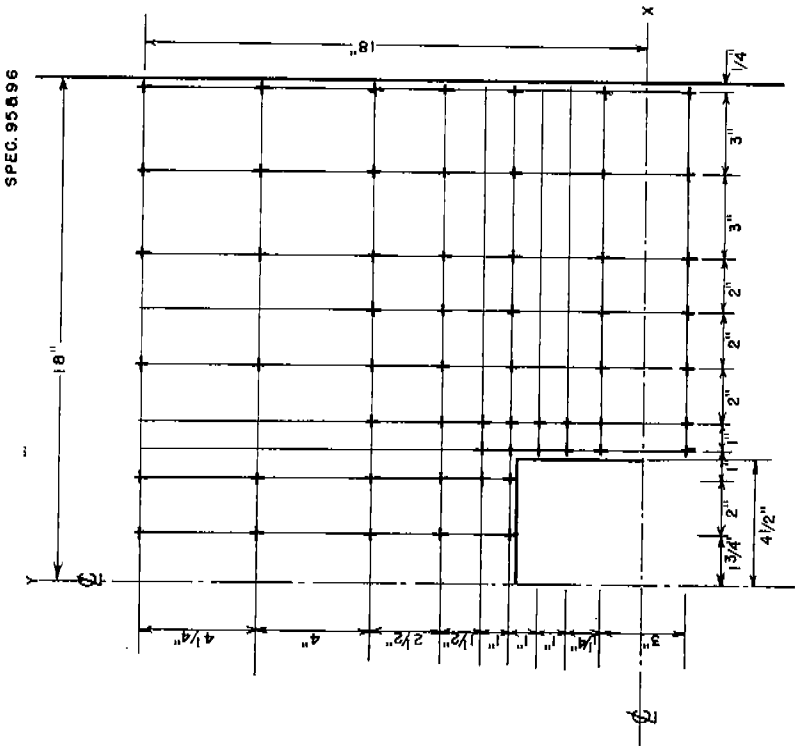

Fig. No. 7 . Arrangement of Grid-Wire Gages for Specs. No. 95 and 96.

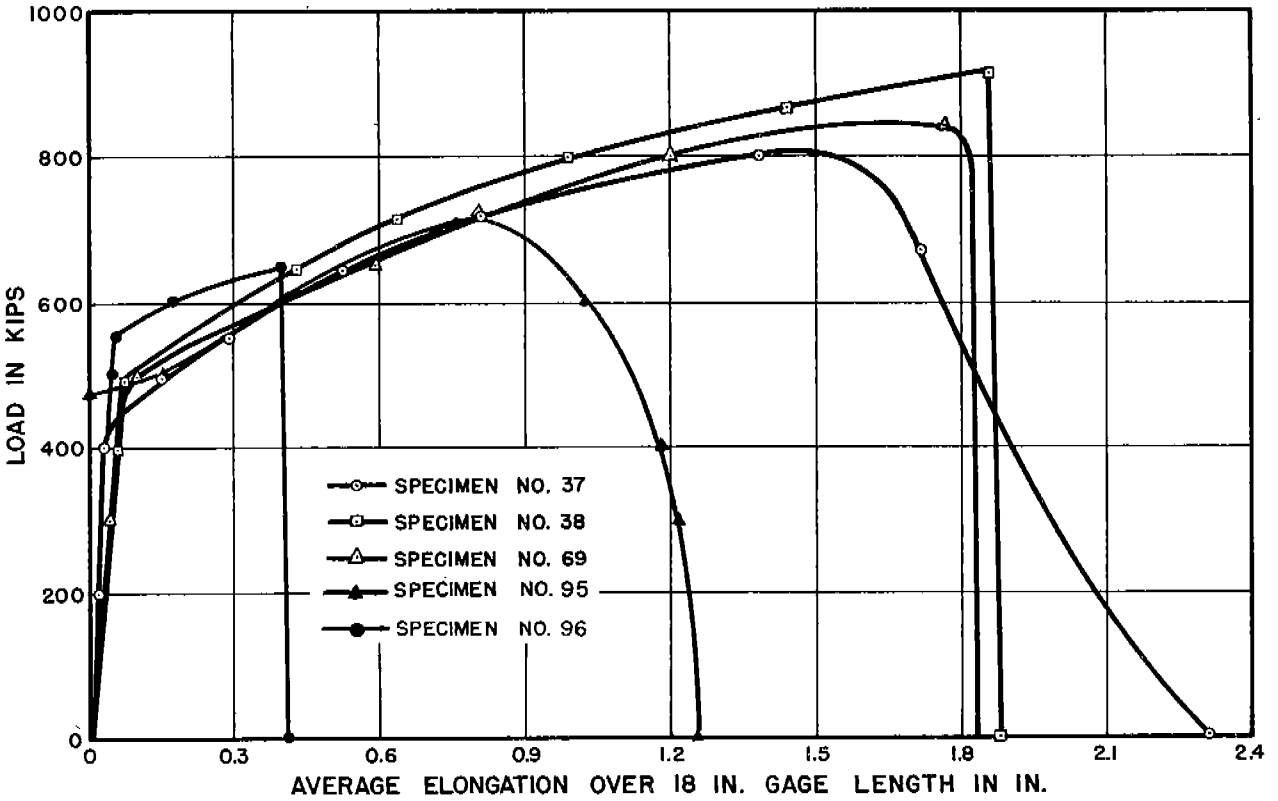

Fig. 9. Load -Average Elongation Curves, Specs. No. 37, 38, 69, 95 and 96.

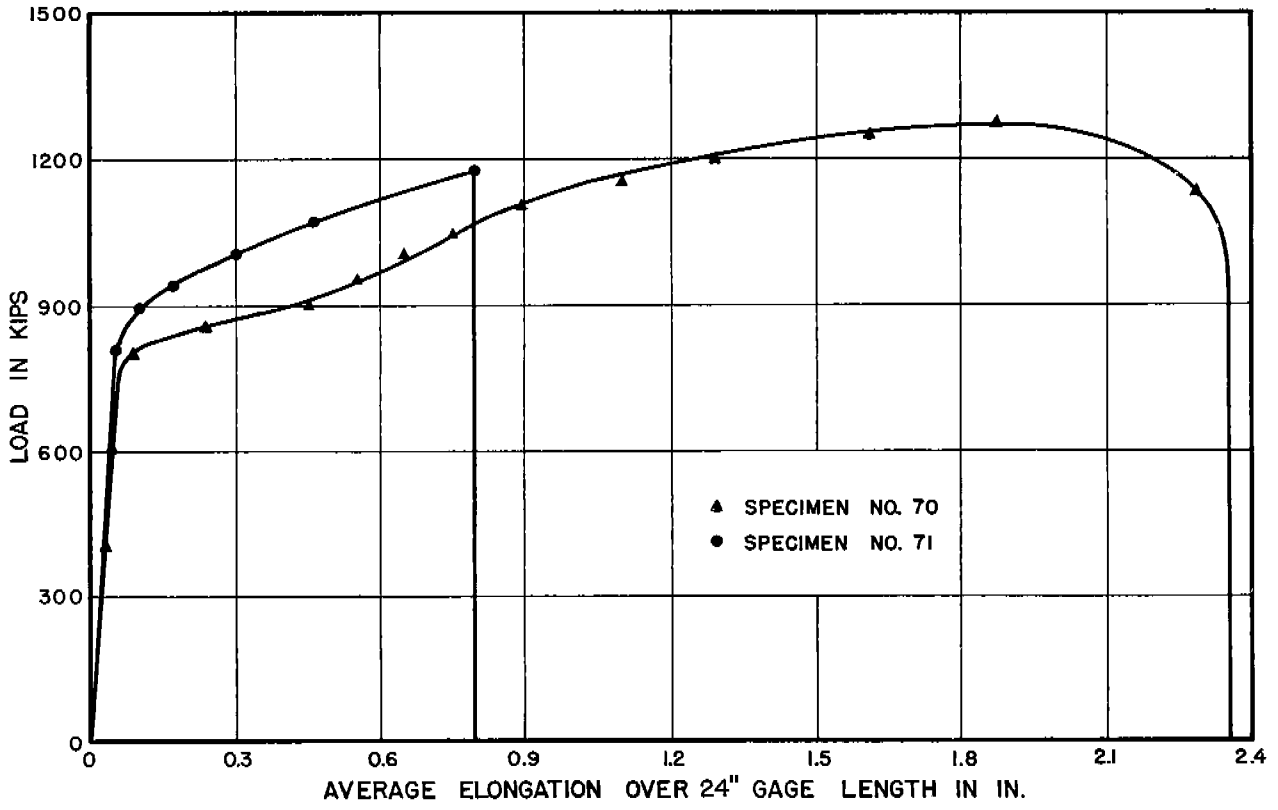

Fig. 10. Load -Average Elongation Curves. Specs. No. 70 and 71.

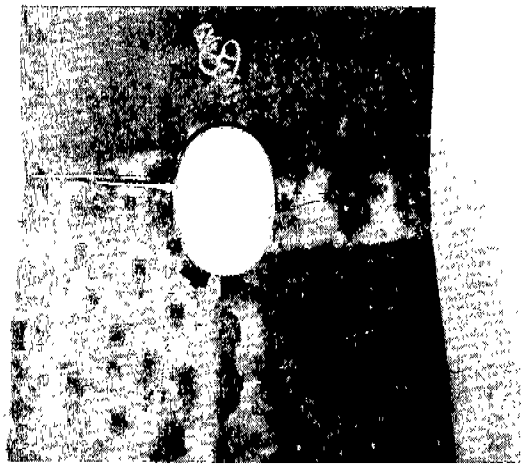

Spec. No. 69

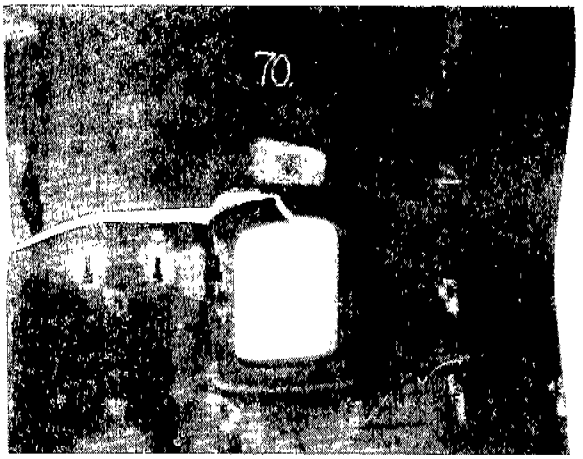

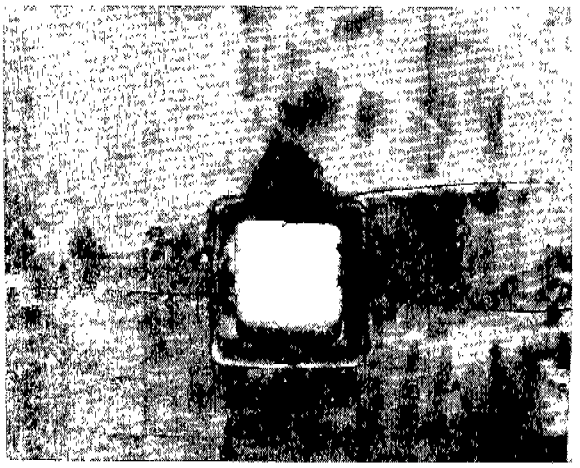

Spec. No. 71

Fig. 11. Photographs of Plates after Failure. Spec. No. 69, 70 & 71.

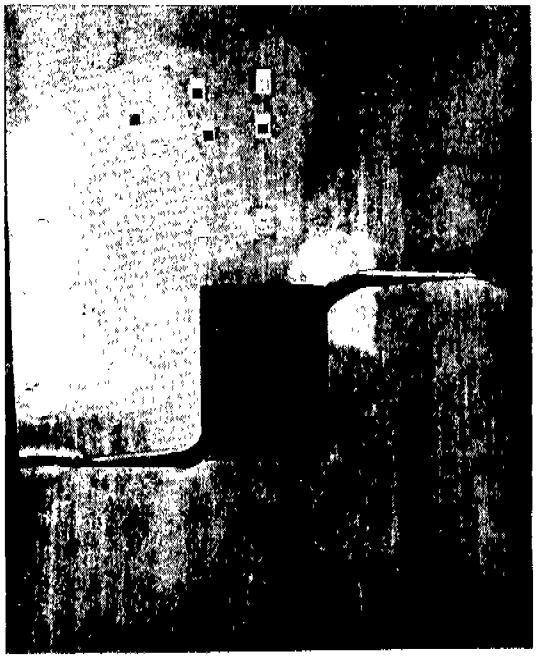

Spec. No. 95

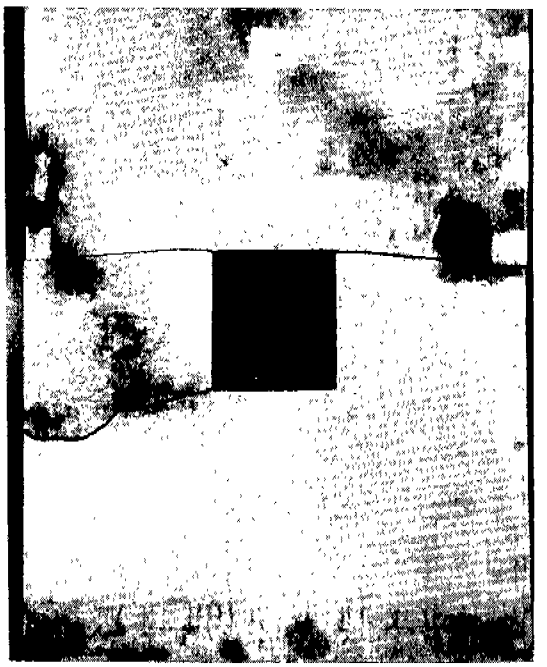

Spec. No. 96

Fig. 12. Photographs of Plates after Failure. Spec. No. 95 and 96.

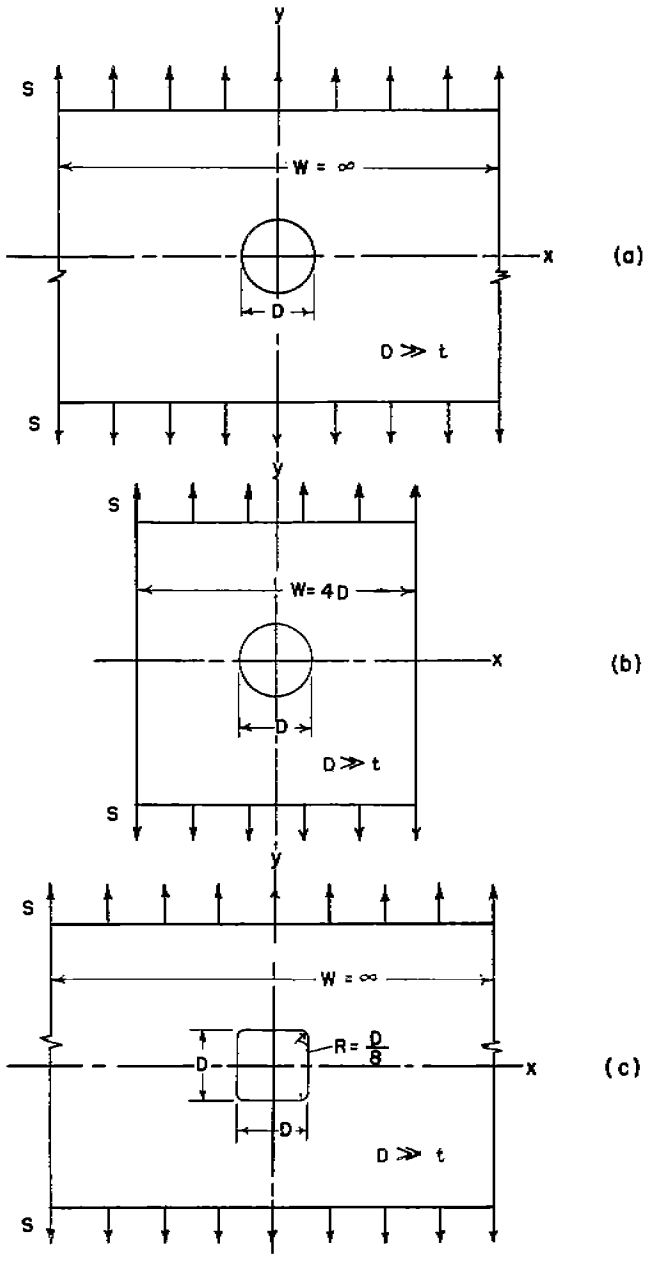

Fig. 13. Particular Cases of Plates with Unreinforced Openings Analyzed by Elastic Theory. Plates (a), (b) and (c).

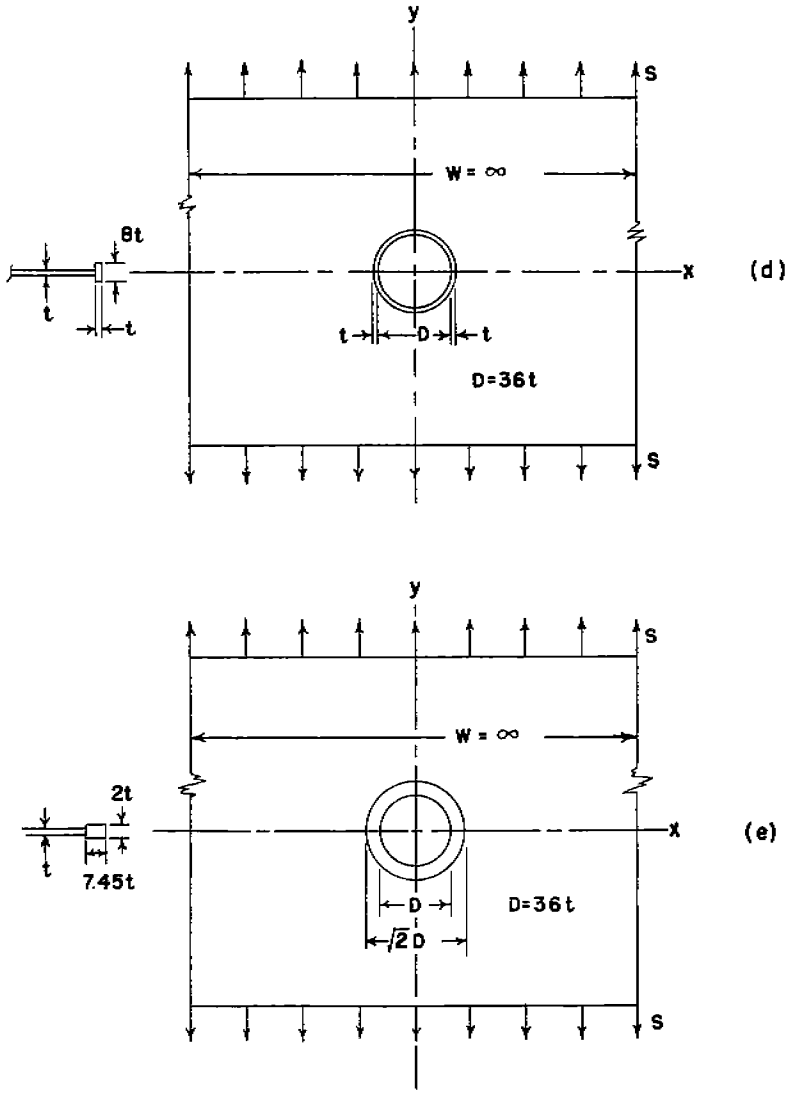

Fig. 14. Particular Cases of Plates with Reinforced Openings Analyzed by Elastic Theory. Plates (d) and (e).

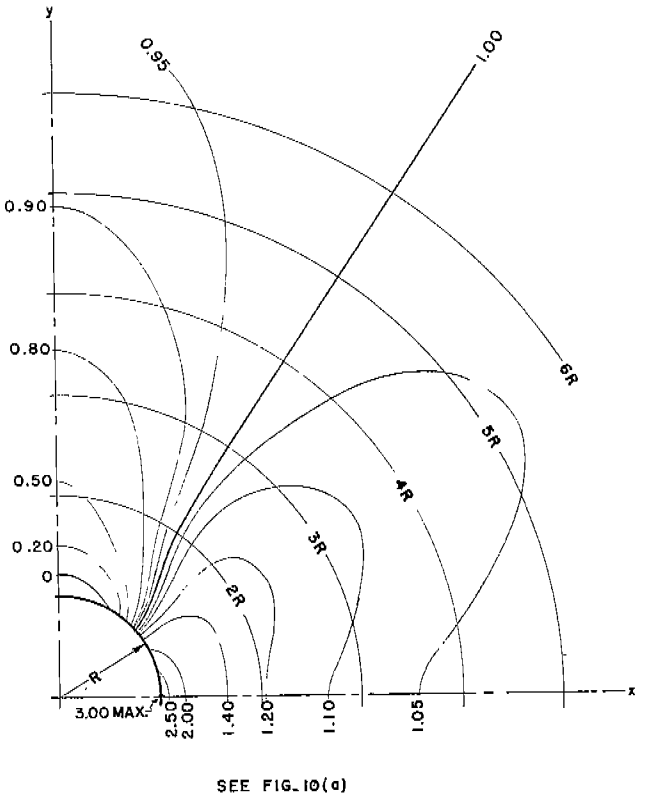

Fig. 15 . Stress Concentration Contours in y-Direction for Plate of Infinite Width with Circular Hole by Elastic Theory. Plate (a).

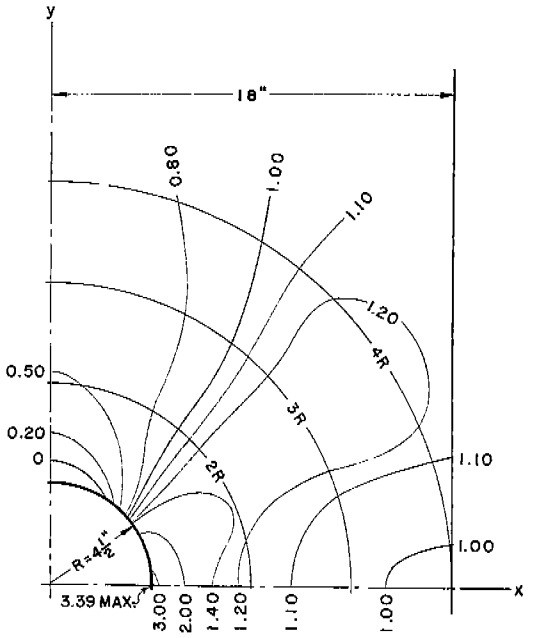

Fig. 17. Elastic Unit Strain Concentration Contours for Plate of Finite Width with Circular Opening Plotted from SR-4 Strain Gage Readings. Spec. No. 69.

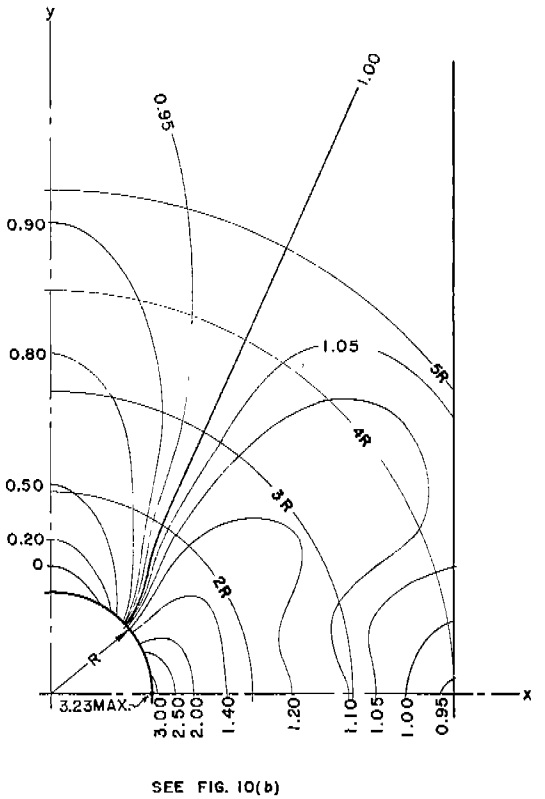

Fig. 16 . Stress Concentration Contours in y-Direction for Plate of Finite Width with Circular Hole by Elastic Theory. Plate (b).

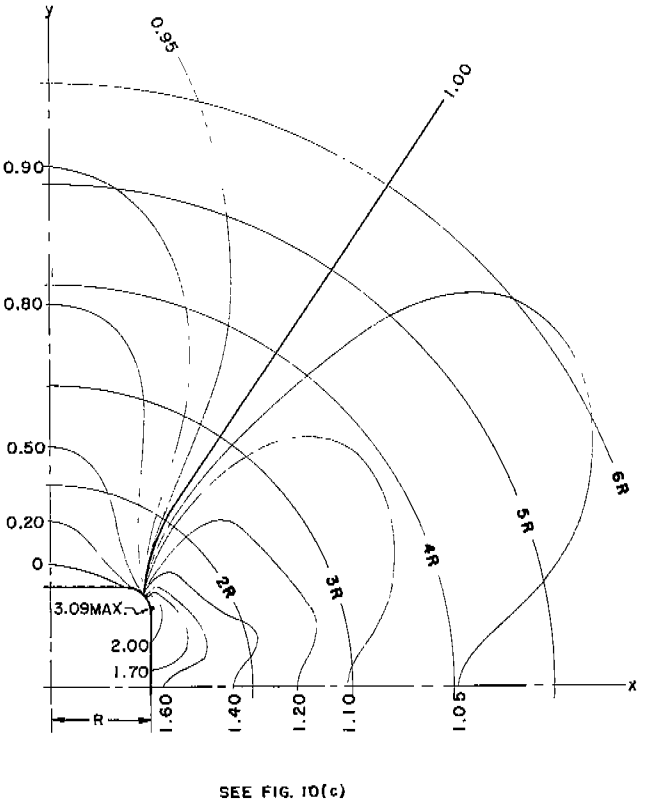

Fig. 18 . Stress Concentration Contours in y-Direction for Plate of Infinite Width with Square Opening with Rounded Corners by Elastic Theory. Plate (c).

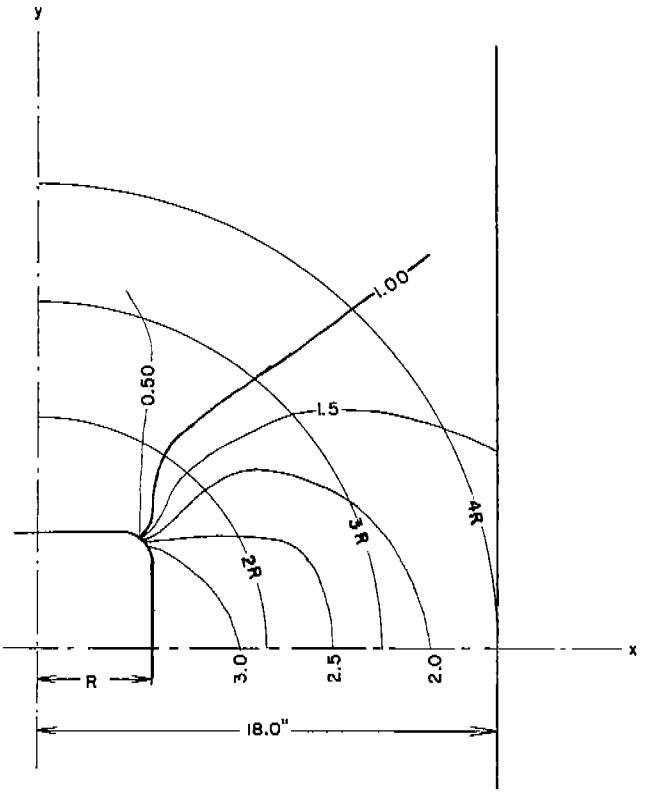

Fig. 19. Elastic Unit Strain Concentration Contours for Plate of Finite Width with Square Opening with Rounded Corners Plotted from SR-4 Strain Gage Readings. Spec. No. 38A.

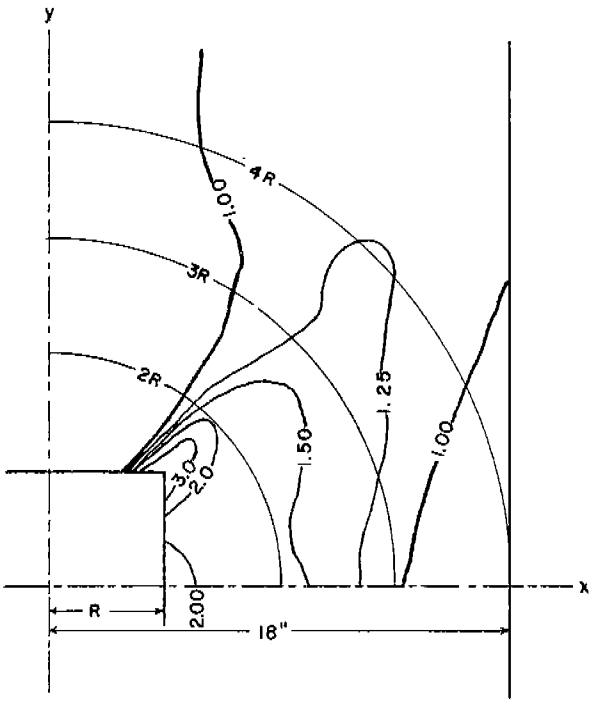

Fig. No. 20. Elastic Unit Strain Concentration Contours for Plate of Finite Width with Square Opening. Plotted from SR-4 Strain Gage Readings. Spec. No. 95. 76 F.

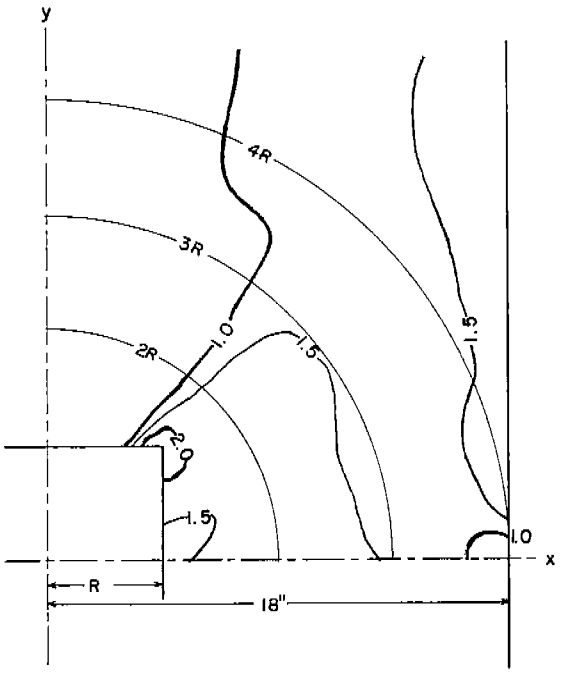

Fig. No. 21. Elastic Unit Strain Concentration Contours for Plate of Finite Width with Square Opening. Plotted from SR-4 Strain Gage Readings. Spec. No. 96. -46 F.

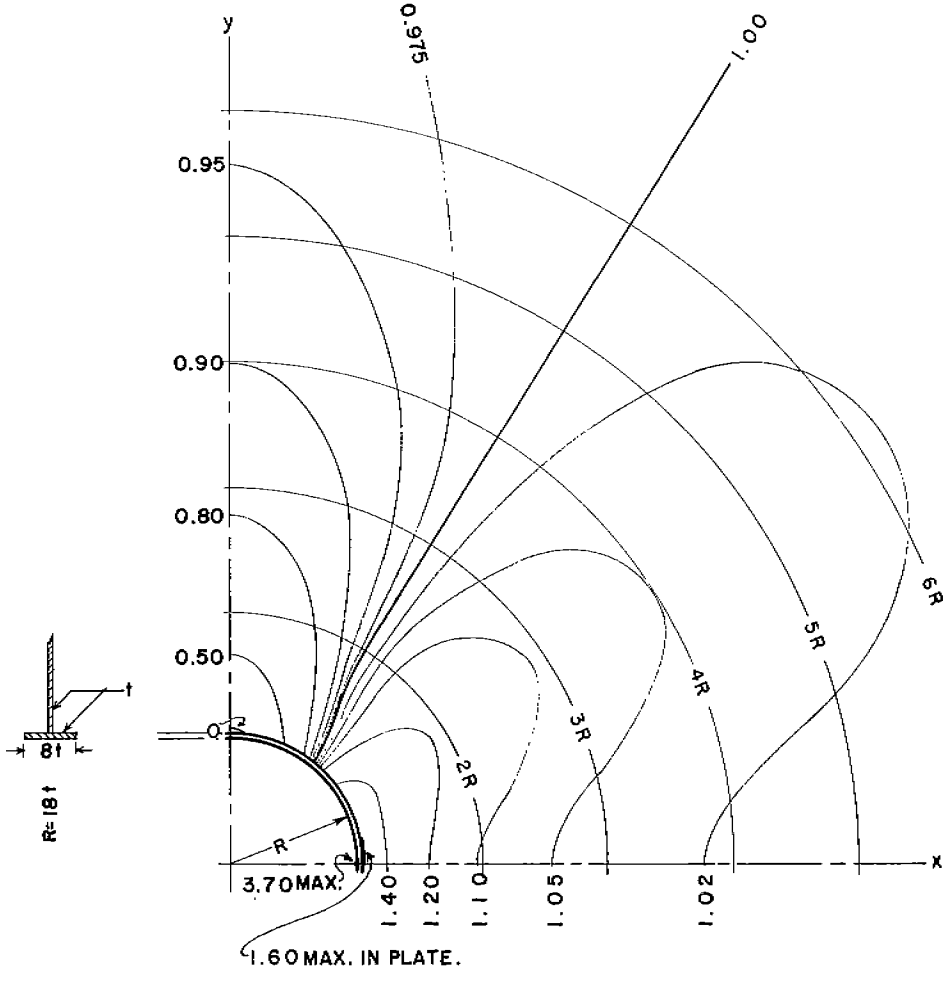

Fig. 22 . Stress Concentration Contours in y-Direction for Plate of Infinite Width with Circular Opening with Face Bar Reinforcement by Elastic Theory. Plate (d).

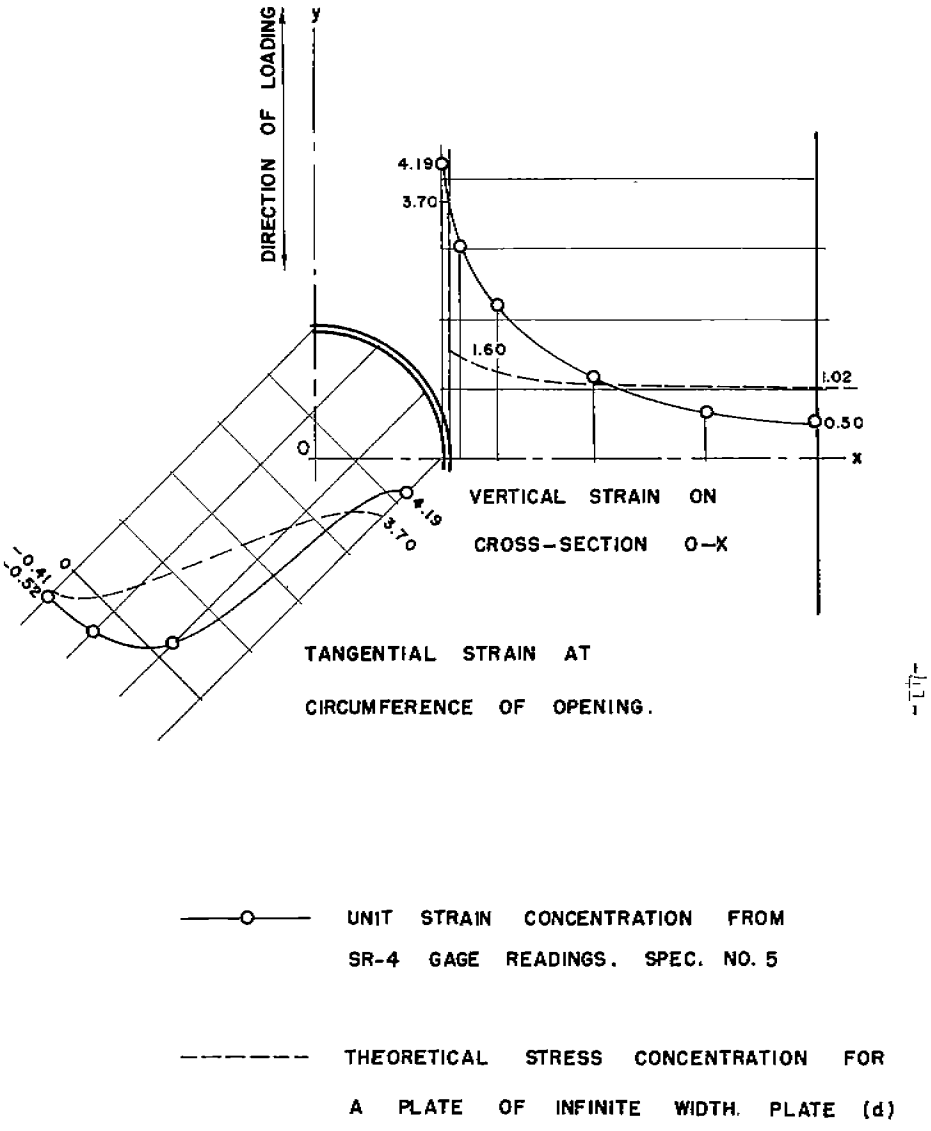

Fig. 23 . Elastic Unit Strain Concentration Curve for Plate of Finite Width with Circular Opening with Face Bar Reinforcement. Spec. No. 5.

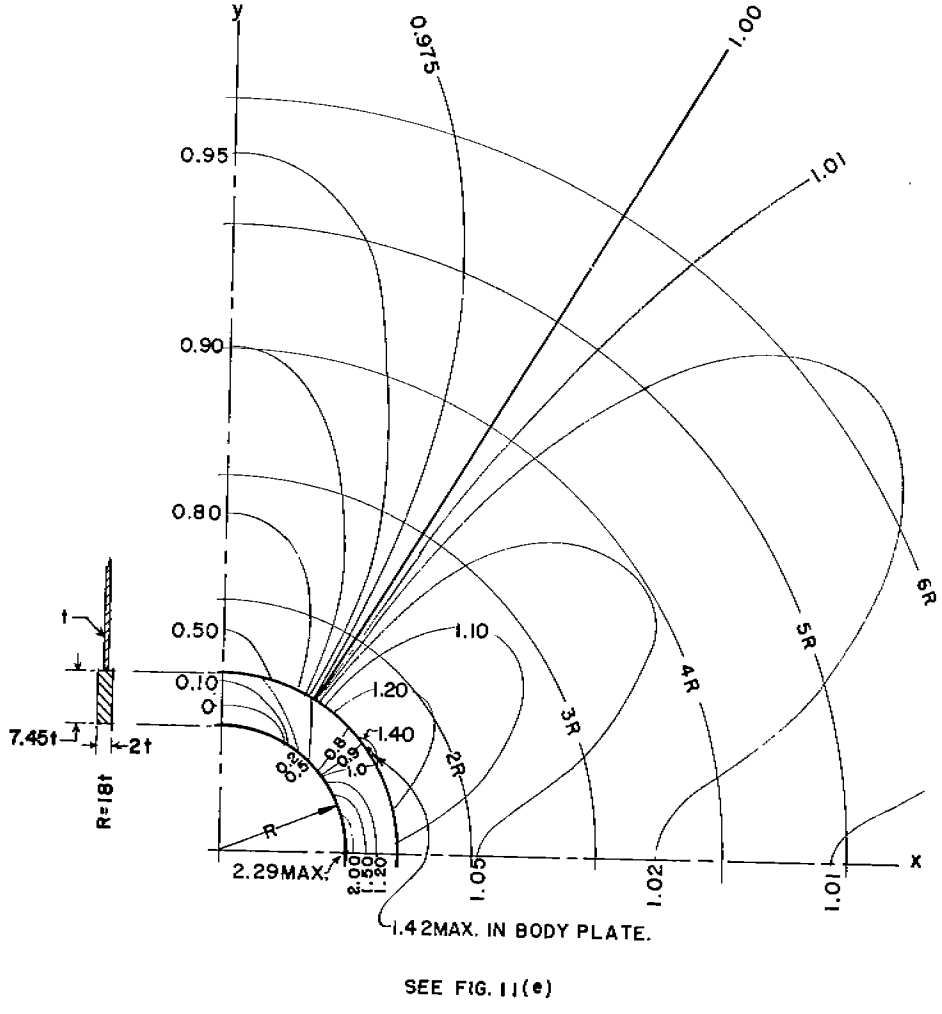

Fig. 24. Stress Concentration Contours in y-Direction for Plate of Infinite Width with Circular Opening with Insert Plate Reinforcement by Elastic Theory. Plate (d).

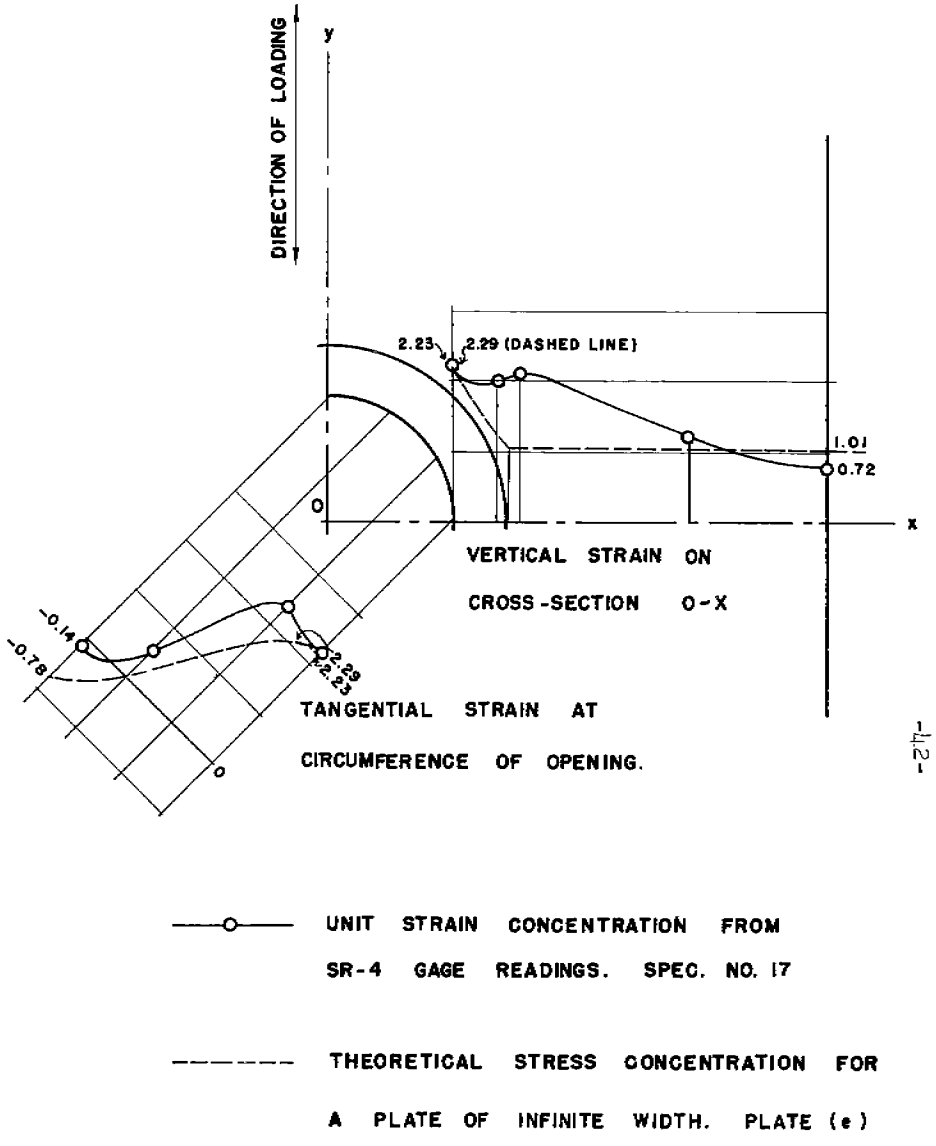

Fig. 25. Elastic Unit Strain Concentration Curve for Plate of Finite Width, Insert Plate Reinforcement. Spec. No. 17.

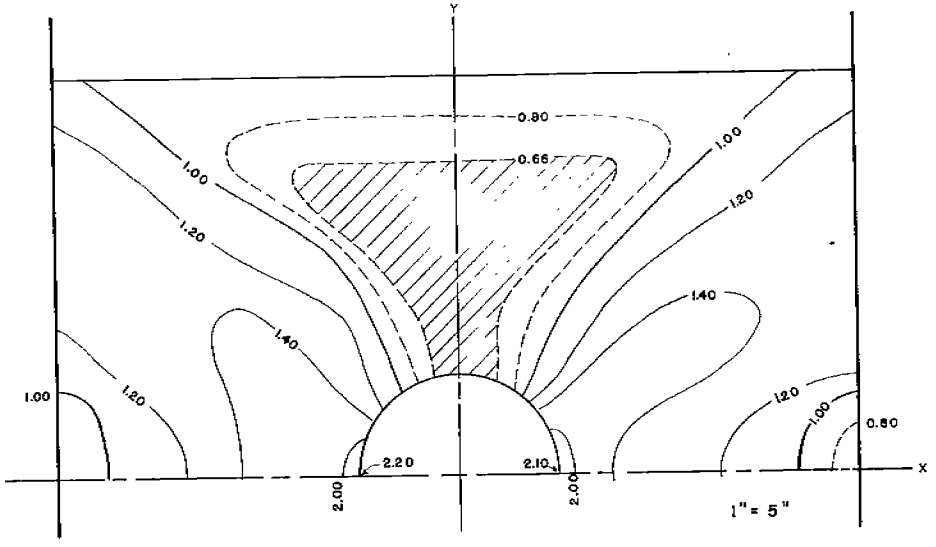

Fig. 26. Stress Concentration Contours for σ_y for Plate with Circular Opening for Load of 650 kips, 77 Per Cent of Maximum Load. Spec. No. 69, 76 F.

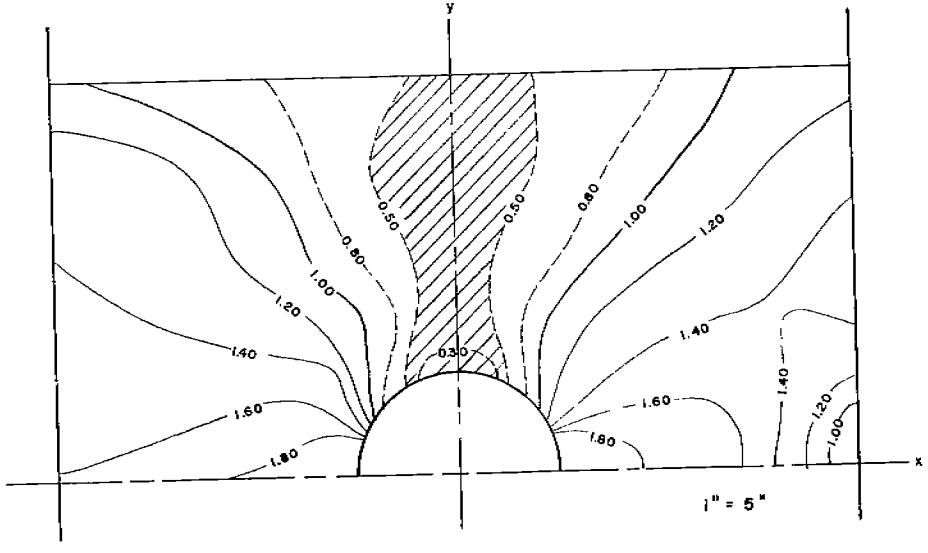

Fig. 27. Stress Concentration Contours for σ_y for Plate with Circular Opening for Load of 845 kips, Maximum Load. Spec. No. 69, 76 F.

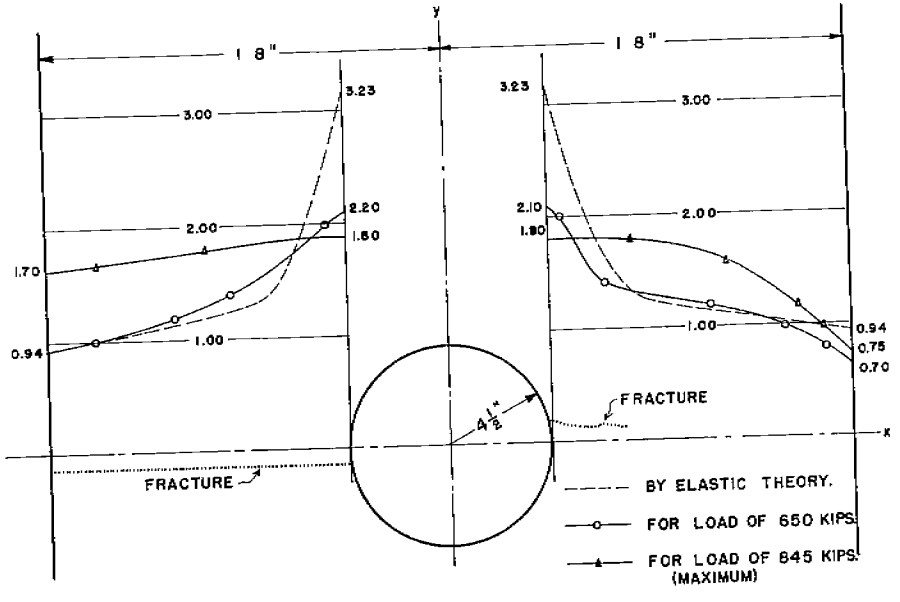

Fig. 28. Comparison of Elastic and Plastic Stress Concentration Curves for σ_y for Plate with Circular Opening. Spec. No. 69.

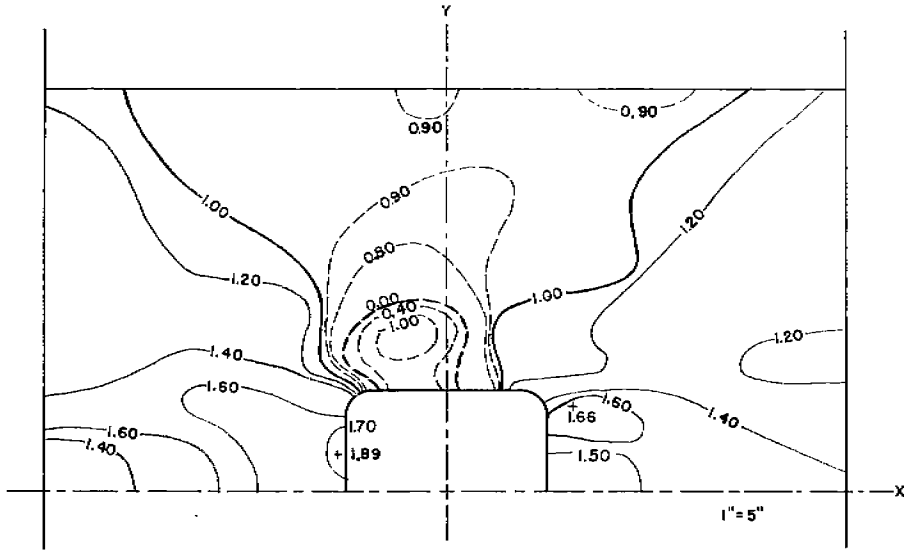

Fig. 29. Stress Concentration Contours for σ_y for Plate with Square Opening, Rounded Corners, Load of 800 kips, Maximum Load. Spec. No. 37, 76F.

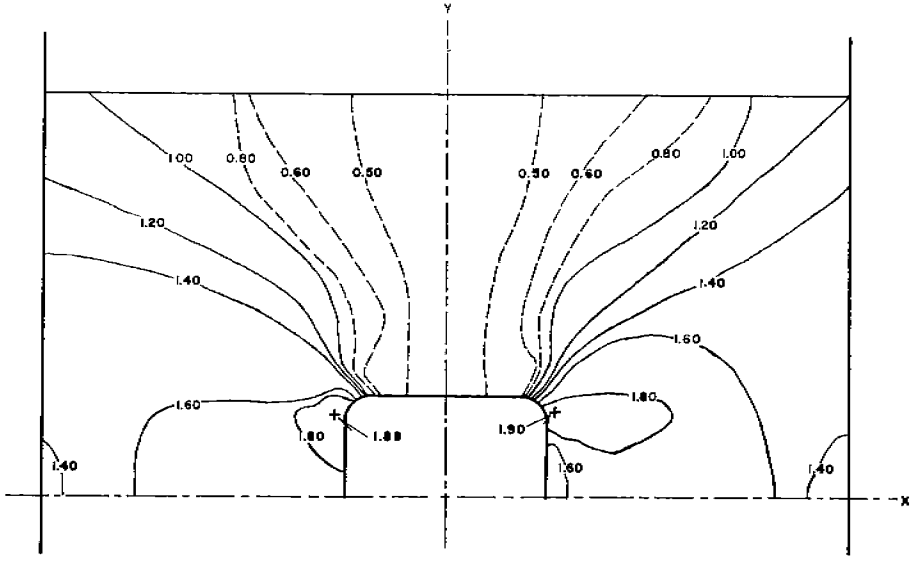

Fig. 31. Stress Concentration Contours for σ_y for Plate with Square Opening with Rounded Corners, Load of 915 kips, Maximum Load. Spec. No. 38, -20 F.

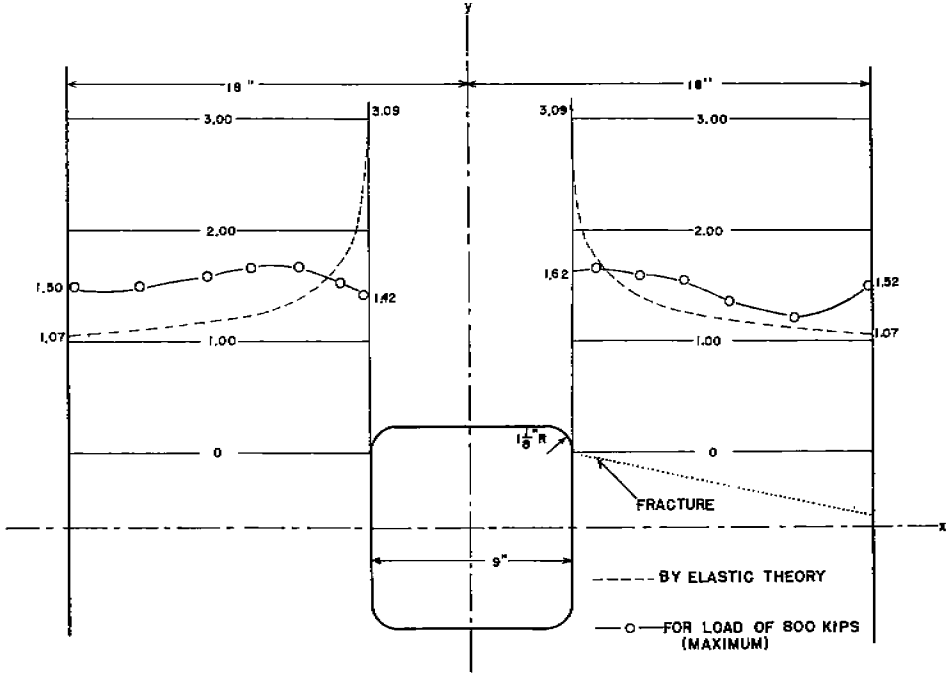

Fig. 30. Comparison of Elastic and Plastic Stress Concentration Curves for Plate with Square Opening with Rounded Corners., Spec. No. 37, 76 F.

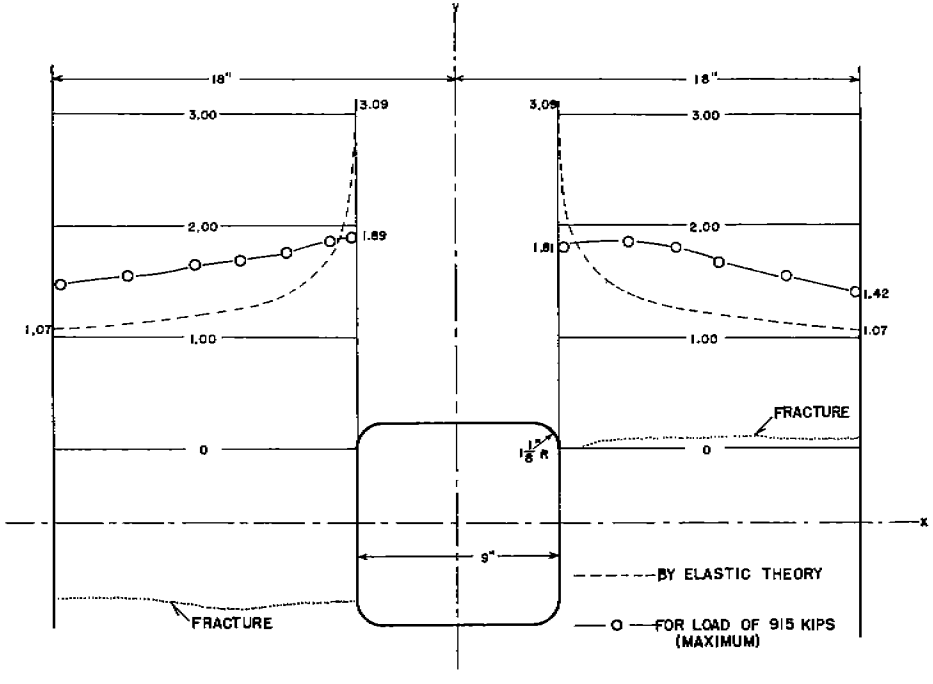

Fig. 32. Comparison of Elastic and Plastic Stress Concentration Curves for σ_y for Plate with Square Opening with Rounded Corners. Spec. No. 38, -20 F.

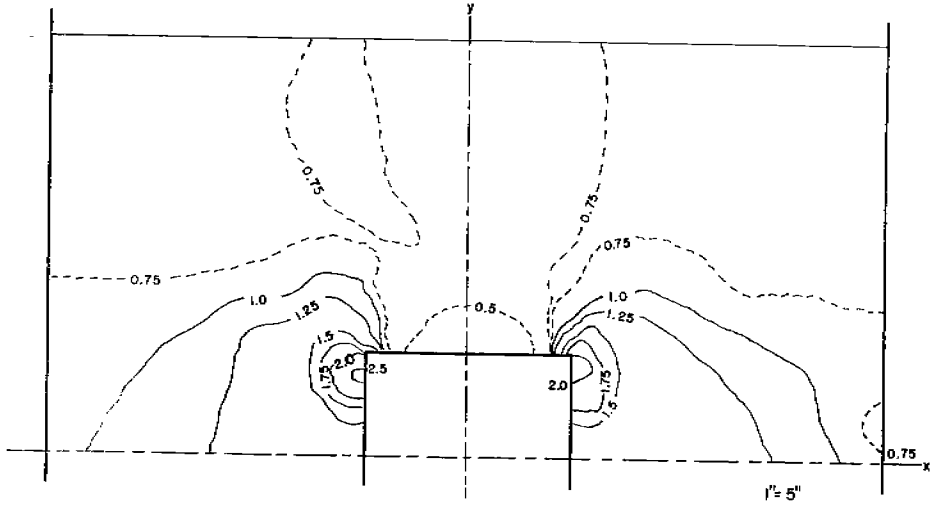

Fig.33. Stress Concentration Contours for σ_y for Plate with Square Opening, Load of 575 kips, 81 Per Cent of Maximum Load. Spec. No. 95. 76 F.

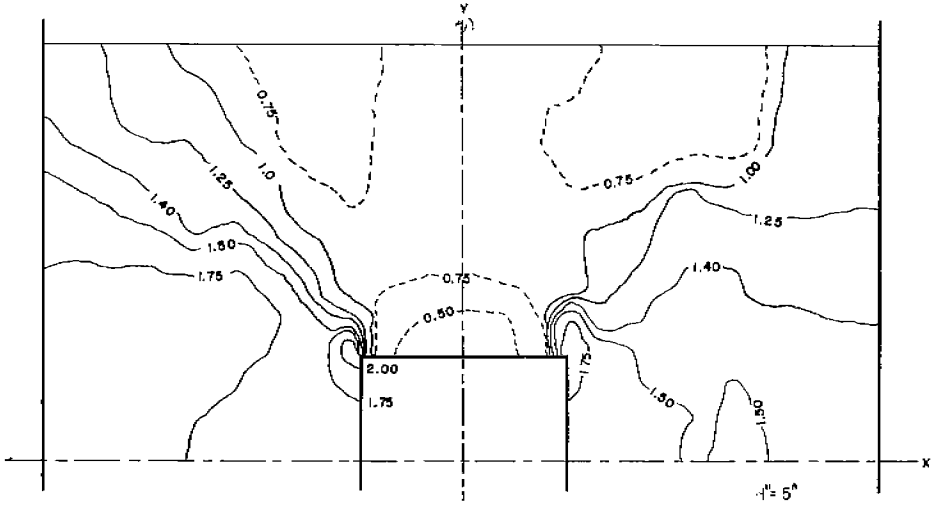

Fig.34. Stress Concentration Contours for σ_y for Plate with Square Opening. Load of 710 kips. Maximum Load. Spec. No. 95. 76 F.

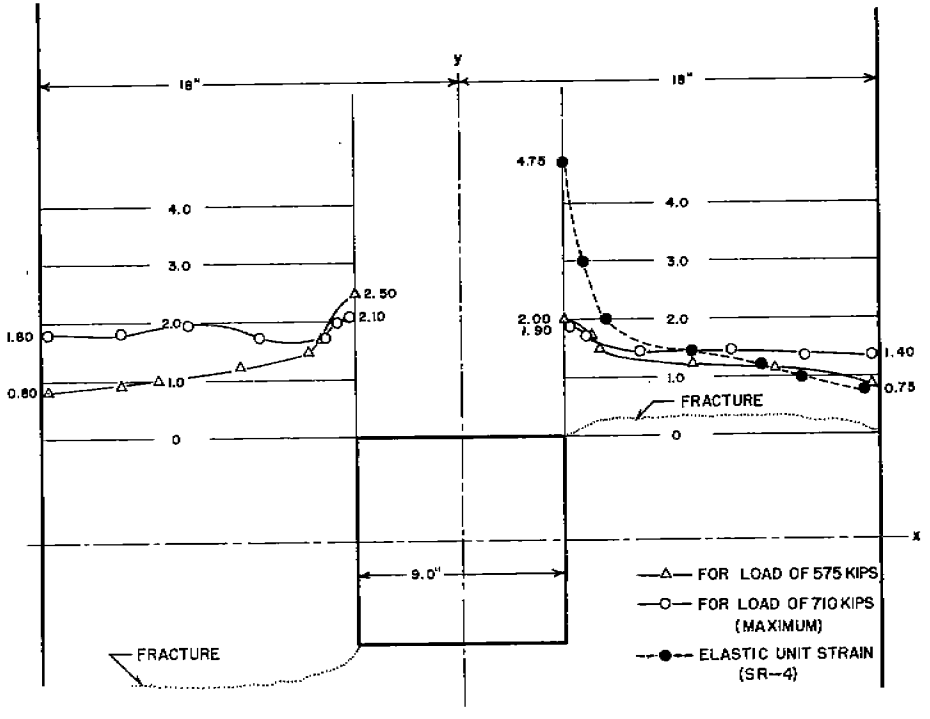

Fig.35. Comparison of Elastic and Plastic Stress Concentration Curves for σ_y for Plate with Square Opening. Spec. No. 95. 76 F.

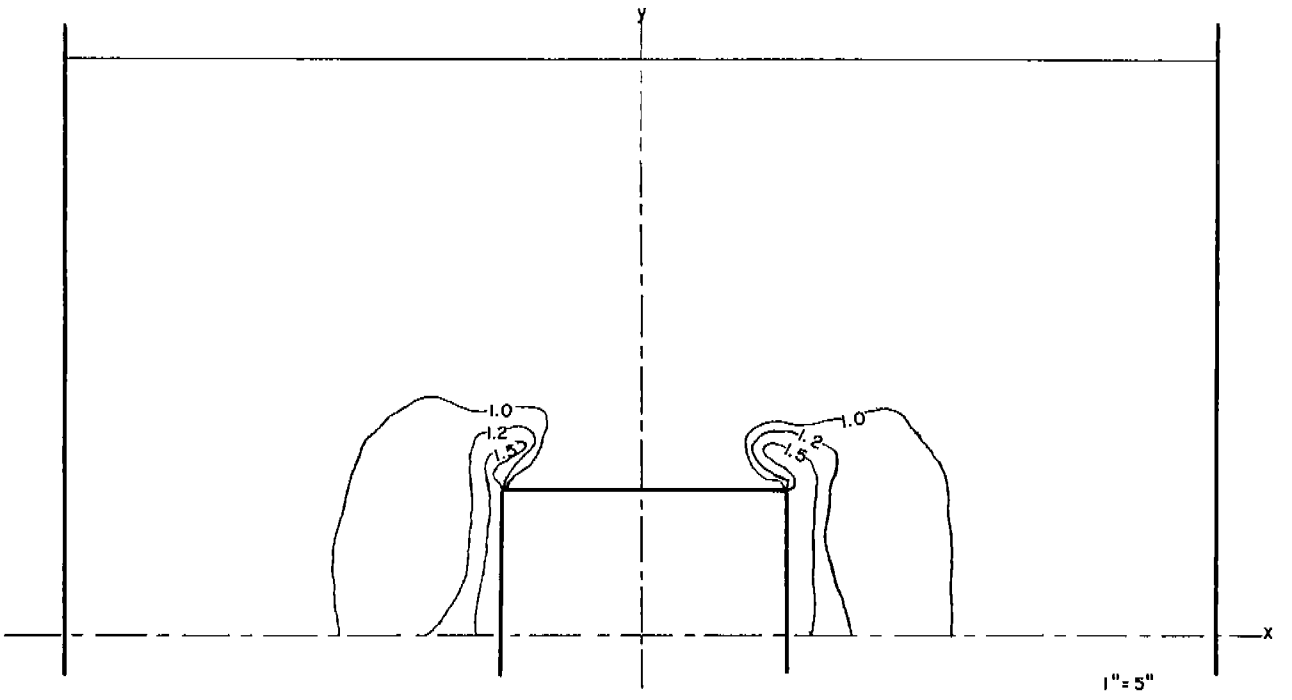

Fig. No. 36. Stress Concentration Contours for σ_Y for Plate with Square Opening. Load of 648 kips. Max. Load. Spec. No. 96. -46 F.

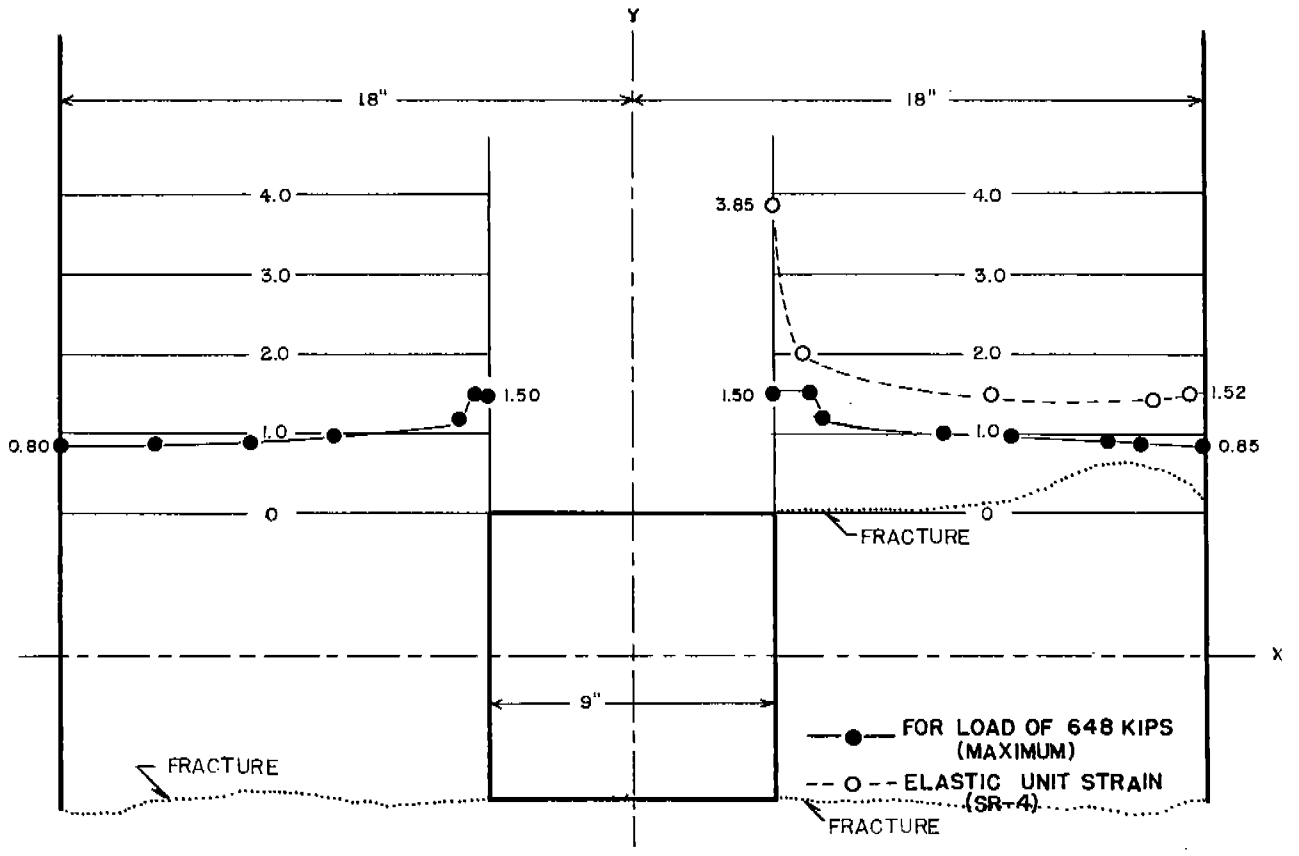

Fig. No. 37. Comparison of Elastic and Plastic Stress Concentration Curves for σ_Y for Plate with Square Opening. Spec. No. 96. -46 F.

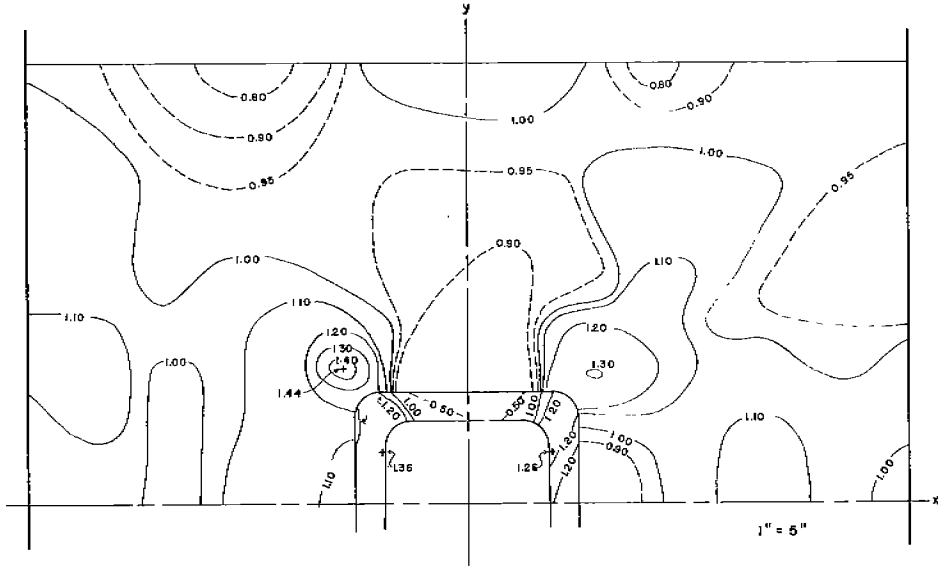

Fig. 38. Stress Concentration Contours for σ_y for Plate with Reinforced Square Opening with Rounded Corners for Load of 1150 kips, 90 Per Cent of Maximum Load. Spec. No. 70, 76 F.

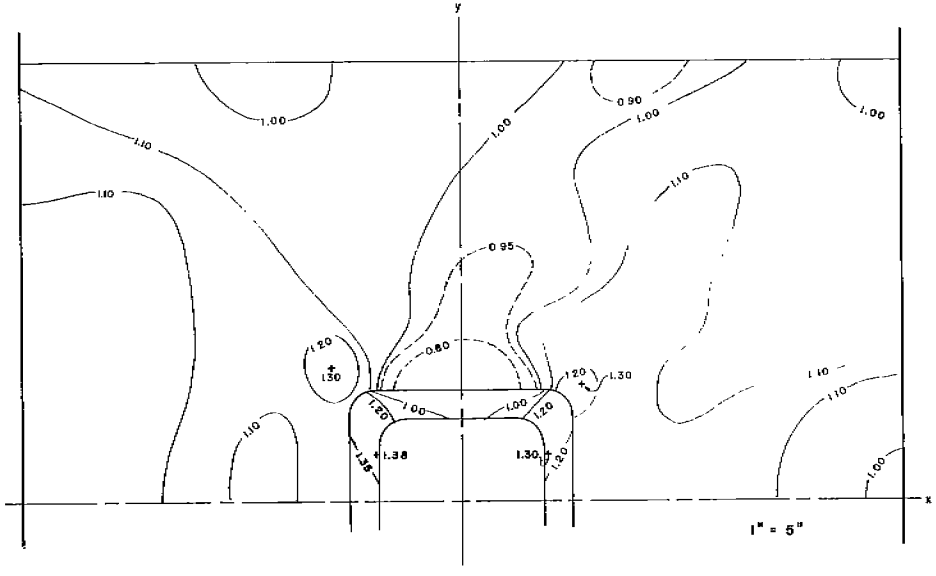

Fig. 39. Stress Concentration Contours for σ_y for Plate with Reinforced Square Opening with Rounded Corners for Load of 1276 kips, Maximum Load. Spec. No. 70, 76 F.

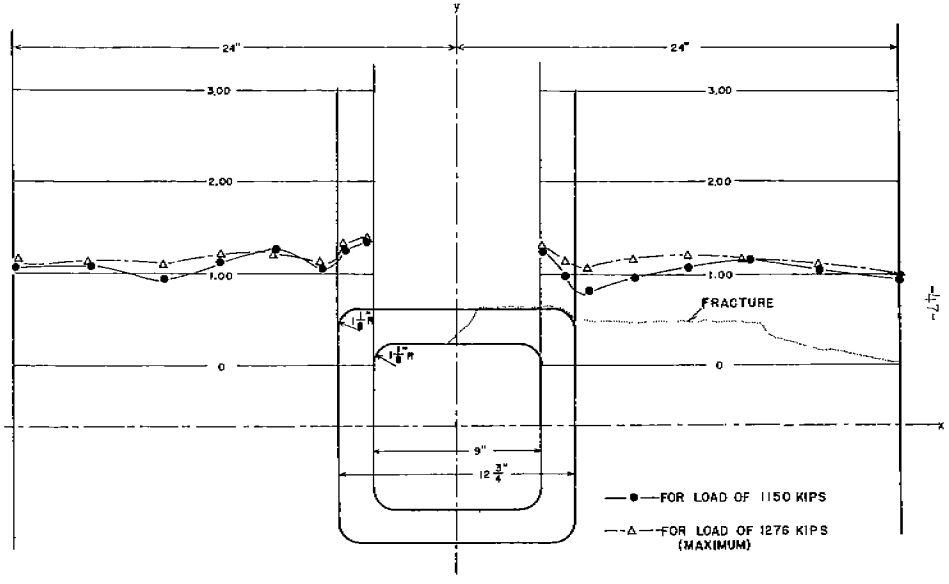

Fig. 40. Comparison of Elastic and Plastic Stress Concentration Curves for σ_y for Plate with Reinforced Square Opening with Rounded Corners. No. 70, 76 F.

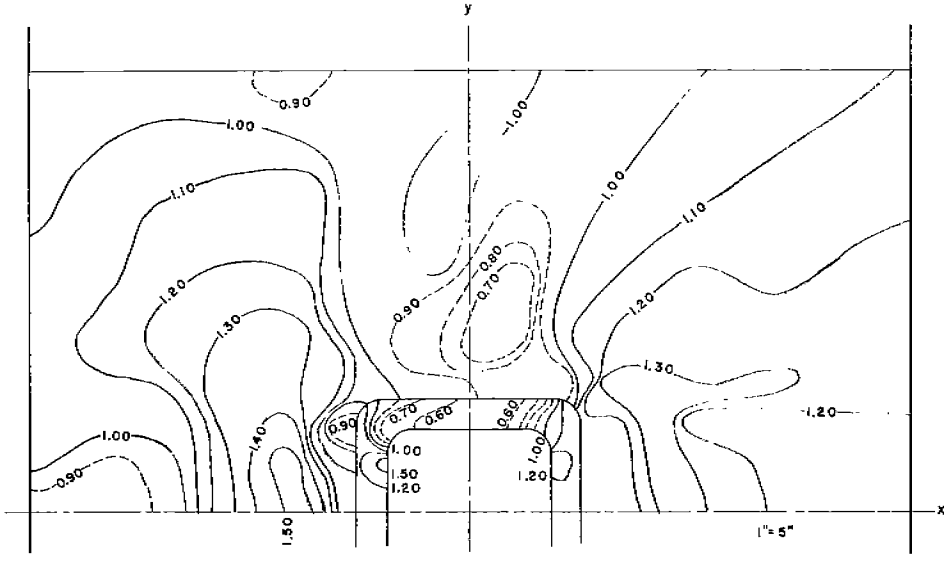

Fig. 41. Stress Concentration Contours for σ_y for Plate with Reinforced Square Opening with Rounded Corners for Load of 1150 kips, 98 per cent of Maximum Load. Spec. No. 71, -46 F.

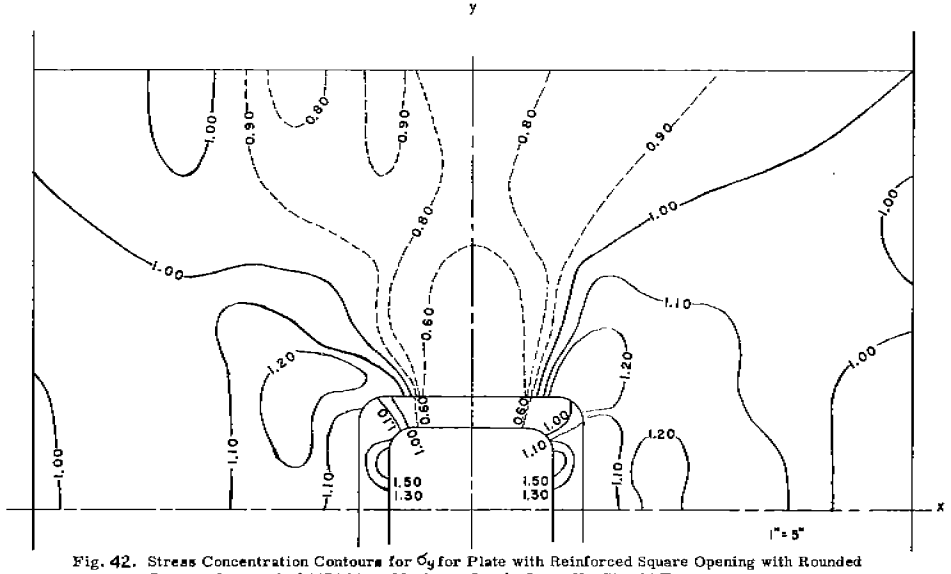

Fig. 42. Stress Concentration Contours for σ_y for Plate with Reinforced Square Opening with Rounded Corners for Load of 1176 kips, Maximum Load. Spec. No. 71, -46 F.

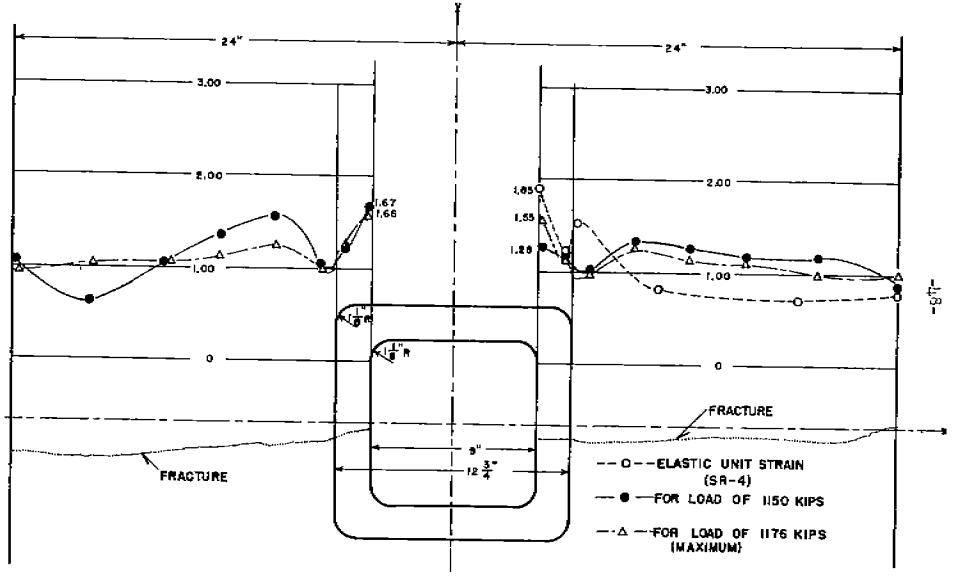

Fig. 43. Comparison of Elastic and Plastic Stress Concentration Curves for σ_y for Plate with Reinforced Square Opening with Rounded Corners. Spec. No. 71, -46 F.

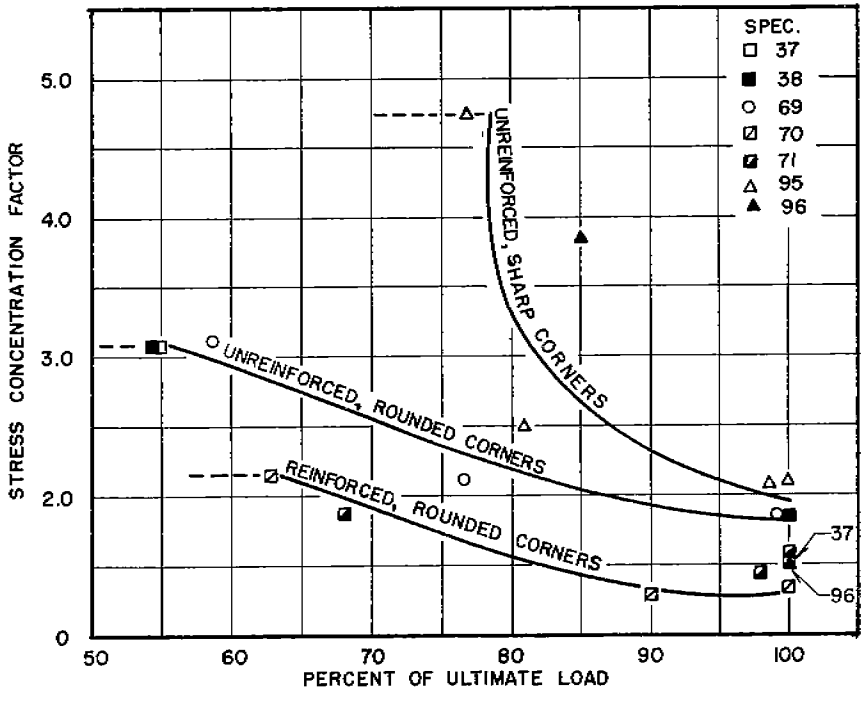

Fig. 44. Stress Concentration Factor in Plastic Range as Failure is Approached.

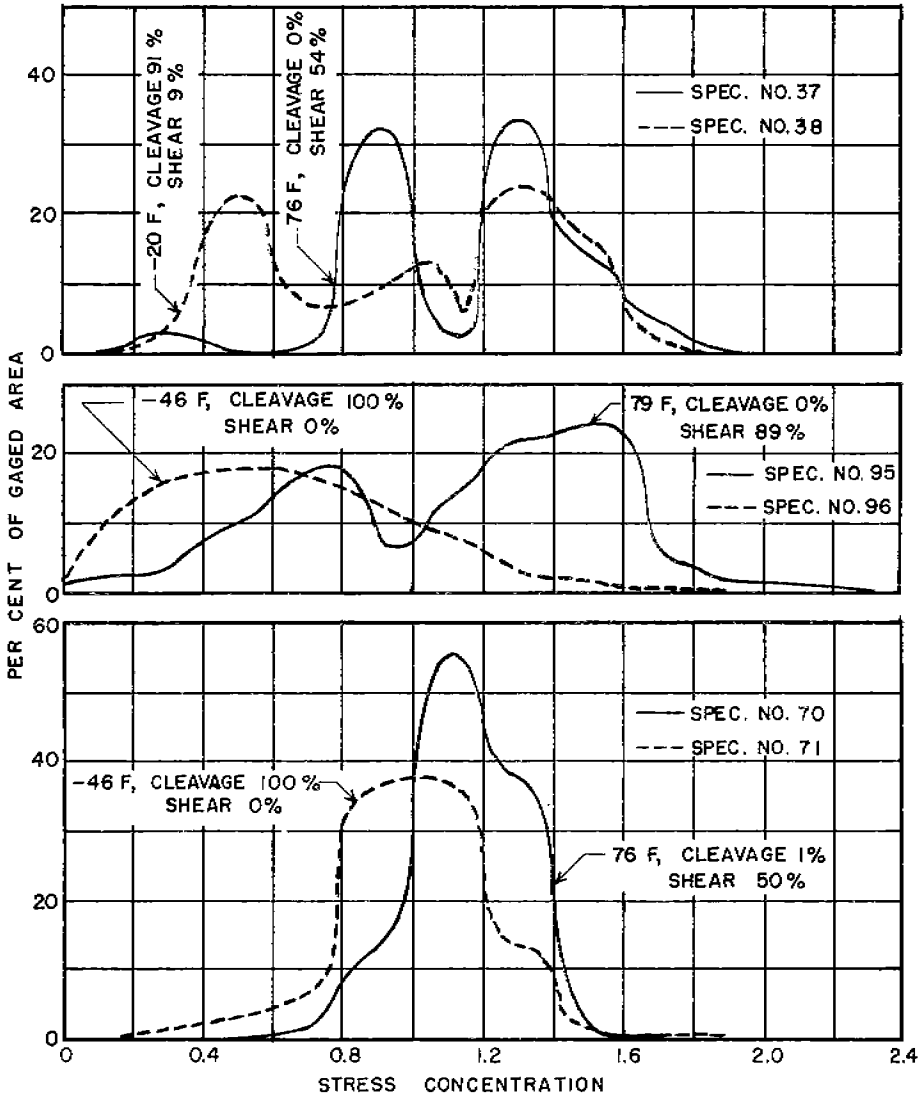

Fig. 45. Effect of Testing Temperature Upon Plastic Stress Distribution at Maximum Load.

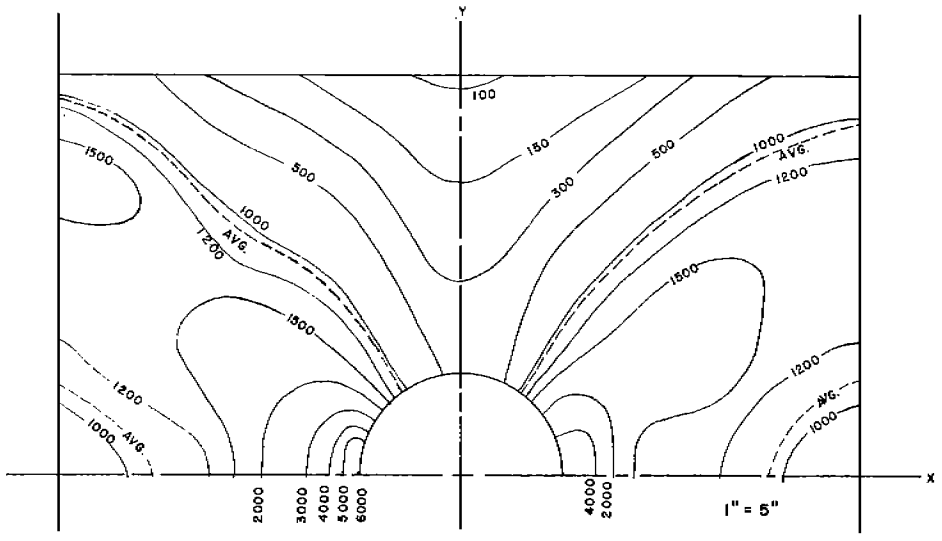

Fig. 46. Unit Strain Energy Contours for Plate of Finite Width with Circular Opening for Load of 650 kips, 77 Per Cent of Maximum Load. Spec. No. 69; 76 F.

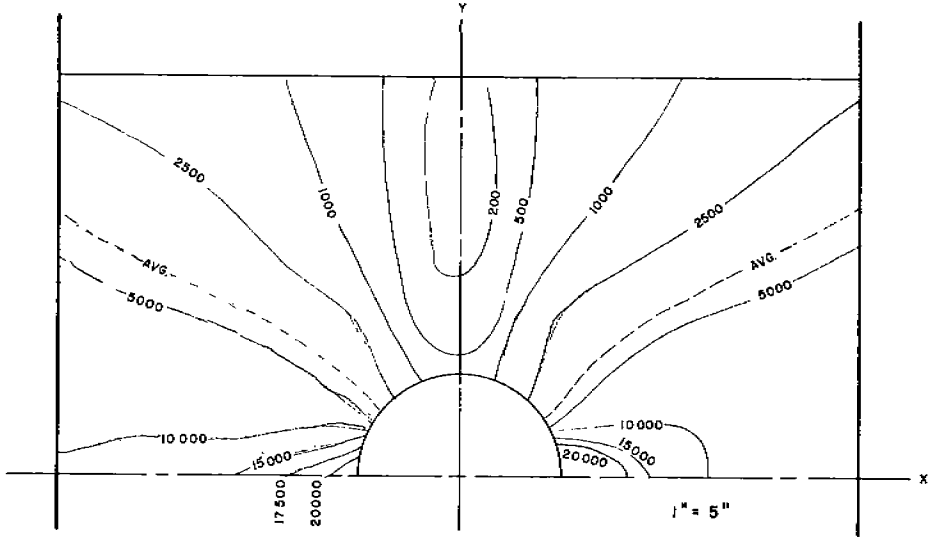

Fig. 47. Unit Strain Energy Contours for Plate of Finite Width with Circular Opening for Load of 845 kips, Maximum Load. Spec. No. 69, 76 F.

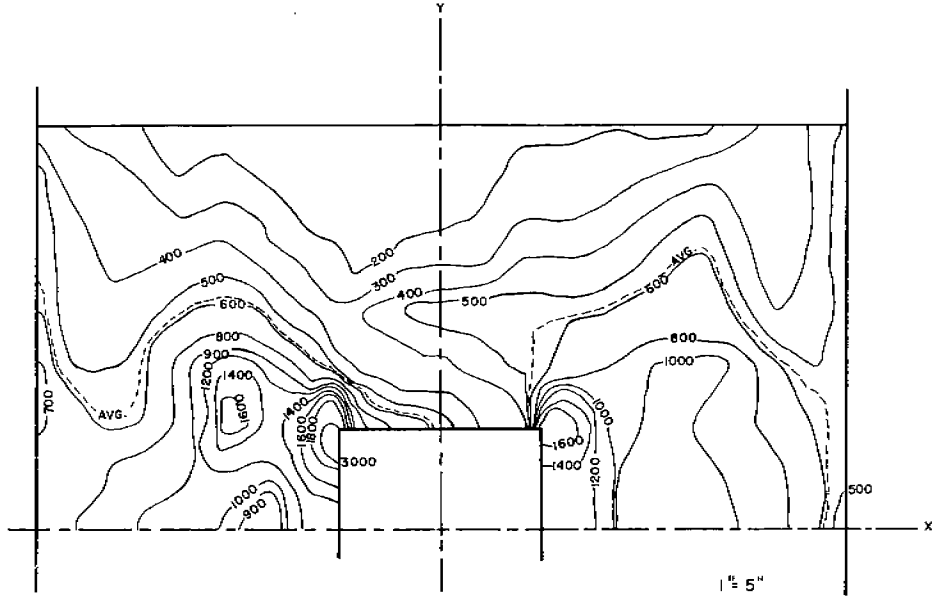

Fig. 48. Unit Strain Energy Contours for Plate of Finite Width with Square Opening, for Load of 575 kips, 81 Per Cent of the Load. Spec. No. 95. 76 F.

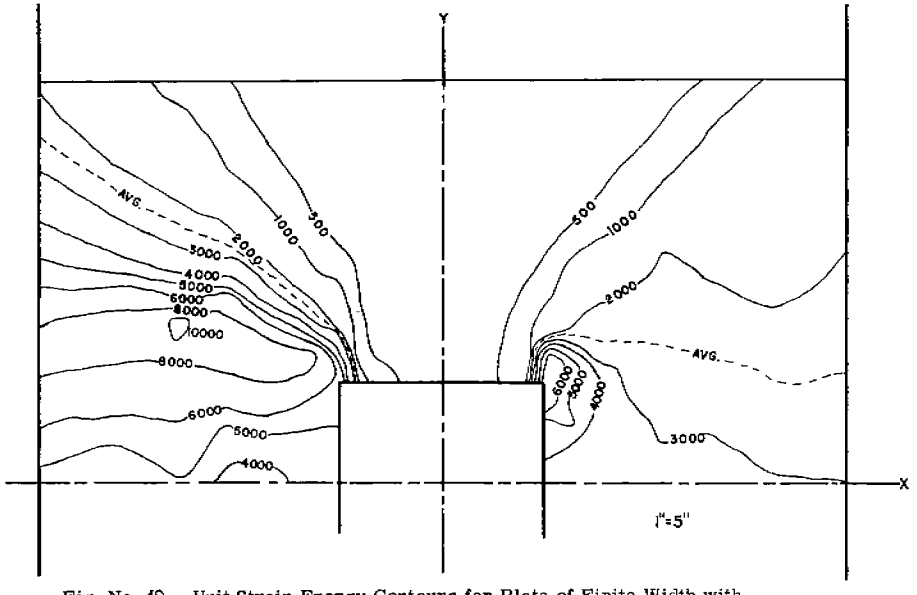

Fig. No. 49. Unit Strain Energy Contours for Plate of Finite Width with Square Opening, for Load of 710 kips, Max. Load. Spec. No. 95. 76 F.

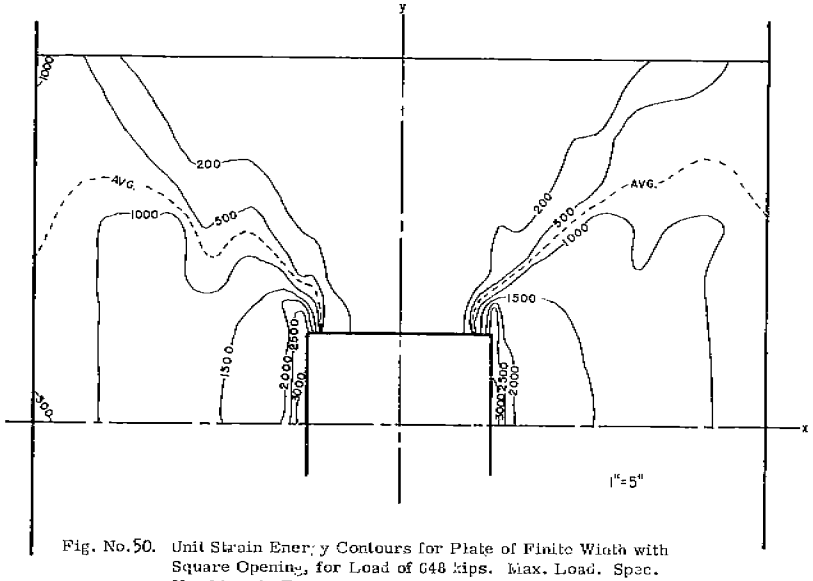

Fig. No. 50. Unit Strain Energy Contours for Plate of Finite Width with Square Opening, for Load of 648 kips. Max. Load. Spec. No. 96. -40 F.

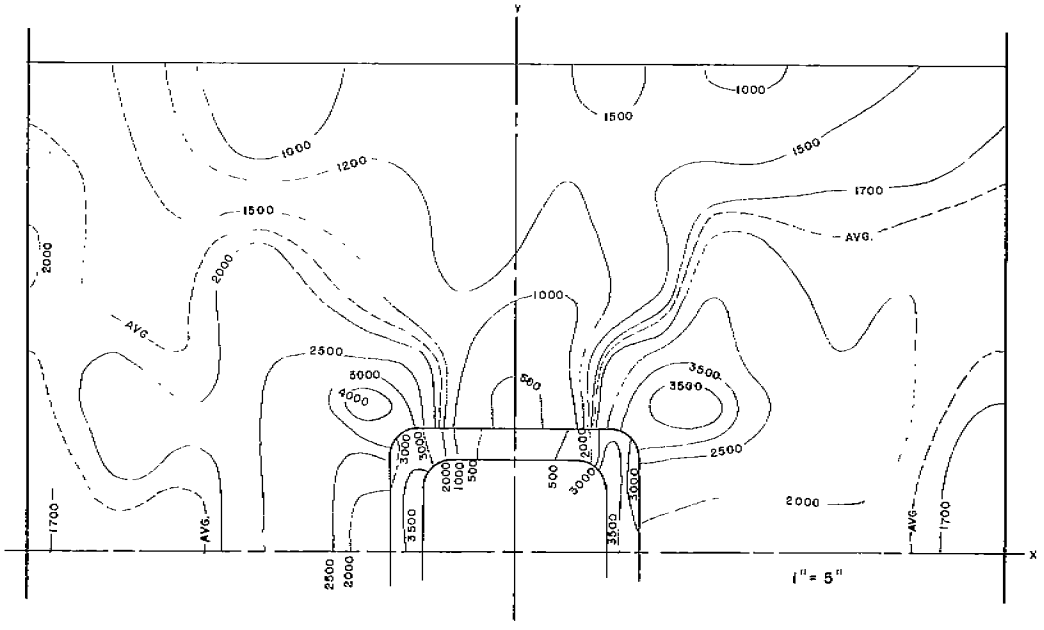

Fig. 51 . Unit Strain Energy Contours for Plate of Finite Width with Reinforced Square Opening with Rounded Corners for Load of 1150 kips, 90 Per Cent of Maximum Load. Spec. No. 70, 76 F.

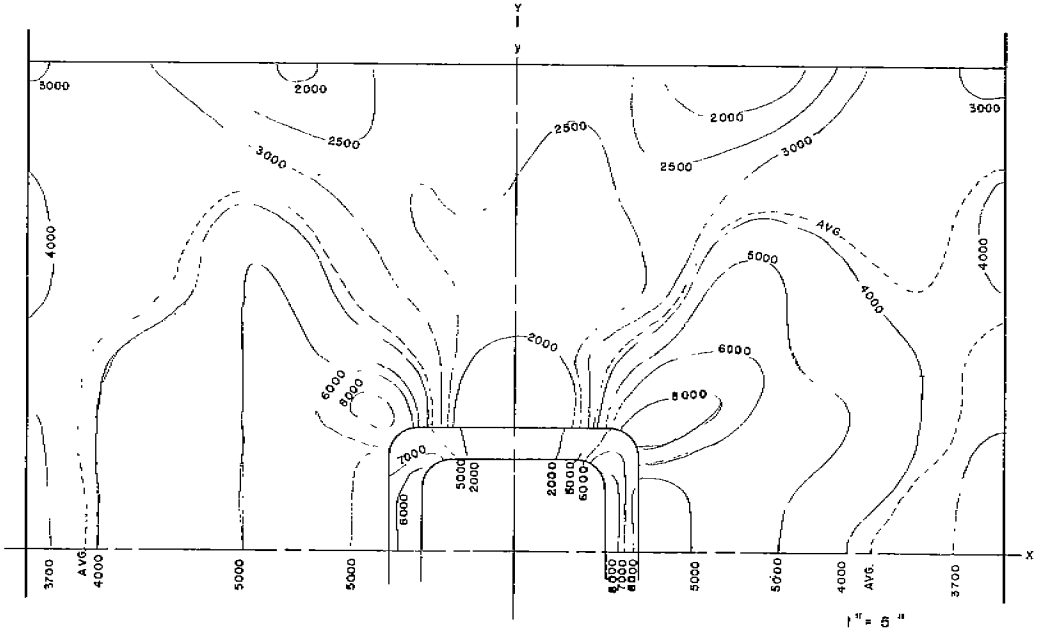

Fig. 52 . Unit Strain Energy Contours for Plate of Finite Width with Reinforced Square Opening with Rounded Corners for Load of 1276 kips, Maximum Load. Spec. No. 70, 76 F.

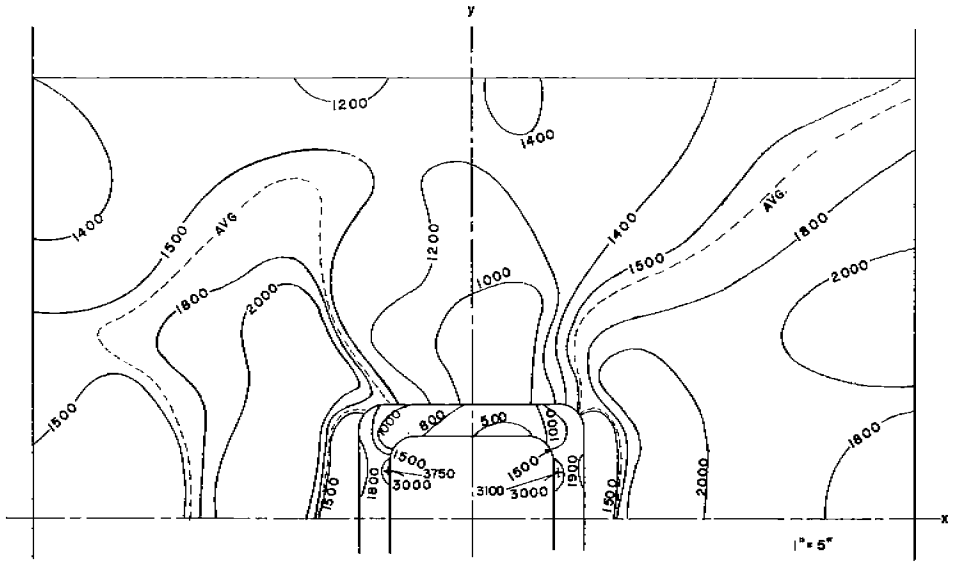

Fig. 53. Unit Strain Energy Contours for Plate of Finite Width with Reinforced Square Openings with Rounded Corners for Load of 1150 kips 98 per cent of Maximum Load. Spec. No. 71, -46 F.

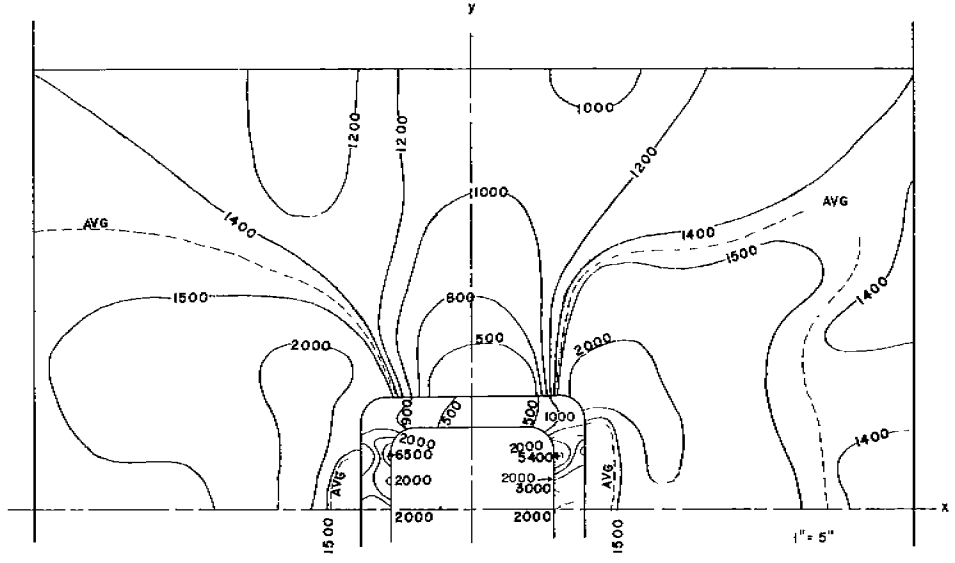

Fig. 54. Unit Strain Energy Contours for Plate of Finite Width with Reinforced Square Opening with Rounded Corners for Load of 1176 kips. Maximum Load. Spec. No. 71, -46 F.

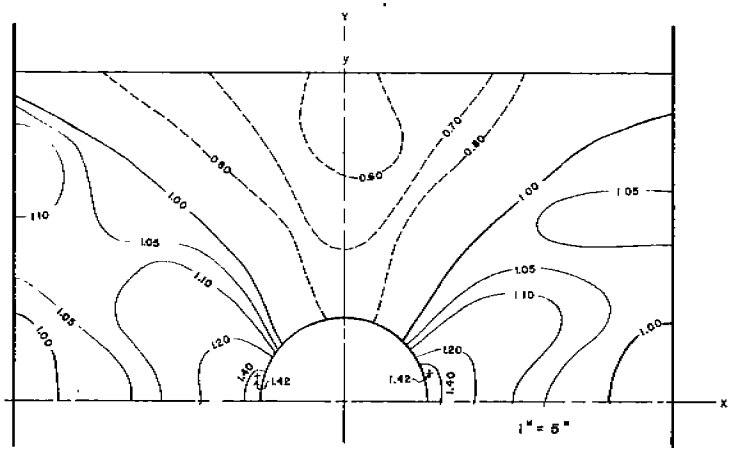

Fig. 55. Contours of Equal Rate of Energy Absorption. Spec. No. 69, 76 F.

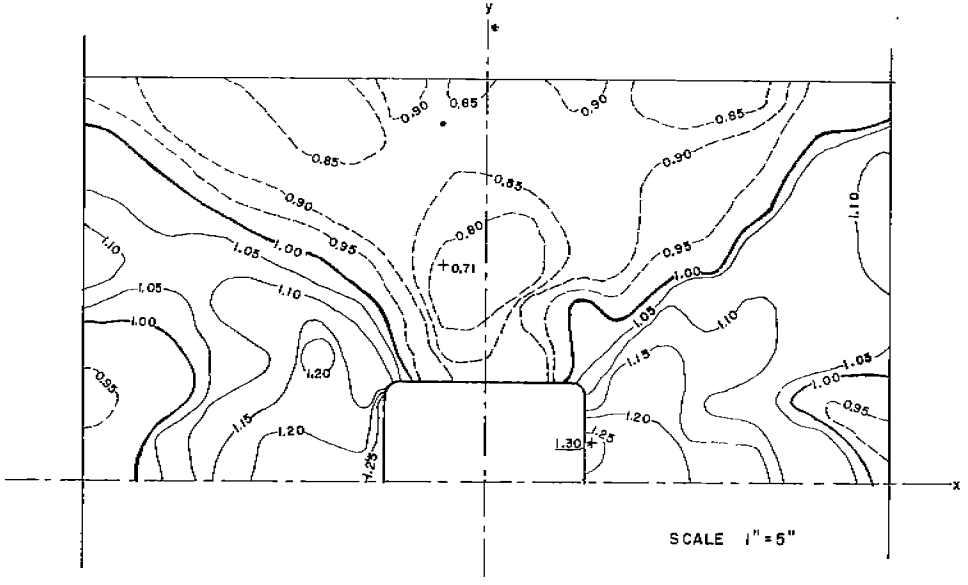

Fig. 56. Contours of Equal Rate of Energy Absorption. Spec. No. 37, 76 F.

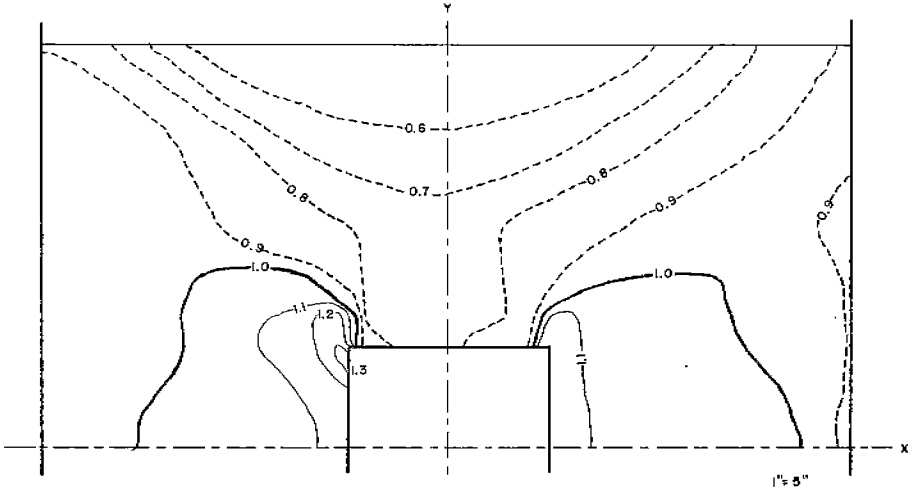

Fig. No.58. Contours of Equal Rate of Energy Absorption. Spec. No. 95. 76 F.

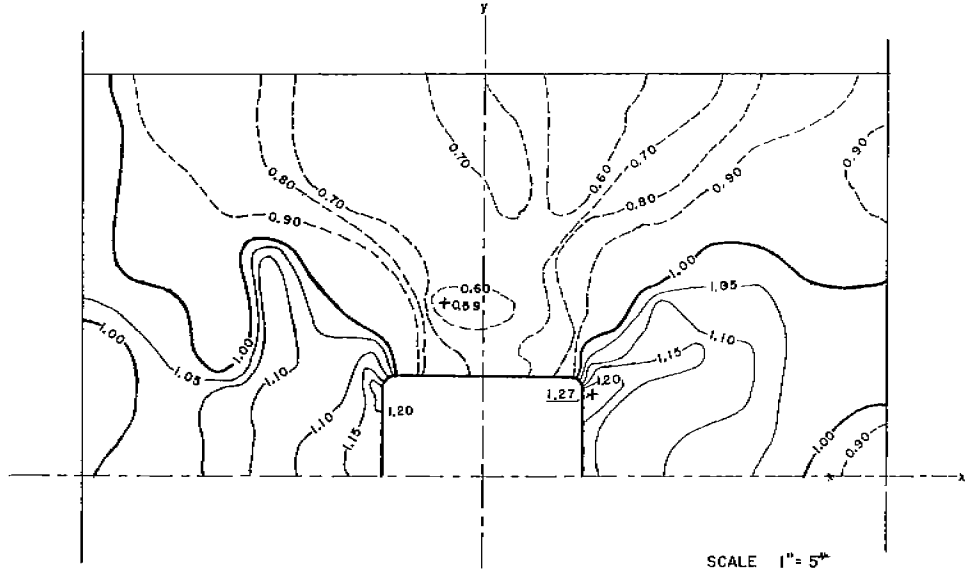

Fig. 57. Contours of Equal Rate of Energy Absorption. Spec. No. 38, -20F.

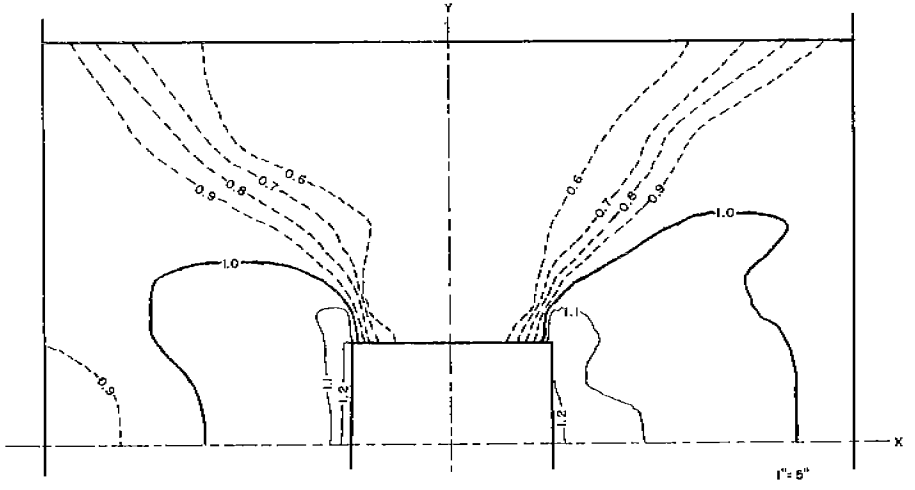

Fig. No. 59. Contours of Equal Rate of Energy Absorption. Spec. No. 96. -46 F.

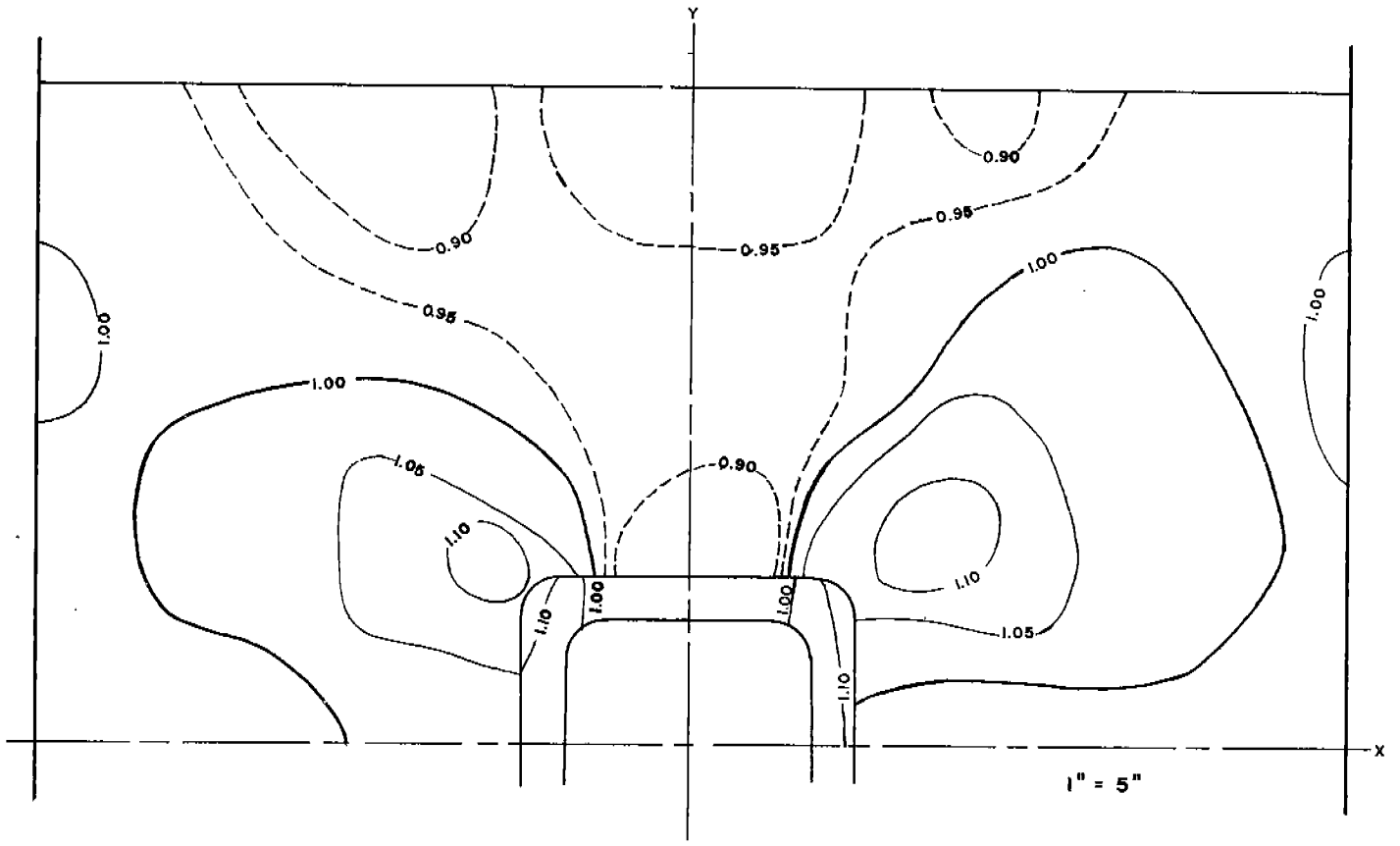

Fig. 60 . Contours of Equal Rate of Energy Absorption. Spec. No. 70, 76 F.

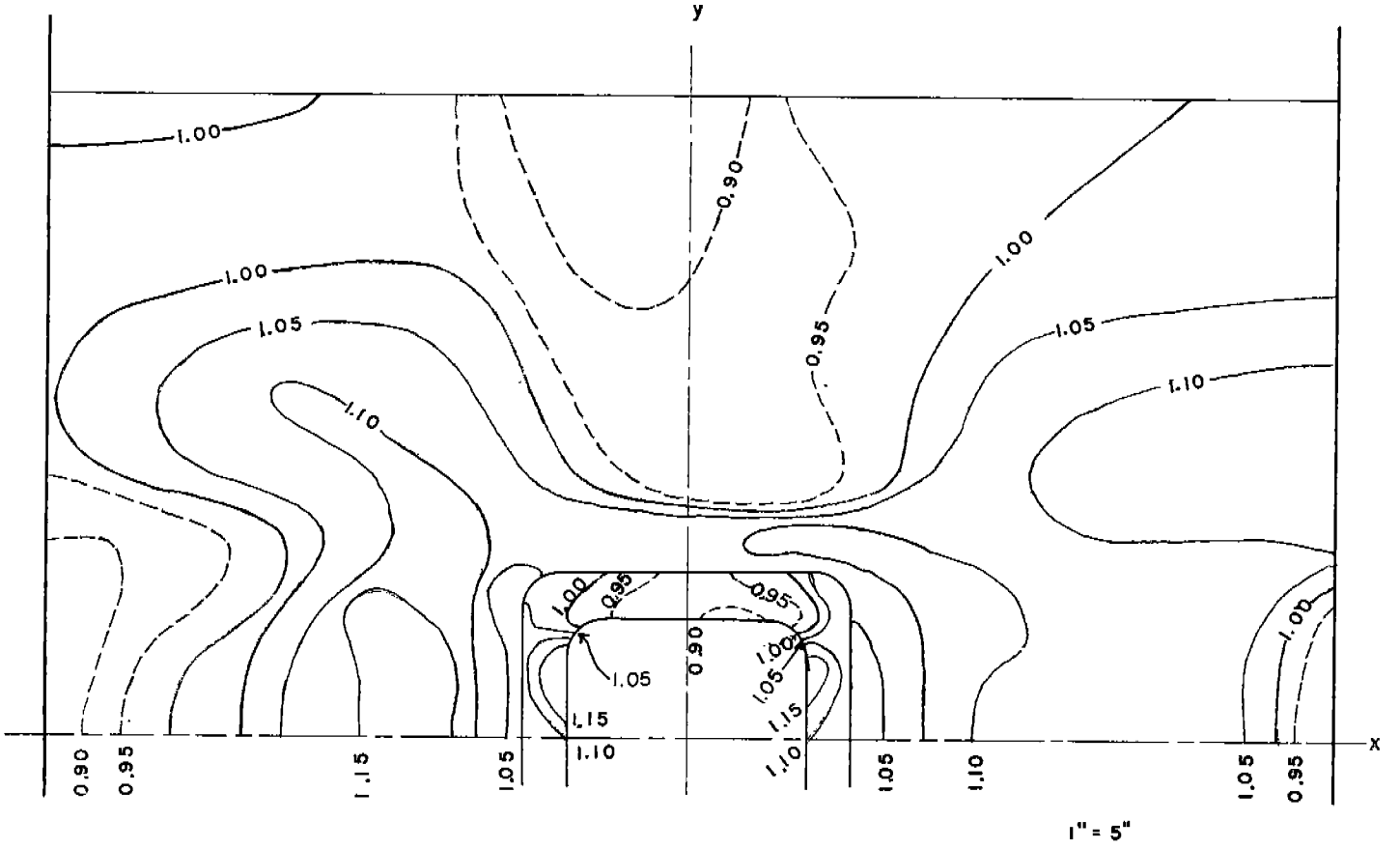

Fig. 61 . Contours of Equal Rate of Energy Absorption. Spec. No. 71, -46 F.

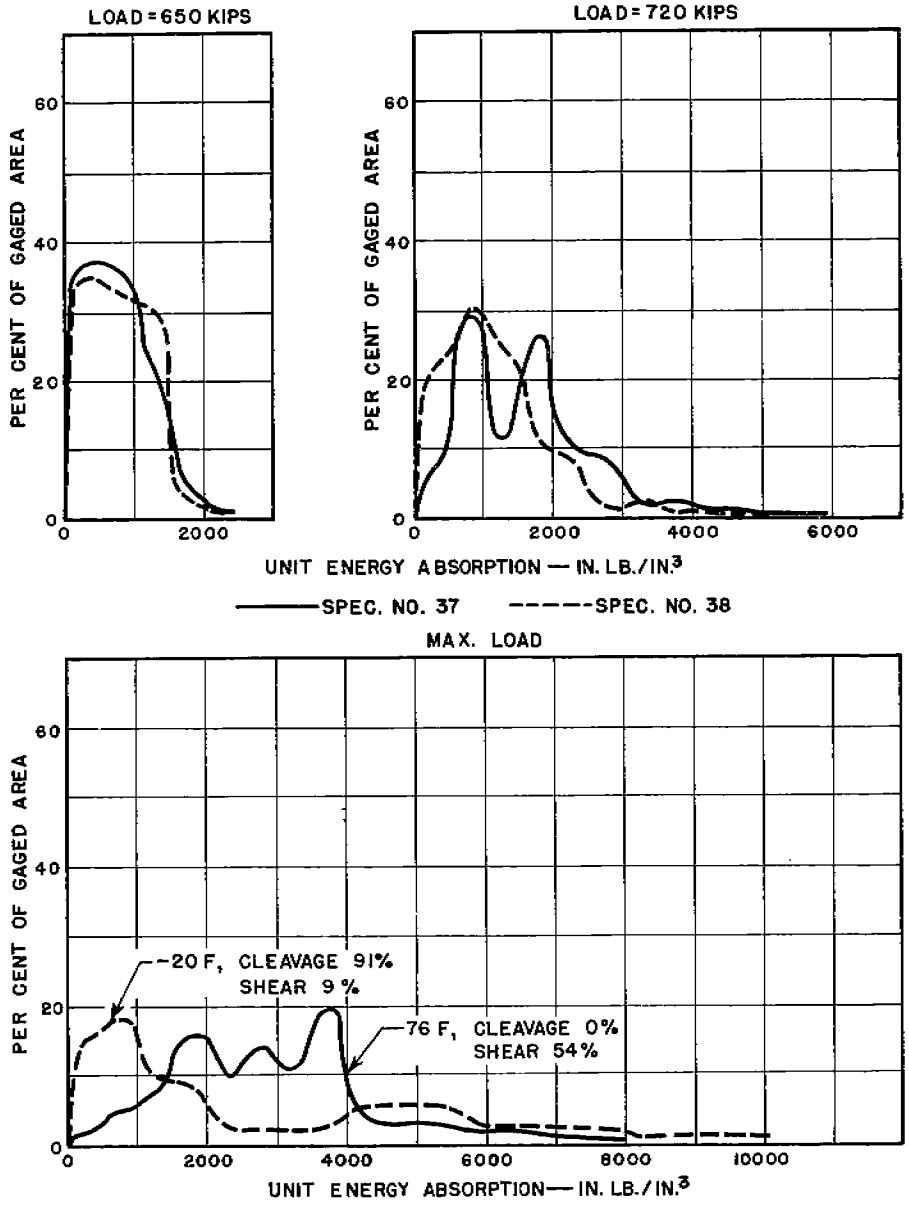

Fig. 62. Effect of Testing Temperature upon Plastic Energy Distribution Specs. No. 37 and 38, at Maximum Load.

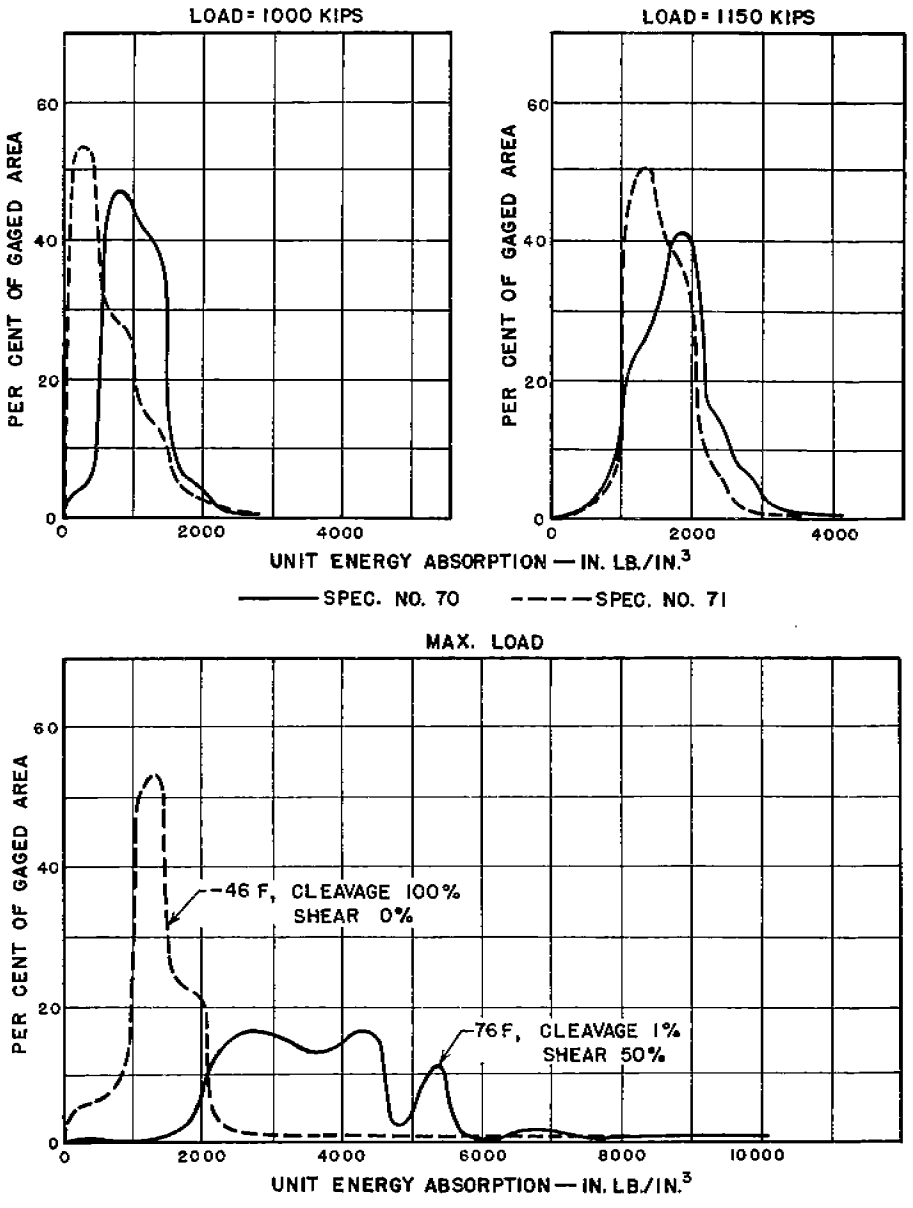

Fig. 63. Effect of Testing Temperature upon Plastic Energy Distribution Specs. No. 70 and 71, at Maximum Load.

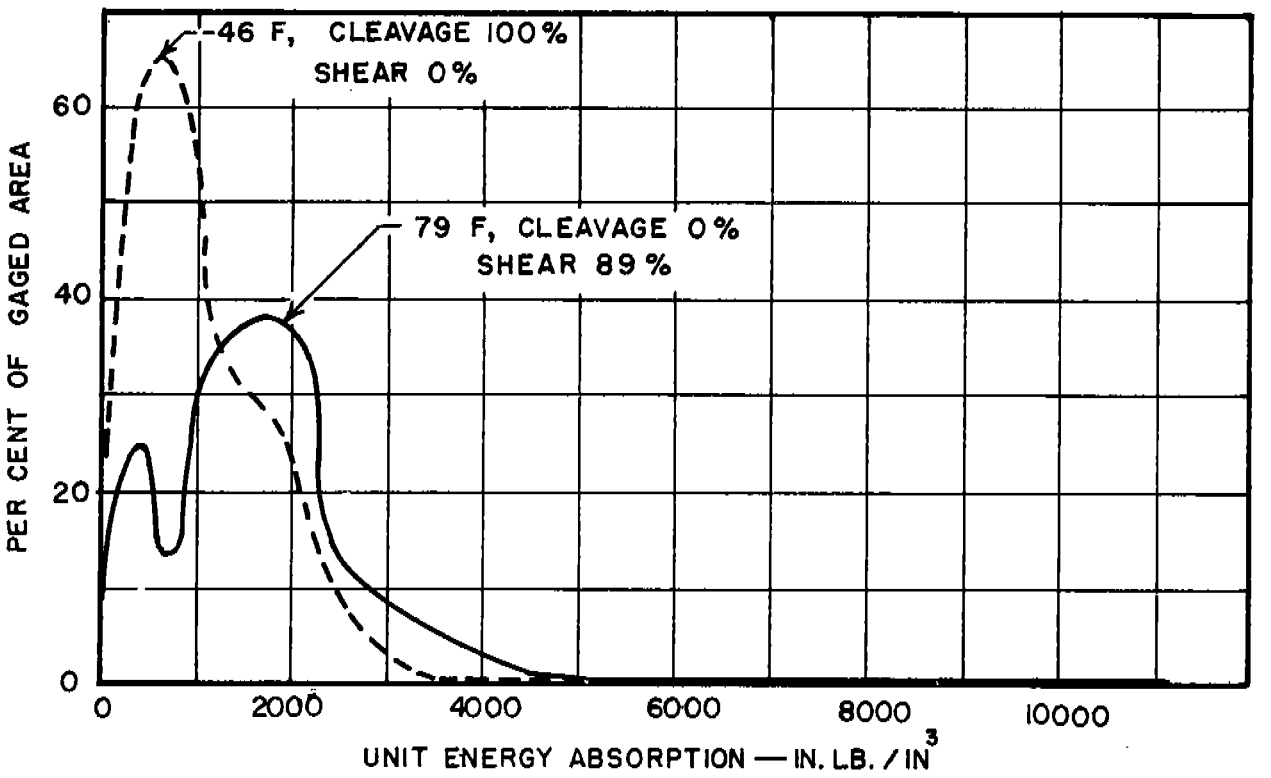

Fig.64. Effect of Testing Temperature upon Plastic Energy Distribution at Maximum Load. Spec. No. 95 and 96.

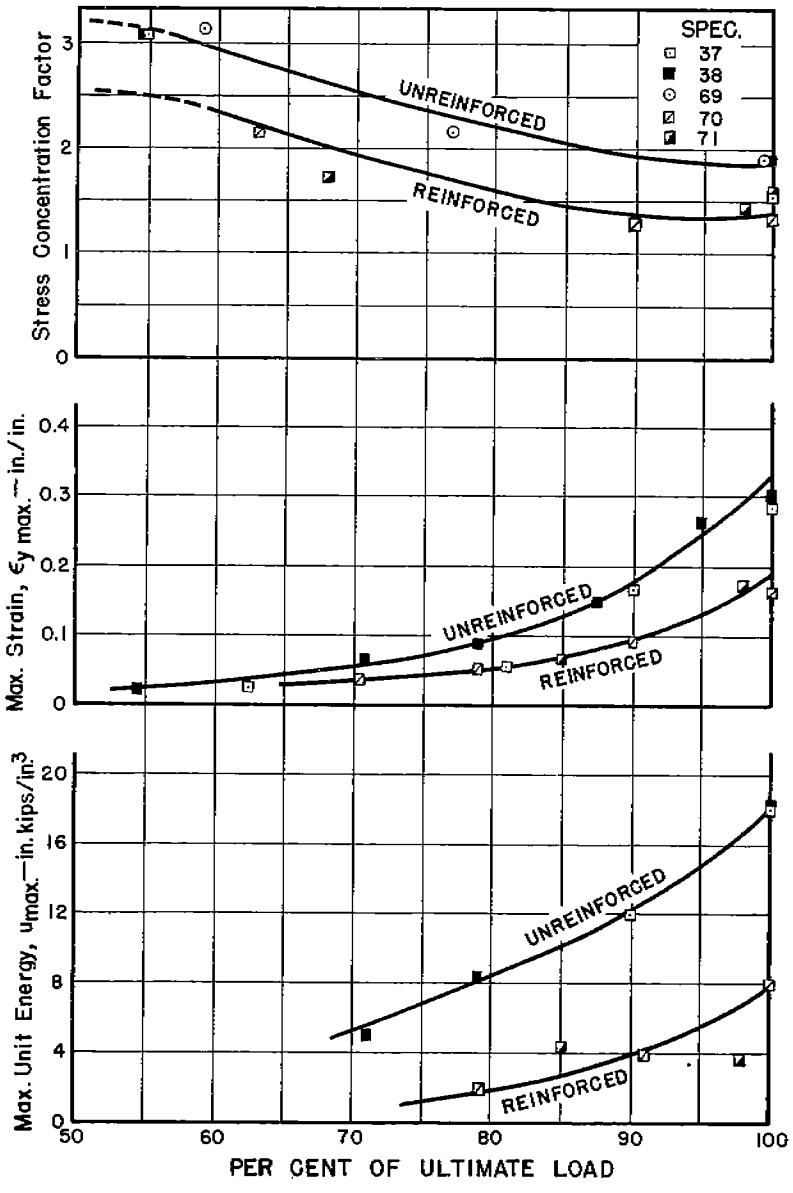

Fig. 65. Stress Concentration Factor, Maximum Strain and Maximum Unit Energy as Fracture is Approached.

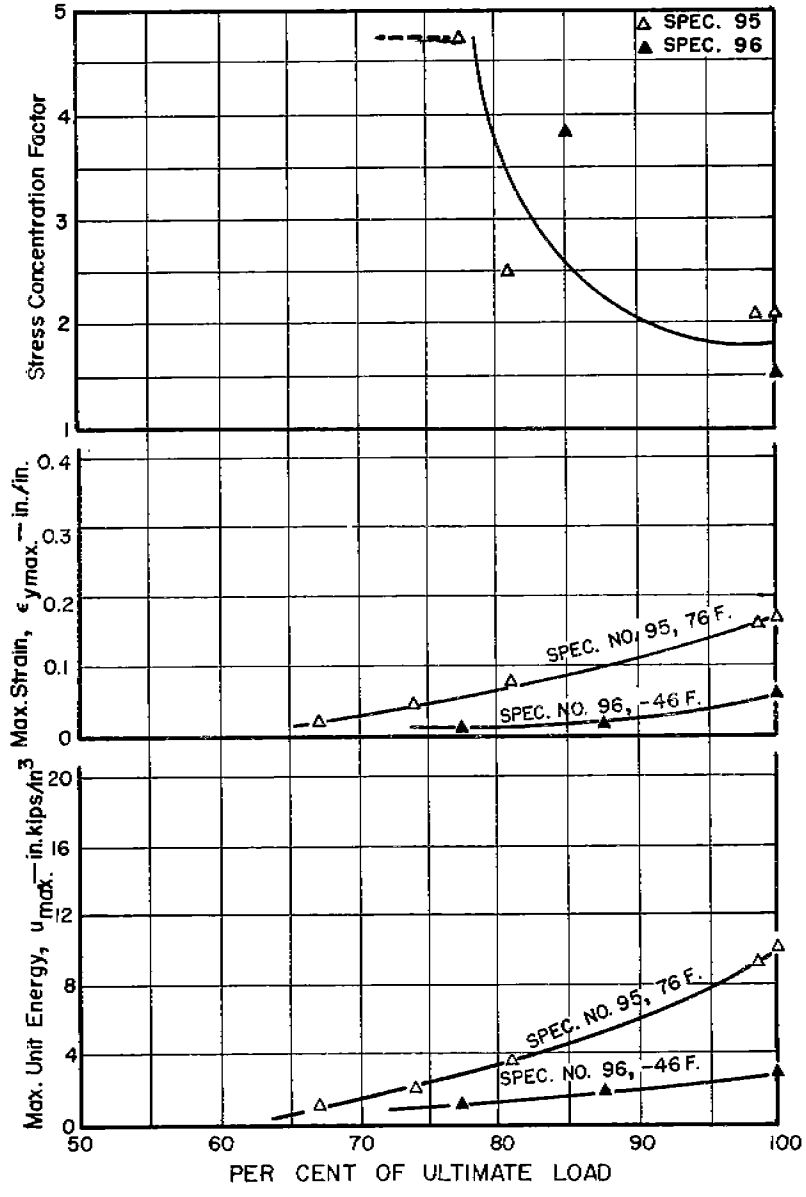

Fig. 66 . Stress Concentration Factor, Maximum Strain and Maximum Unit Energy as Fracture is Approached.

APPENDIX A

CALIBRATION TENSILE TESTS

The data of the calibration tensile tests are given in this appendix. The details of the tensile specimen, the procedure for these tests, and the application of the resulting data to the plastic energy and stress computations were described in the Second Progress Report (2).

The test results are summarized in Table Ia and plotted in Figs. 1a-4a.

TABLE A-1

RESULTS OF CALIBRATION TENSILE TESTS*

Plate No.	Used for Spec. No.	Direction** of Test	Testing Temp.	Upper Yield Point	Ultimate Strength	Elong. in 12 in.	Reduction of Area	Poisson's Ratio
			deg. F.	psi	psi	per cent	per cent	
26	37	P	76	36,900	61,800	35	62	0.48
		T	76	36,500	61,100	31	54	0.46
4	38	P	76	34,900	60,200	32	61	----
		T	76	35,200	61,500	#	52	----
		P	-20	42,500	68,500	32	60	0.51
		T	-20	38,900	64,100	#	50	0.46
3	69, 70, 71	P	76	34,900	61,200	33	62	0.47
		T	76	38,100	62,600	30	52	0.45
		P	-46	44,300	70,900	29	56	0.50
		T	-46	43,900	72,000	#	49	0.51
1	95, 96	P	76	36,600	62,400	28	56	0.45
		P	-46	42,300	69,900	23*	51	0.48

* See second Progress Report for sketch of specimen.
** P, parallel to direction of rolling. T, transverse to direction of rolling.
\# Specimen broke outside gage length.

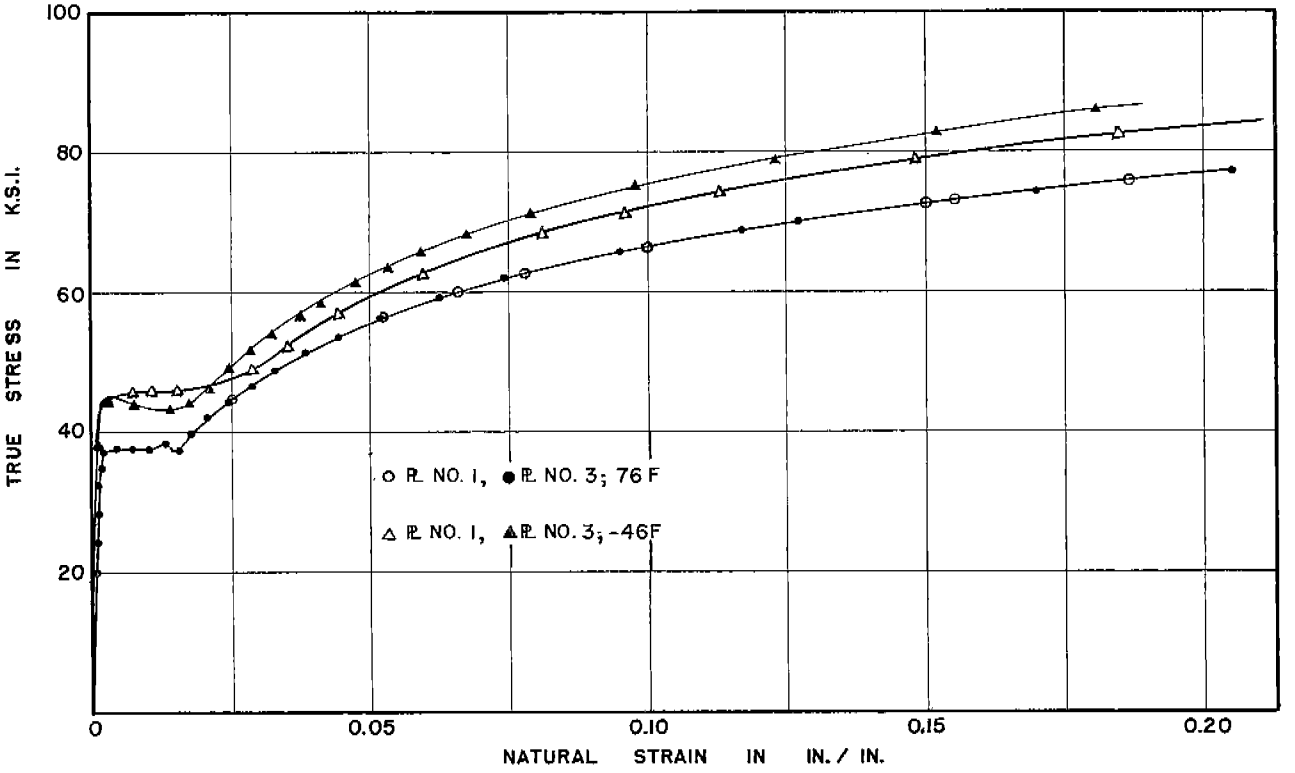

Fig. 1a. Calibration Test. True Stress-Strain Curve.

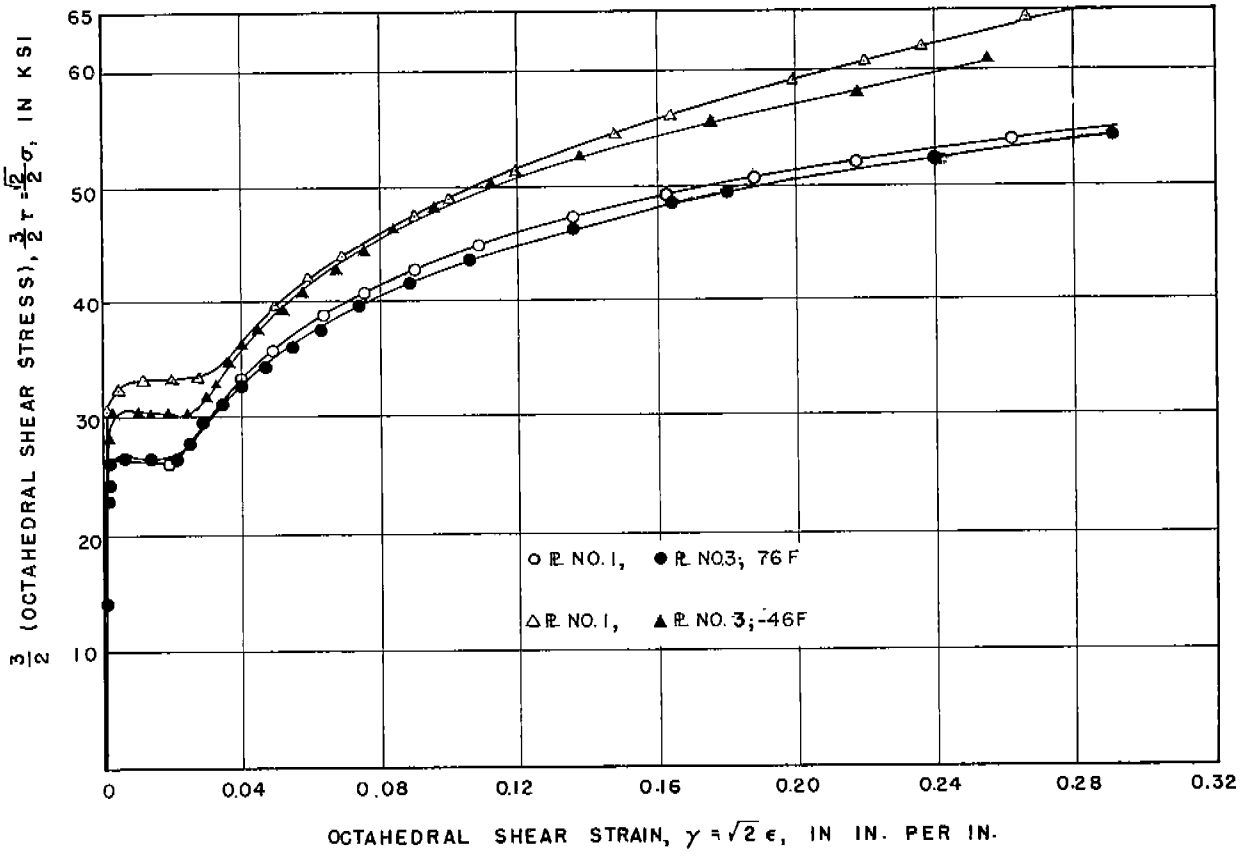

Fig. 2a. Calibration Test. Octahedral Stress-Strain Curve.

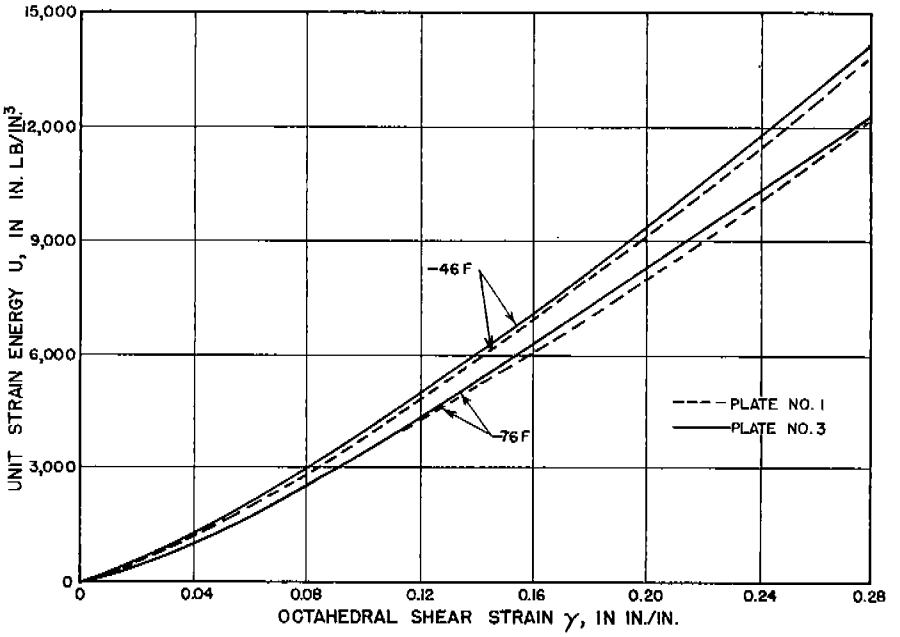

Fig. 3a. Relation of Unit Strain Energy Absorption and Octahedral Shear Strain for Calibration Test Specimen.

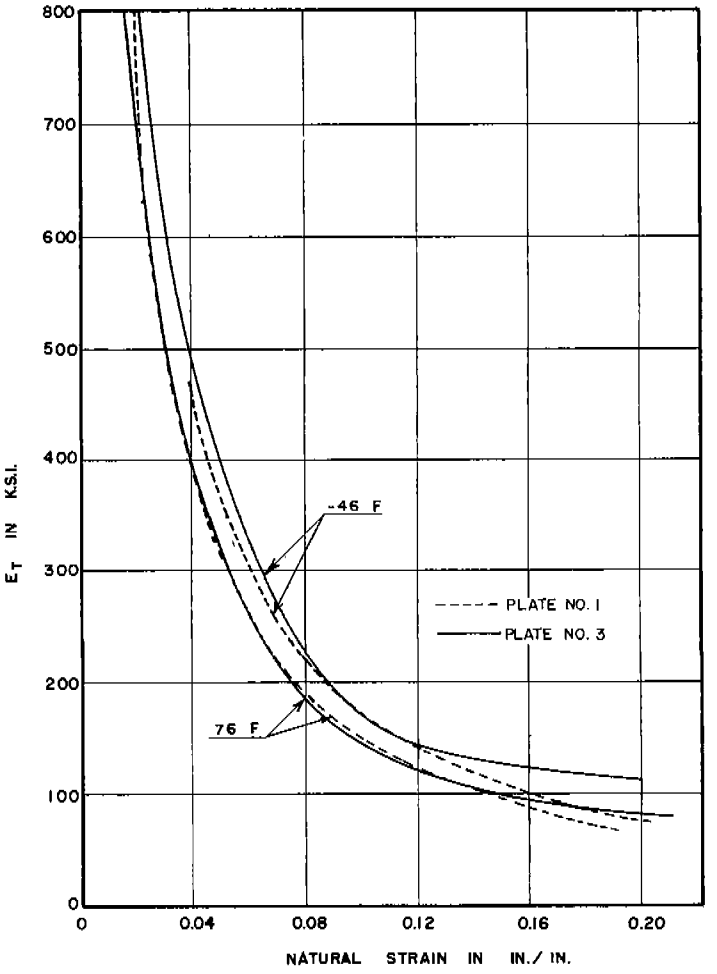

Fi . 4a Plot of E_T as a Function of Natural Strain.

APPENDIX B

TEST OF SPECIMEN NO. 85

Specimen No. 85 was a 36" x 1/4" plate, with a square opening with rounded corners. The reinforcement combined a face bar and an insert plate, the details of which are shown on Fig. 1b.

The test of the specimen and the recording of the results followed exactly the procedures described in the First Progress Report (1) for similar specimens. The results are given in Tables Ib and IIb. The test results are plotted in Figs. 2b-4b.

These results may be compared with those in the First and Third Progress Reports (1,3) and they will be incorporated along with previous results in the Final Report.

TABLE Ib

DESCRIPTION AND TEST RESULTS, SPEC. NO. 85

Description of Specimen		
Opening:	9" x 9" Square, 1-1/8" Corner Radius	
Reinforcement:	1-1/2" x 1/4" Face Bar in 14" x 14" x 1/2" Square Insert	
Percentage of Reinforcement:		77.8
Cross Section Area:	Net	8.50 sq.in.
	Gross	9.00 sq.in.
Testing Temperature:		76F
Strength and Energy Absorption		
General Yielding:	Load	295,000 lb.
	Av. Gross Stress	32,780 psi
	Av. Net Stress	34,710 psi
Ultimate Strength:	Load	493,000 lb.
	Av. Gross Stress	54,780 psi
	Av. Net Stress	58,000 psi
Energy Absorption:*	To Ultimate Load	1,442,000 in-lb
	To Failure	1,747,500 in-lb
Efficiency Compared with 1/4-In. Plain Plate		
General Yielding:	Load	77%
	Av. Net Stress	81%
Ultimate Strength:	Load	84%
	Av. Net Stress	89%
Energy Absorption:	To Ultimate Load	36%
	To Failure	29%

* Energy Absorption in 36-In. Gage Length.

II. b.

GENERAL YIELDING AND FRACTURE OF SPEC. NO. 85

Load in Kips at				Location of First Luders Lines, First Crack, Max. Unit Strain Concentration
First Luders Lines	General Yielding	First Crack	Ultimate Load	
260	295	494	494	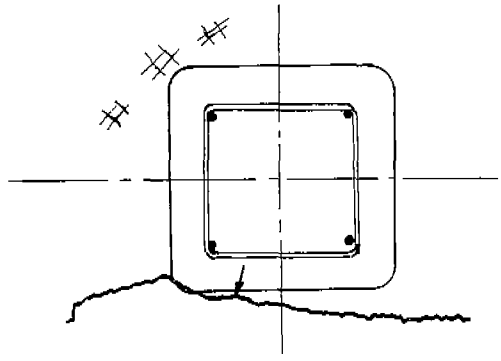

Legend:

- Max. unit strain concentration according SR-4 readings.

Luders lines appearing before general yielding of the specimen.

← Point of first crack.

— Fracture.

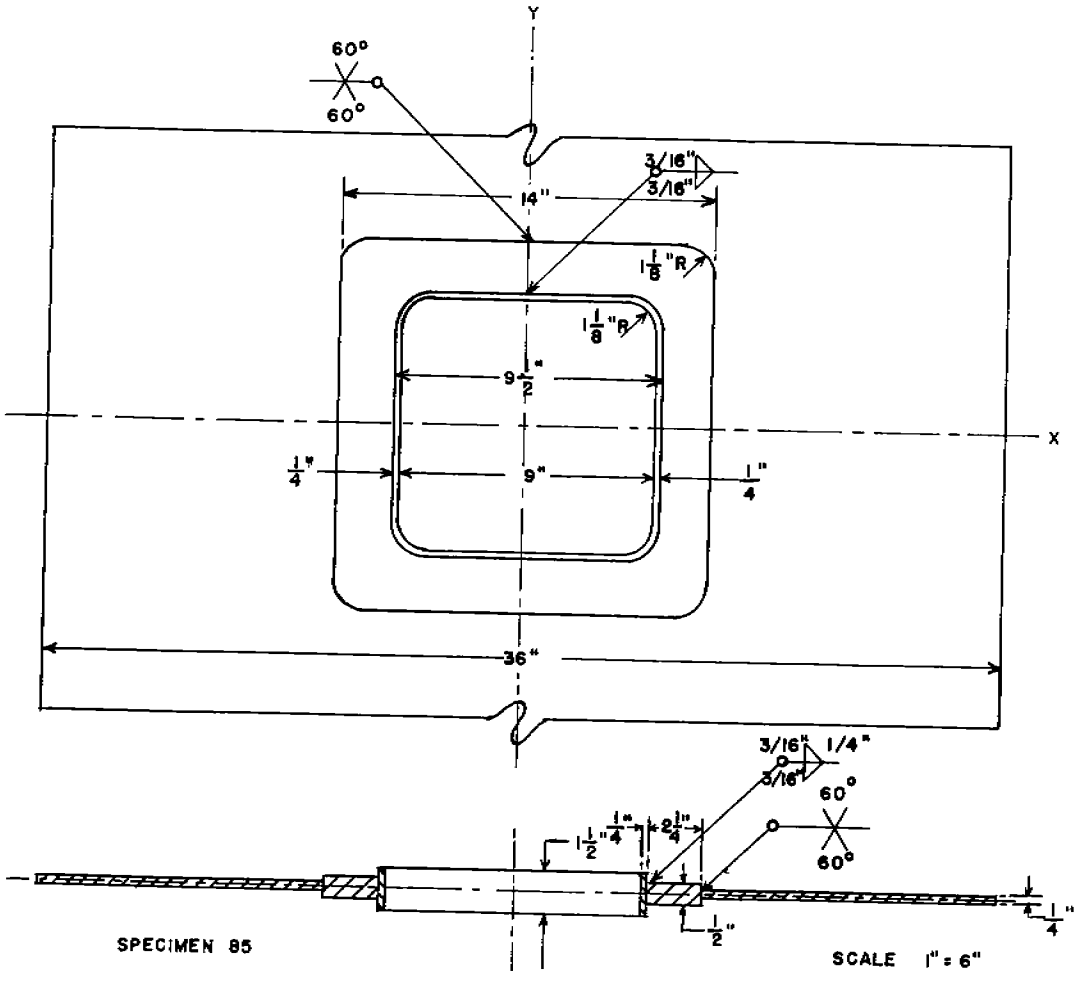

Fig. 1b. Details of Spec. No. 85.

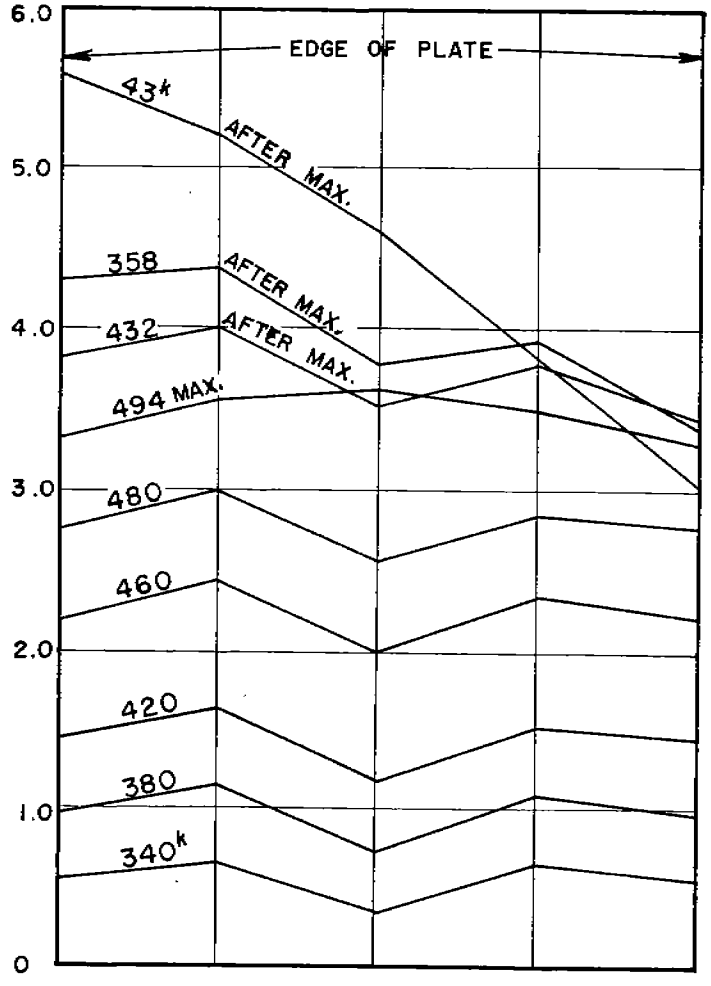

Fig. 2b. Distribution across Plate of Elongation on 36-In. Gage Length. Spec. No. 85. Square Opening with Rounded Corners, Face Bar and Insert Plate Reinforcement.

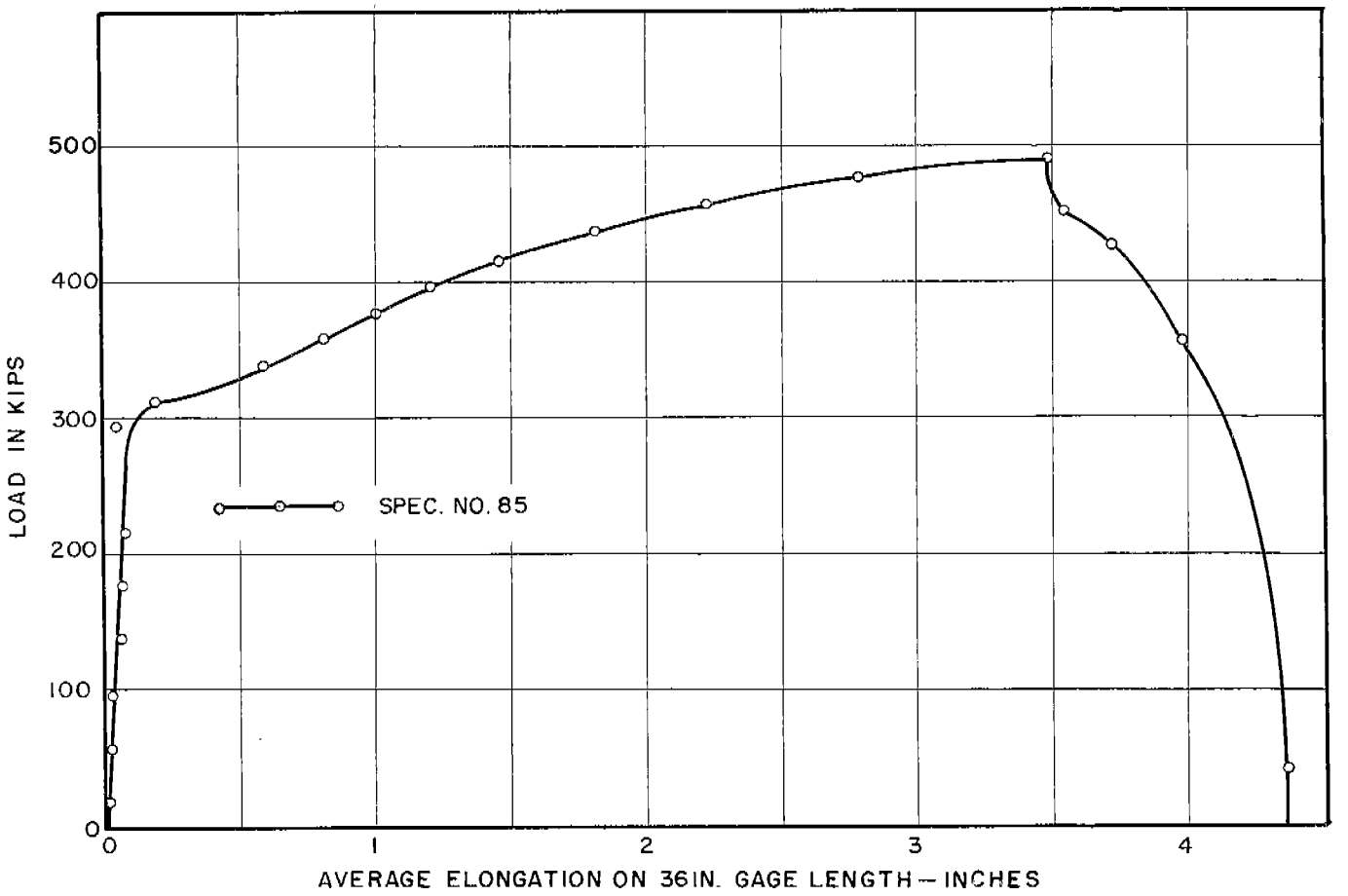

Fig.3b. Load and Average Elongation on 36-In. Gage Length for Spec. No. 85.

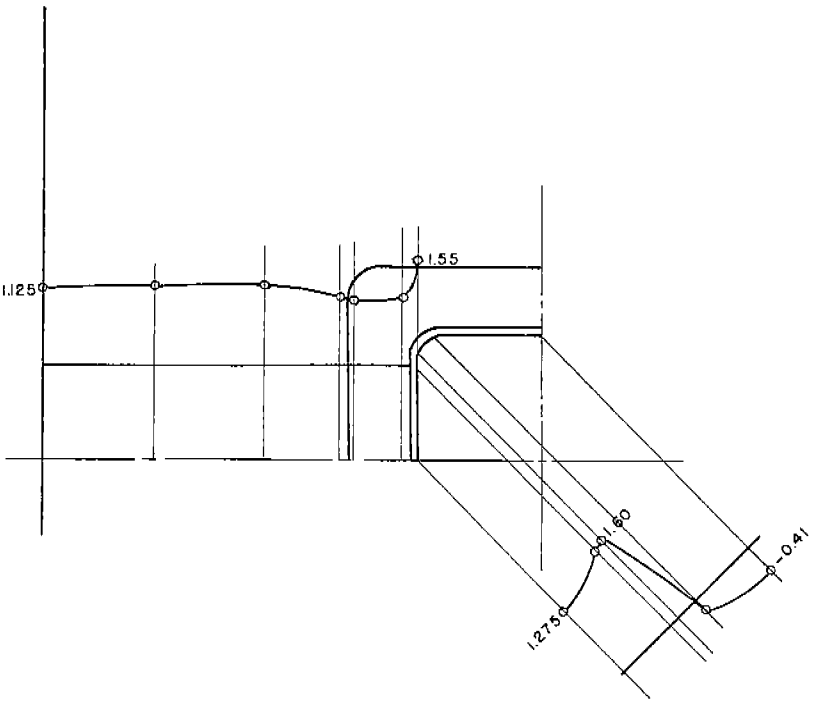

Fig.4b. Unit Strain Concentration in Region of Opening. Spec. No. 85.

Fig. 5b. Photograph of Spec. No. 85 after Failure.